# FIBROBLAST GROWTH FACTOR SIGNALING REGULATES TUMOR ANGIOGENESIS AND CANCER METABOLISM

A Dissertation

by

JUNCHEN LIU

Submitted to the Office of Graduate and Professional Studies of
Texas A&M University
in partial fulfillment of the requirements for the degree of

DOCTOR OF PHILOSOPHY

| | |
|---|---|
| Chair of Committee, | Fen Wang |
| Committee Members, | Wallace L. McKeehan |
| | Nora M. Navone |
| | Jiang Chang |
| | Mingyao Liu |
| Head of Department, | Warren Zimmer |

December 2017

Major Subject: Biomedical Sciences

## ABSTRACT

Acquisition of ectopic expression of type 1 receptor for the fibroblast growth factor receptor type1 (FGFR1) in prostate cancer (PCa) is well documented. However, while it is known that FGFR confers a growth advantage and promotes cell survival, how this aberrantly expressed transmembrane receptor tyrosine kinase contributes to PCa progression is not fully understood. Therefore, we investigated the roles of FGF signaling in both cancer metabolism and tumor angiogenesis. In first part of our study, we used a TRAMP mouse model with tissue specific deletion of fibroblast growth factor receptor substrate 2α (Frs2α), a key adaptor protein of the FGF signaling, in the prostate epithelium to investigate whether epithelial FGF signaling affects blood vessel cell functionality. Results showed that deletion of Frs2α decreased the blood vessels in prostate tumors. Similarly, conditioned medium of Frs2α knockdown prostate cancer cells inhibited the tube formation of human umbilical vein endothelial cells (HUVEC). Frs2α knockdown also decreased the ability of tumor cells to recruit HUVECs. We also discovered that ablation of Frs2α decreased the production of vascular endothelial growth factor A (VEGFA) primarily through preventing the binding of transcription factors HIF1α and c-Jun to its promoter region in prostate cancer cells and *in vivo*. We also demonstrated that hyperactivity of Frs2α, as well as upregulation of c-Jun and HIF1α, were positively associated with vessel density and progression of human PCa. In the

second part of this study, we reported that FGFR1 tyrosine kinase promoted aerobic glycolysis via regulating the expression pattern of lactate dehydrogenase (LDH): it tyrosine phosphorylated type A LDH (LDHA) and enhanced its stability, which favors the conversion of pyruvate to lactate, and therefore, decreases oxidative phosphorylation. Concurrently, FGFR1 downregulated the expression of type B LDH (LDHB) via increasing promoter methylation, which favors the conversion of lactate to pyruvate. Furthermore, consistent with the expression level of ectopic FGFR1, high levels of phosphorylated LDHA accompanied by diminished LDHB were associated with short overall survival and biochemical recurrence free survival time in PCa patients. This suggests that the dysregulated expression of LDH isozymes is of clinical value for PCa prognosis.

## ACKNOWLEDGEMENTS

Appreciation and deepest gratitude goes to the following persons who in one way or another have made this study possible.

Dr. Fen Wang gave me the opportunity to conduct my research in his lab. Thanks for his continuous support and guidance throughout the last seven years. He offered me freedom and responsibility for executing the work and trained me to think independently, which will be my greatest assets in my future academic pursuits. Dr. Wang would go through my slides and make notes so that I could better understand my problems on the presentation and writings. Besides, he and his family also gave me tremendous help my wife and I to settle down in America as a foreign student. The achievements that Dr. Wang has made in his scientific career and personal life set the bar so high that I know I will have to work extra hard to reach.

Dr. Wallace McKeehan frequently exchanged ideas with me on my projects, and he posed intriguing and incisive questions, which made me to think deeper in a wider scope. He also urged me to perfect my writings and speaking English to achieve a successful career in biomedical sciences. Since retirement, Dr. McKeehan has diligently taken time from his farming and ranching to attend my committee meetings and continue to interact, advise and encourage at other times

Dr. Nora Navone offered me generous advice and suggestions. Her warm and constructive advice on my project and career gave me the strength to carry on. The collaboration between our two labs broadened my perspective in prostate cancer bone metastasis.

Dr. Jiang Chang offered me valuable advice on my project design and on how to better organize and present my research work. He also provided me with gracious help on out collaborating project regarding FGF signaling in cardiovascular system.

Dr. Mingyao Liu gave me valuable advice on my career and personal life. He would talk to me about the details of experiments so that I can better understand the scientific questions I want to address. He also introduced me to Dr. Wang's lab.

Dr. Stefan Siwko helped me with the proofreading of my manuscripts and other writings. He offered informative, interesting and inspiring advice.

I thank my family for their long-time support and unconditional love.

Thanks go to my friends and colleagues, Yanqing Huang, Jue Zhang, Julia Chang, Yang Xiao, Yuepeng Ke, Zhiduan Cai, Guo Chen, Zezhen Liu, Xin Fu, Shaoyou Liu, Wenjiao Li, Ji Jing, Xianglai Xu, Shanshan Gao, Cong Wang, Pan You, Tomoaki Hamana, Xiangfeng Zeng, Yi Liang, and Jonathian Few.

## CONTRIBUTORS AND FUNDING SOURCES

This work was supervised by a thesis (or) dissertation committee consisting of Professors Fen Wang [advisor], Wallace McKeehan, Jiang Chang, Mingyao Liu of the Department of Center for Translational Cancer Research and Professor Nora Navone of the Department of Genitourinary Medical Oncology of the University of Texas MD Anderson Cancer Center.

The clinical data analysis for Chapter III and IV was conducted by Professor Weide Zhong of the Department of Urology, Guangdong Key Laboratory of Clinical Molecular Medicine and Diagnostics, Guangzhou First People's Hospital and Guangzhou Medical University.

All other work conducted for the thesis (or) dissertation was completed by the student independently.

Funding support: This work was supported by the NIH CA96824, TAMU1400302, and CPRIT 110555 to Fen Wang.

## TABLE OF CONTENTS

Page

## LIST OF FIGURES

Page

## LIST OF TABLES

Page

# CHAPTER I

# INTRODUCTION

Cancer cells, in order to meet the needs of rapid proliferation, rewire their metabolism and signaling pathways to generate ATP and other metabolic components that are essential for cellular processes (1-5). One of the characteristics of tumor cells is a shift from oxidative phosphorylation to glycolysis even though oxygen is sufficient, a phenomenon that is termed as the Warburg effect (6). ATP, oxygen and other metabolic building blocks contribute to the building of new cell mass during cell division. Glucose and other nutrients are from the environment that eventually becomes hypoxic due to the depletion of oxygen and nutrients as tumor growth outstrips the ability of the local vasculature to supply increasing demand. To expand and metastasize, tumor cells interact with the environment and induce the generation of new blood vessels to transfer nutrients from other parts of a human body. Therefore, tumor angiogenesis and cancer metabolism are both adaptations that tumor cells need to employ to meet their changing needs (3).

Weinberg proposed several hallmarks of cancers acquired during the development of human tumors. They include sustained proliferation signals, loss of tumor suppressors, induction of angiogenesis, activation of invasion and metastasis, cell death resistance, deregulated energy metabolism, enabling replicative immortality, and loss of immune checkpoints (7). Of note, these processes are not independent of or irrelevant to each other. In fact, the

signaling pathways that modulate these processes often overlap. For example, hypoxia-inducible factor 1α (Hif1α) stimulates the expression of VEGF-A to activate angiogenesis (8), but it also upregulates genes such as Glut1 and Ldha that are essential for glycolysis. Major oncogenes that operate in tumors, such as Myc and Ras, can upregulate angiogenesis factors in endothelial cells, and they can also regulate genes that are important for energy metabolism. Importantly, FGF is able to induce angiogenesis either through activating the proliferation of endothelial cells or by inducing VEGF-A which has been discussed earlier. Moreover, a recent study shows that FGF signaling activates angiogenesis by stimulating HK2 mediated glycolysis (9). Collectively, such observations reveal that cancer occurrence is a multi-step and well organized process that can be regulated by the same driver genes.

The relationship between glycolysis and angiogenesis has also been under investigation regarding the order of these two processes during tumor progression. Emerging evidence has shown that the “glycolytic switch” occurs before the “angiogenic switch” and tumors do not become vascularized until the basement membrane separating epithelium and blood vessels is breached (10). The glycolytic switch initially occurs due to hypoxia in the tumor microenvironment. Increased glycolysis results in an acidic tumor environment (low PH), which facilitates the degradation of the extracellular matrix (ECM). The acidic environment is toxic to nearby normal cells but not cancer cells (3). Although it is commonly believed that the altered metabolism is a result of

genetic changes including mutations in oncogenes and tumor suppressors, the induction of glycolysis is as important as the mechanism of it. There is a hypothesis arguing that the shift to aerobic glycolysis is the defining moment when normal cells become cancerous (3).

Prostate glands, which lie under the bladder and surround the urethra, produce fluids that form 25-30% of semen. Prostate cancer (PCa) is one of the leading causes of death in North America. Its progression is a multi-step process that develops relatively slowly and it often manifests in aged men. In the US, 1 out of 5 men are diagnosed with prostate cancer, although most patients with prostate cancer do not die from this disease. It usually arises within the peripheral zone of prostate glands which is distinct from the benign hyperplasia that occurs mainly in the transition zone (11). Early staged prostate cancer can be treated by physical removal of the tumors or with antigen deprivation therapy. However, metastatic prostate cancer migrates to bone, lung and brain and becomes castration resistant and deadly. Therefore, it is important to diagnose prostate cancer at relatively early stages. The prostate-specific antigen (PSA) test, transrectal ultrasound, transrectal magnetic resonance imaging (MRI) and biopsy can be used to detect and diagnose prostate cancer.

Stromal cells and epithelial cells compose the two major compartments of prostate. Prostate epithelium has three major cell types: basal cells, luminal cells and neuroendocrine cells. These three cell types can be distinguished by molecular markers, morphology, function and relevance to the progression of

prostate cancer (12). Luminal cells, which are column-shaped secretory cells, are the major type of prostate epithelium. They primarily express androgen receptors (AR), cytokeratin 8 and 18, and the CD57. Basal cells, residing between the basement membrane and the luminal cells, primarily express p63, cytokeratin 5 and 14, and CD44. Although the lineage of basal cells is still controversial, evidence shows that they are the sources of epithelial stem cells and transiently amplifying cells (13,14).

FGF signaling is comprised of at least 18 FGF ligands and 4 FGF receptors. By binding with FGF ligands along with heparan sulfate (HS), the active FGF/FGFR/HS complex recruits and activates downstream pathways such as the MAP kinase and PI3K pathways through its adaptor protein-Frs2α. Alternatively, FGF can bind and activate phospholipase C-gamma (PLCγ) through the C-terminal tail of the FGFR kinases (15,16) and this process is independent of Frs2α. FGF regulates a broad spectrum of cell activities, such as proliferation, apoptosis, differentiation and autophagy in contexts ranging from tissue regeneration to tumor progression.

The FGF is a proangiogenic factor that stimulates the proliferation of endothelial cells (17). However, whether aberrant FGF signaling, which is commonly observed in tumor cells, is directly involved in prostate tumor angiogenesis of prostate cancer remains unclear. Frs2α mediates FGF signaling from FGF receptors to downstream pathways such as MAPK and AKT pathway. Activation of Frs2α is correlated with multiple cancers including high grade serous ovarian

cancer, metastatic renal cell carcinoma, pancreatic cancer, and high grade liposarcoma (18-20).

Metabolic reprogramming has emerged as an emerging hallmark of cancer. Studies have shown that increased glycolysis is associated with late stages PCa and poor prognosis (21). A glycolytic gene, fructose-2,6-biphosphatase 4 (PFKFB4) was also found hyperactivated in PCa, further supporting the idea of targeting glycolysis pathways to treat advanced staged PCa (22). In addition to PFKFB4, intensive studies have shown that glycolytic enzymes, such as pyruvate kinase M2 form (PKM2), (glucose transporter) GLUT1, monocarboxylate transporter (MCT), LDHA, and others are implicated in multiple cancers (23). Furthermore, cancer cell chemoresistance is largely due to increased levels of aerobic lactate production (24). Despite a wealth of information that has been generated regarding cancer metabolism, little has been translated to clinical applications. One of the obstacles researchers are facing is a lack of animal models to recapitulate metabolism in the human body. Also a lack of understanding of mutual interactions between the tumor environment (cancer types), genetic features, and the tumor's metabolic dependencies also impedes development of new therapies.

# CHAPTER II

# HYPERACTIVATED FRS2α - MEDIATED SIGNALING IN PROSTATE CANCER CELLS PROMOTES TUMOR ANGIOGENESIS AND PREDICTS POOR CLINICAL OUTCOME OF PATIENTS*

## Introduction

Tumor angiogenesis is a crucial step for tumor cells to acquire oxygen and other nutrients. It involves the proliferation, migration and tube formation of endothelial cells and pericytes. The angiogenic switch, firstly described by Judah Folkman, is a process that tumor cells utilize to gain more nutrients and oxygen since these are not available locally when tumors grow to a certain size (25). Tumor cannot reach 1-2 $mm^3$ without getting nutrients from new blood supply supported by endothelial cells (26). The tumor microenvironment becomes hypoxic and acidic due to the extensive of utilization of oxygen and increased aerobic glycolysis by tumor cells. Hypoxia, stabilizing Hif1a, triggers the adaptations of tumor cells to the changing environment. Vascular endothelial growth factors (VEGFs), primarily secreted from tumor cells, along with other angiogenic factors such as FGFs and platelet-derived growth factor B (PDFG-B), activate

* Part of the data reported in this chapter is reprinted with permission from "Hyperactivated FRS2α-mediated signaling in prostate cancer cells promotes tumor angiogenesis and predicts poor clinical outcome of patients" by J Liu, P You, G Chen, X Fu, X Zeng, C Wang, Y Huang, L An, X Wan, N Navone, C-L Wu, WL McKeehan, Z Zhang, W Zhong and F Wang,2016. Oncogene, 35, 1750-1759, Copyright [2016] by Junchen Liu.

the proliferation and migration of endothelial cells within the microenvironment. The angiogenic switch can also be activated by inhibiting anti-angiogenic factors (27). The balance between pro-angiogenic and anti-angiogenic signals controls the rate of tumor angiogenesis, and eventually determines the growth and survival of tumors. Since angiogenesis is considered as a fundamental step for the progression of aberrantly proliferating tumor cells, it's crucial to understand what signaling pathways activate and control angiogenesis. This will lead to another questions, including whether we can target angiogenesis to treat tumors such as prostate cancer (PCa).

FGF-2 was one of the first pro-angiogenic factors to be discovered. Secreted by tumor, stromal and even endothelial cells, FGF2 also induced the expression of VEGF in blood vessels cells through paracrine and autocrine mechanisms. Recombinant adenovirus expressing soluble FGFR, which inhibited FGF function, reduced the growth of pancreatic tumors through interfering with the vasculature of tumor cells (17). In a murine pancreatic neuroendocrine tumor model, tumors cells treated with anti-VEGF therapy develop resistance due the upregulation of FGF2, suggesting of the cross-talk between FGF signaling and VEGF signaling (28). The detailed mechanism of this cross talk might be essential to effectively target tumor progression through inhibiting angiogenesis. FGF2 also synergistically promoted rumor angiogenesis with another proangiogenic factor PDGF-BB. Vascular smooth muscles cells (VSMCs) treated with PDGF-BB respond to FGF2 effectively via FGFR1 promoter activity

(29). Since FGFR1 is hyperactivated in ~40% of prostate cancers, FGFR-mediated signals could play essential roles in stimulating the disorganized vasculature in tumor outgrowth and metastasis.

Microvessel density (MVD), which reflects the expansion of the vasculature within tumors, serves as an essential marker for the histological analysis of tumor angiogenesis (6). Studies have suggested that MVD can be used as a predictive marker for prostate cancer (6,30).

Herein we show that overexpression and elevated phosphorylation of FRS2α is associated with tumor angiogenesis as well as clinical features of human PCa. Ablation of *Frs2α* in prostate epithelial cells compromised angiogenesis in the TRAMP mouse prostate tumor model. Depleting Frs2α expression in human PCa cells also reduced their ability to recruit human umbilical cord endothelial cells (HUVEC) in vitro and host endothelial cells in vivo. A detailed analysis revealed that Frs2α-mediated signals in PCa cells contributed to tumor angiogenesis via promoting production of VEGF-A through the HIF1α and cJUN pathways in the cells. This in turn recruited endothelial cells to the tumor. Thus, the results reveal a novel mechanism by which Frs2α-mediated signaling in PCa epithelial cells facilitated tumor angiogenesis within the microenvironment, unraveling the potential of overexpressed Frs2α as a biomarker for PCa diagnosis, and providing a rationale for treating PCa by inhibiting Frs2α-mediated signaling in epithelial cells or pro-angiogenic factors controlled by it.

## Materials and Methods

### *Animals and isolation of tissues*

All animals were housed in the Program of Animal Resources of the Institute of Biosciences and Technology, Texas A&M Health Science Center, and were handled in accordance with the principles and procedures of the Guide for the Care and Use of Laboratory Animals. All experimental procedures were approved by the Institutional Animal Care and Use Committee. Mice carrying the ARR2PBi-Cre, Frs2α floxed and TRAMP transgenic alleles were maintained and genotyped as previously described. A total of 40 TRAMP mice were generated for this study. No randomization was used in this study.

### *Histology and immunostaining*

Prostate or PCa tissues were fixed, dehydrated, embedded, and sectioned according to standard procedures. Antigens were retrieved by boiling in the citrate buffer (10 mM) for 20 minutes or as suggested by manufacturers. All sections were incubated with primary antibodies diluted in PBS at 4°C overnight. The rabbit anti-cJUN antibody (1:200) was purchased from Cell Signaling Technology (Beverly, MA); rabbit anti-HIF1α (1:200) and rabbit anti- CD31 (1:200) from Abcam (Cambridge, MA); mouse anti-CD31 (1:200) antibody from Novus Biologicals (Littleton, CO); rabbit anti-Frs2α from Santa Cruz (Santa Cruz, CA); rabbit anti-NG2 antibody from Chemicon (Billerica, MA); biotinylated-isolectin B4 from Vector Labs (Burlingame, CA). Specifically bound antibodies

were detected with alkaline phosphatase staining or FITC-conjugated secondary antibodies (Life Technologies, Grand Island, NY).

For expression of Frs2α and CD31 in human PCa, the Massachusetts General Hospital (MGH) PCa TMA was used. It includes 240 consecutive patients with PCa who underwent radical prostatectomy at the MGH from September 1993 to March 1995. For analyses of Frs2α phosphorylation in PCa, the human PCa TMA from the Shanghai Outdo Biotech Co, LTD (Shanghai, China, Cat No: HPro-Ade180PG-01) was used. It includes 99 primary PCa and 81 adjacent non-cancerous prostate tissues with the pathological features characterized by the vendor. Two experienced pathologists independently scored the results without any information about the samples. Only epithelial staining was counted. The scores were compared, and discrepant scores were subjected to re-examination by both individuals to achieve a consensus score. Immunostaining of PCa and stromal cells was evaluated separately. The percentage of positive cells was calculated and categorized as following: 0, 0 %; 1, 1–10 %; 2, 11–50 %; 3, 50 –75%; and 4, 75–100%. The staining intensity was visually scored and defined as 0, negative; 1, weak; 2, moderate; and 3, strong. Final immunoreactivity scores (IRS) were calculated for each case by multiplying the percentage and the intensity score. The specificities of the antibodies were validated as shown in online Fig. 2.

### *Matrigel plug*

Young adult (8-week-old) male nude mice were used for the Matrigel plug assay.

Cells (1X106) were infected with control or shFrs2 lentivirus before being mixed with 0.5 ml Matrigel on ice, for a final Matrigel concentration of 10 mg/ml. The Matrigel-cells mixtures were then implanted into the right flank of the mice. The plugs were harvested 14 days after the implantation.

***Cell culture and conditioned medium collection***

PC3 and DU145 cells were cultured in 10% FBS-DMEM medium. HUVECs were purchased from ScienCell Research Laboratories and grown in ECM medium (ScienCell, Carlsbad, CA). Conditioned medium was collected from confluent PC3 cell cultures 24 hours after changing the medium to 0.2% DMEM + FBS. The medium was filtered with 0.22 μm filters prior to being used.

***Cell proliferation***

PCa cells infected with shCtrl and shFrs2α lentivirus for 24 hours were seeded in 96-well plates at a density of 5,000 cells per well. After being cultured in 37°C for 48 hours, the cell densities were measured with the Cell Counting Kit-8 (Dojindo, Gaithersburg, MD). Data represent the mean ± sd of four wells.

***Endothelial recruitment***

PCa cells (2.5x104/well) seeded in 24-well plates were transfected with the indicated siRNAs. After being cultured at 37°C for 48 hours, the cells were washed with PBS and the culture media were replaced with EGM + 0.2% FBS. Each well was then received a chamber with an 8.0 μm pore size membrane

(BD Falcon) containing 1x105 serum-starved HUVECs in 0.5 ml 0.2% FBS-ECM medium. After the co-culture for 32 hours at 37°C, HUVEC cells were fixed with 4% paraformaldehyde and stained with hematoxylin. Three randomly pick areas in each insert were imaged and numbers of migrated HUVEC cells in each imaged area were counted. Data are mean ± sd of 3 replicates.

***Aortic ring assay***

Collagen was added to ice-cold DMEM to a final concentration of 1 mg ml. The pH was adjusted with a few drops of 5-N NaOH: ~20 µl per 10 ml to a final pH of 7.2. 50 µl of collagen matrix was transferred to each well of a 96-well plate, a few wells at a time, so that the matrix does not polymerize before addition of aortic rings. The 96-well plate format is essential for efficient aortic ring sprouting in collagen; aortic rings embedded in collagen in larger wells produce less growth factor and thereby support microvessel growth to a lesser extent. Plates were left undisturbed for 10–15 min at room temperature and then incubated at 37 °C/5% CO2 for 1 h. 150 µl of Opti-MEM culture medium supplemented with 2.5% (vol/vol) FBS and VEGF (final concentration of 30 ng/ml) was added to each well. Penicillin-streptomycin was added in the medium unless the rings had been transfected or transduced. Growth medium was changed first on day 3 or day 4 and then approximately every other day until the experiment ended by removing 130 µl of old medium and replacing with 150 µl of fresh medium.

### *Scratch wound healing*

HUVECs (1 x 105 cells/well) were seeded in six-well plates pre-coated with 0.1% gelatin. The cells were grown to confluence, followed by serum-starvation overnight and 5ug/ml mitomycin treatment to stop cell proliferation. A scratch in each well was made with a pipette tip. The cells were then cultured in the EGM containing 0.5% FBS with or without supplemented with PC3-conditioned media. The number of HUVECs that migrated were counted using a phase contrast microscope.

### *HUVEC tube formation*

HUVECs ($2x10^4$) were seeded in 24-well plates containing 0.5 ml solidified Matrigel (10 mg/ml) and cultured in EGM medium with or without supplementation of PC3 conditioned medium for 8–12 hours at 37°C. Images were acquired with a phase-contrast microscope. Average numbers of tubes were counted in three individual wells and presented as mean ± sd.

### *Gene silencing with siRNA or shRNA*

siRNA targeting Frs2αα, Hif1a, Ap2 and Sp1 were purchased from Dharmacon, GE health (Lafayette, CO, Catalog number: L-006440-00-0005, J-026959-08-0002, J-006348-06-0002 and J-004018-08-0002. PC3 cells were transfected with siRNA 48 hours before being used for functional assays. The coding sequences for shRNAs were cloned into the pLL3.7 plasmid for integration into

lentivirus. GIPZ lentiviral shRNA targeting Frs2αα was obtained from Dharmacon, GE health (Lafayette, CO, Clone ID: V2LMM_90453). Stable cell lines containing Frs2α or non-silencing shRNAs were acquired by G418 selection.

***Gene expression***

Total RNA was extracted with the Ribopure RNA isolation reagent (Ambion, TX). Reverse transcription was carried out with SuperScript III (Life Technologies, Grand Island, NY) and random primers. Real-time PCR was performed on MX3000 (Strategene), using the SYBR Green JumpStart Taq ReadyMix (Sigma, St. Louis, MO) with the primers list in Table 1 and following the manufacturer's protocol. The ratio between expression levels in the two samples was calculated by relative quantification, using β-actin as a reference transcript for normalization.

**Table 1. Primers for angiogenesis related genes**

| Gene Name | | Sequence (from 5'-3') |
|---|---|---|
| human-Vegf-a | forward | CGAACGTACTTGCAGATGTG |
| | reverse | CTGTTCTGTCGATGGTGATG |
| human-Hif1a | forward | TCCAAGAAGCCCTAACGTGT |
| | reverse | TGATCGTCTGGCTGCTGTAA |
| human-cJun | forward | TTTCAGGAGGCTGGAGGAAG |
| | reverse | CTGCCACCAATTCCTGCTTT |
| human-sp1 | forward | TTGAAA AAGGAGTTGGTGGC |
| | reverse | TGCTGGTTCTGTAAGTTGGG |

**Table 1. Continued**

| Gene Name | | Sequence (from 5'-3') |
|---|---|---|
| human-Frs2α | forward | TCCAGGATTTGCTGCTCAGA |
| | reverse | TTTCCGCTCTTCTTGCACAC |
| human-Ap2 | forward | TGGATCCTCGCAGGGAC ACAG |
| | reverse | GTTGGACTTGGACAGGGACAC G |
| human-GAPDH | forward | GAAGGTCGGAGTCAACGGATT |
| | reverse | TGACGGTGCCATGGAATTTG |
| mouse-Vegfa | forward | ACCTCCACCATGCCAAGT |
| | reverse | TCAATCGGACGGCAGTAG |
| mouse-Hif1a | forward | GTGAACAGAATGGAACGGAG |
| | reverse | CACAATCGTAACTGGTCAGC |
| mouse-c-Jun | forward | CATAGCCAGAACACGCTTCC |
| | reverse | TTGAAGTTGCTGAGGTTGGC |
| mouse-sp1 | forward | TGGTCATATTGTGGGAAGCG |
| | reverse | AATAAGGGCTGAAGGAGTGG |
| mouse-Frs2α | forward | GAGCTGGAAGTCCCTAGGACACCT |
| | reverse | GCTCTCAGCATTAGAAACCCTTGC |
| mouse-Ap2 | forward | GATGAAATCACCGCAGACGA |
| | reverse | TCCTTTGGCTCATGCCCTTT |
| mouse-VEcadherin | forward | TTGGGCTTTCTGACTGTTGT |
| | reverse | CAGGGACTTCGTGGGTTT |
| mouse-beta-actin | forward | GCACCAAGGTGTGATGGTG |
| | reverse | GGATGCCACAGGATTCCATA |

***Western blot***

Tumors or cultured cells were dissociated in 1% Triton X-100/PBS containing Proteinase and Phosphatase Inhibitors. Cells were lysed in RIPA buffer. The lysates (2ug) were separated on SDS-PAGE and blotted onto PVDF

membranes. The membranes were treated with 5% non-fat milk and incubated with primary antibodies overnight. Mouse anti-β-actin (1:2000) and rabbit anti cJUN (1:10000) antibodies were from Cell Signaling Technology; rabbit anti-VEGF (1:200) and mouse anti- VEGF antibodies were from Abcam; rabbit anti-HIF1α (1:1000) from Novus Biologicals. After washing with the TBST buffer, the membranes were incubated with horseradish peroxidase conjugated rabbit antibodies (1:10000) at room temperature for 1 hour. The specifically bound antibodies were visualized by using the ECL-Plus chemoluminescent reagents purchased from GE Healthcare Life Sciences. For quantitative analysis, the films were scanned with a densitometer.

***Chromatin immunoprecipitation (ChIP)***

Cells transfected with control or shFrs2α lentivirus for 72 hours were lysed and subjected to ChIP analyses using the EZ-ChIP Kit from Millipore (Billerica, MA) according to the manufacturer's protocols. Rabbit anti-cJUN antibodies and control IgG were purchased from Cell Signaling Technology (Beverly, MA). Mouse anti-HIF1α antibody was obtained from Novus Biologicals (Littleton, CO). The real-time PCR primers for the AP1-binding site regions were: Vegf-AP1 Forward (TAAGGGCCTTAGGACACCAT) and Vegf-AP1 Reverse (GGAATGCAGCAATTTCCCTC), and HIF1α-binding regions were: Vegf-HRE Forward (CAGGAACAAGGGCCTCTGTCT) and Reverse (TGTCCCTCTGACAATGTGCCATC).

### *Statistical analysis*

Statistical analysis was performed by the two tailed t test, significance set to $P < 0.05$. Correlation between Frs2α and CD31 was determined by Pearson's correlation test. Survival analysis was examined using the Prism 6 software. Error bars indicate standard deviation.

## Results

### *Ablation of Frs2a decreases angiogenesis in TRAMP tumors*

Ablation of Frs2a inhibits prostate tumor initiation, growth, and progression in the TRAMP mouse prostate tumor model (31). To investigate whether prostatic Frs2α regulates tumor angiogenesis in the TRAMP model, we knockout *Frs2α* in the prostatic epithelium by crosing a minimal probasin-ARR2Pbi-Cre strain with the floxed *Frs2α (Frs2α$^{flox}$)* mouse strain (Fig. 2.1). The resultant *Frs2α$^{flox/flox}$Cre*+ mice have no Frs2α activity in prostate epithelium. We further crossed the knockout mice with the TRAMP mice to generate mice that spontaneously develop prostate cancer but lack Frs2α expression in the prostate.

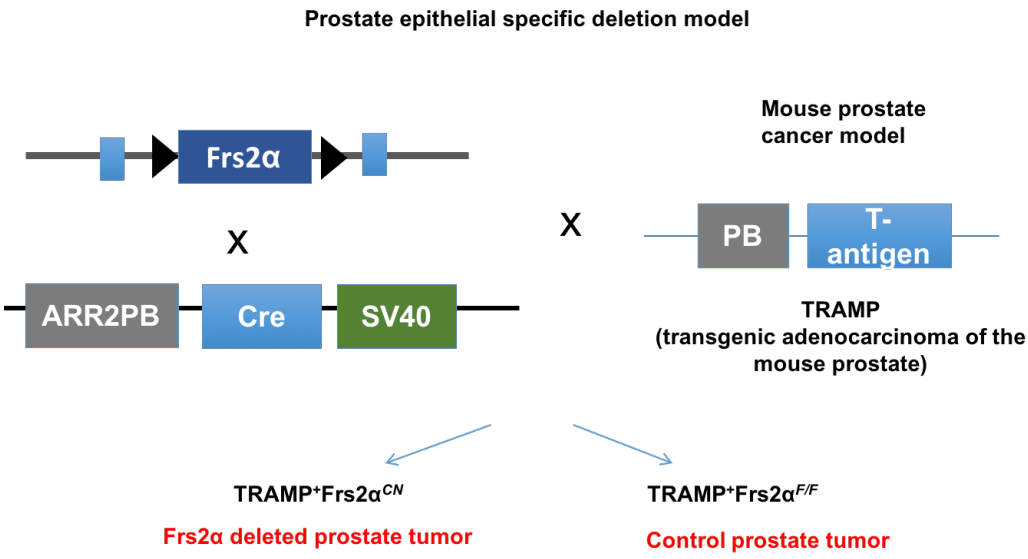


**Fig. 2. 1. Strategy of prostate-specific deletion of Frs2α in TRAMP mouse prostate tumor model.**

Prostatic deletion of *Frs2α* was achieved by crossing mice carrying the floxed *Frs2α* (*Frs2α*$^{f/f}$) with mice carrying *Cre* under the direction of minimal ARR2PB promoter. *Frs2α* $^{cn}$ mice were then crossed with TRAMP mice to get mice with *Frs2α* deletion in prostate tumors. PB, probasin promoter; TRAMP, transgenic adenocarcinoma of the mouse prostate.

We then sought to determine whether FRS2 is required for prostate tumor angiogenesis. Tumors from TRAMP and *Frs2α* Deleted TRAMP mice were sectioned and stained for the endothelial marker CD31 to determine the microvascular density. The *Frs2α* deletion reduced the number of blood vessels in PCa, suggesting Frs2α mediated FGF signaling is essential for the vasculature in the microenvironment of prostate cancer (Fig. 2.2 A). To confirm this result, we also used anti-NG2 antibodies to stain pericytes that typically abide around endothelial cells. NG2 positive blood vessels were also decreased in tumors that lack of *Frs2α* compared with control tumors (Fig. 2.2 B). Lectin-stained endothelial cells (another marker of endothelial cells) were reduced in *Frs2a* knockout tumors compared to control tumors (Fig. 2.2 C). In addition, the relative expression of CD31, NG2, and VE-cadherin mRNA was significantly lower in tumors that lack Frs2α compared with controls (Fig.2.3). Together, our data strongly indicate that Frs2α-mediated FGF signaling is crucial for the abundance of blood vessels in TRAMP tumors.

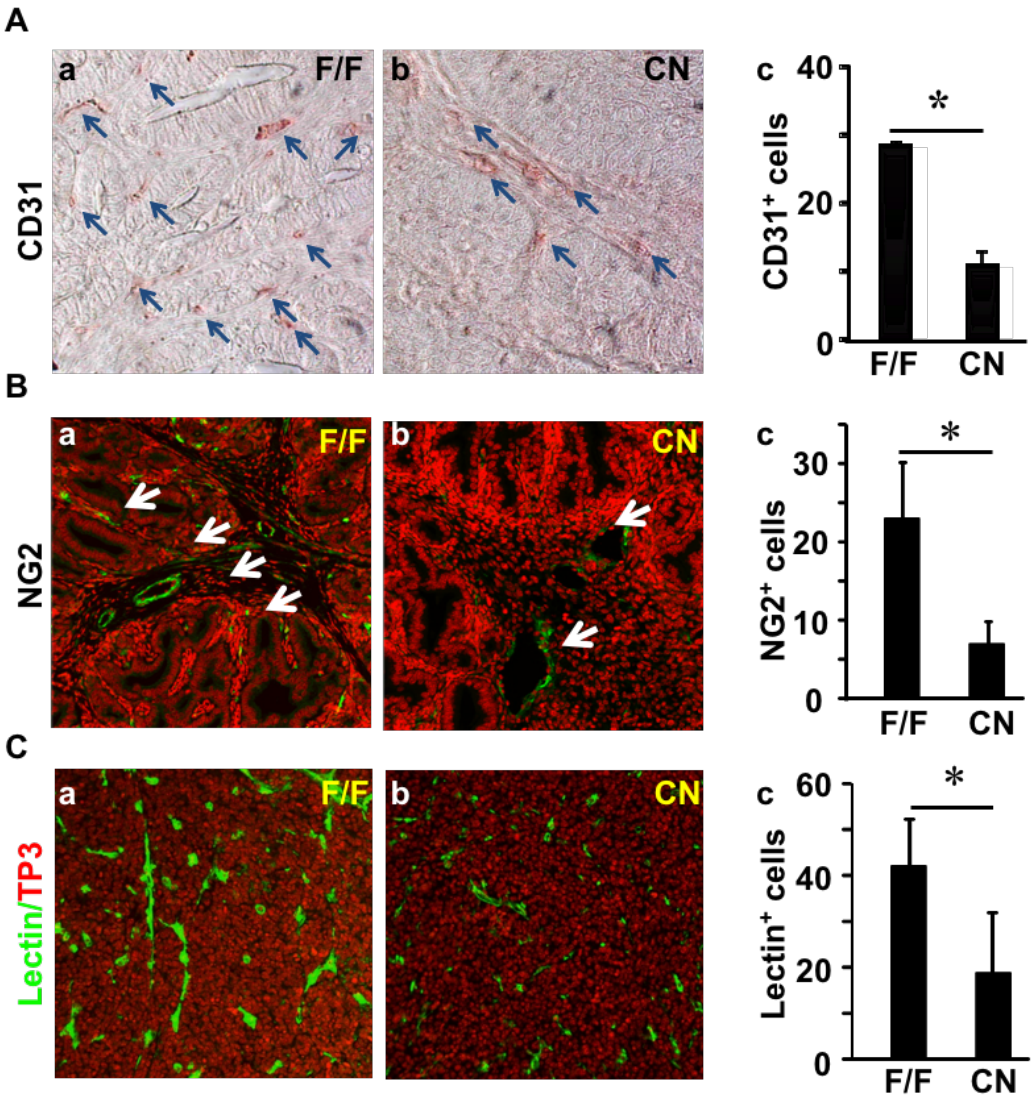


**Fig. 2. 2. Ablation of *Frs2α* in prostate epithelial cells reduces angiogenesis in mouse TRAMP tumors.**

**A–C.** Prostate tumor sections of 5-month-old TRAMP mice bearing floxed (F/F) (n=7) or epithelial-specific null (CN) (n=8) *Frs2α* alleles were stained with the indicated antibodies or lectins. The average number of stained cells per viewing frame was scored as indicated in panel c. TP3, To-Pro3.

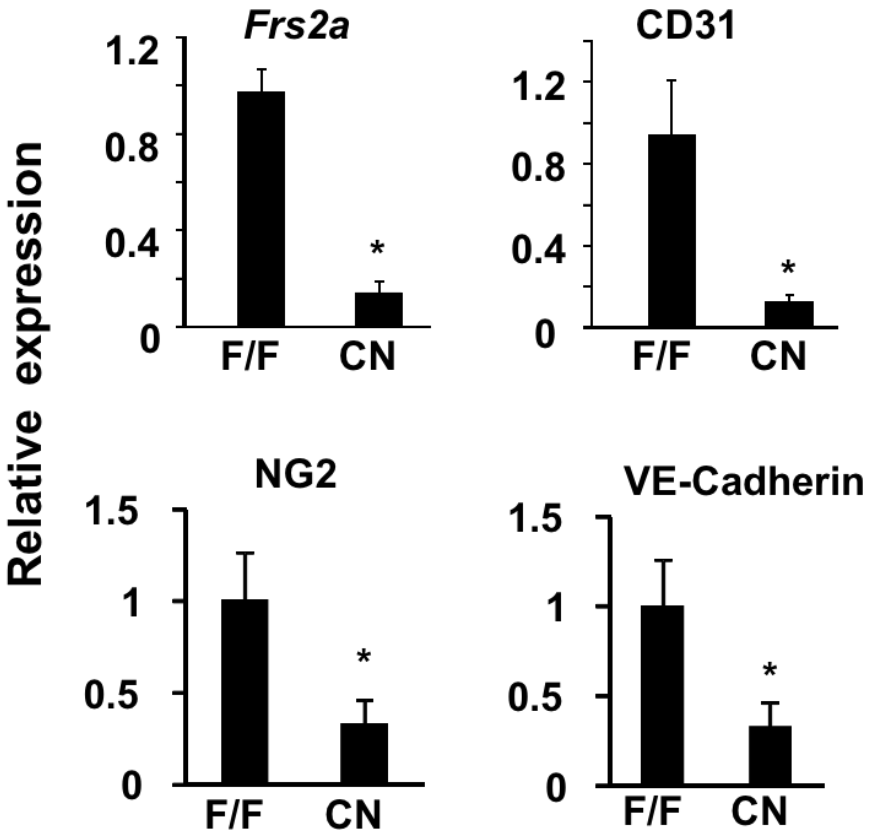


**Fig. 2. 3. *Frs2α* deletion reduced angiogenesis.**

Real-time RT-PCR analyses of the indicated mRNA in TRAMP tumors with or without Frs2α ablation. mRNA levels of Frs2α, CD31, NG2 and VE-Cadherin significantly decreased in conditional knockout tumors compared with controls. Data were normalized with β-actin and were expressed as mean ± sd from triplicate samples. CN, conditional knockout; *, $P<0.05$.

***Depletion of Frs2α decreased the ability of prostate cancer cells to recruit endothelial cells.***

Epithelial depletion of Frs2α decreased the amount of tumor blood vessels indicated that Frs2α altered the interaction between tumor cells and endothelial cells. We next sought to determine whether deletion of Frs2α in prostate cancer cells affects the function of endothelial cells *in vitro*. To model the interaction between tumor and endothelial cells, we co-cultured PC3 and HUVECs using a Transwell system with PC3 cells with or without Frs2α expression seeded in the lower chamber while HUVECS were planted in the upper chamber therefore to allow us to analyze the capacity of tumor cells to recruit HUVECs (Fig. 2.4. A). We found that HUVECs co-cultured with PC3 cells lacking Frs2αA migrated slower than those co-cultured with control PC3 cells, suggesting that Frs2 deletion impaired the capacity of tumor cells to recruit endothelial cells (Fig. 2.4. C).

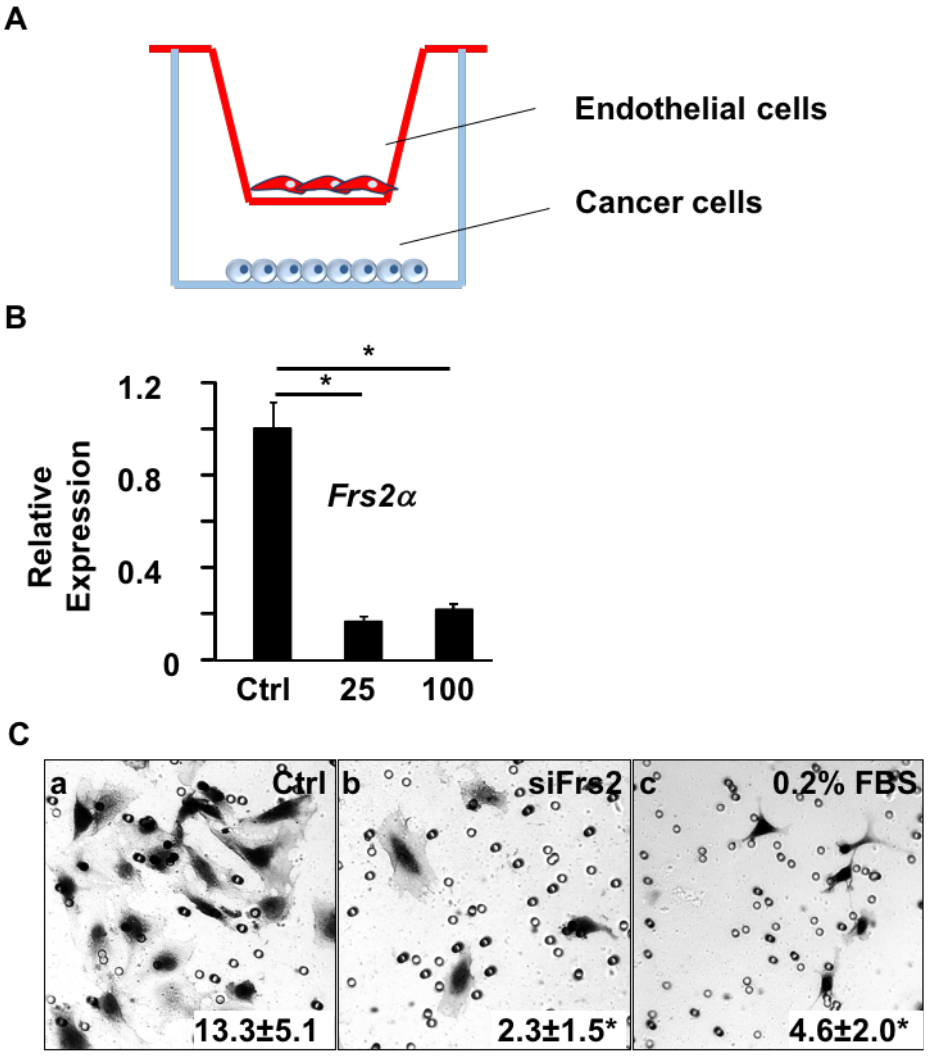


**Fig. 2. 4. Depletion of FRS2α in PC3 cells reduces their ability to induce HUVEC migration**

**A.** Schematic picture of HUVEC recruitment assay. **B.** Real-time RT-PCR analyses of FRS2α expression in PC3 cells treated with control or FRS2α siRNA at the indicated concentration. **C.** Transwell assays with HUVECs in the upper chamber and 10% PC3 cell-conditioned medium or 0.2% FBS in the lower chamber. Number of cells that migrated through the membrane was counted from triplicate samples and shown as mean ± sd.

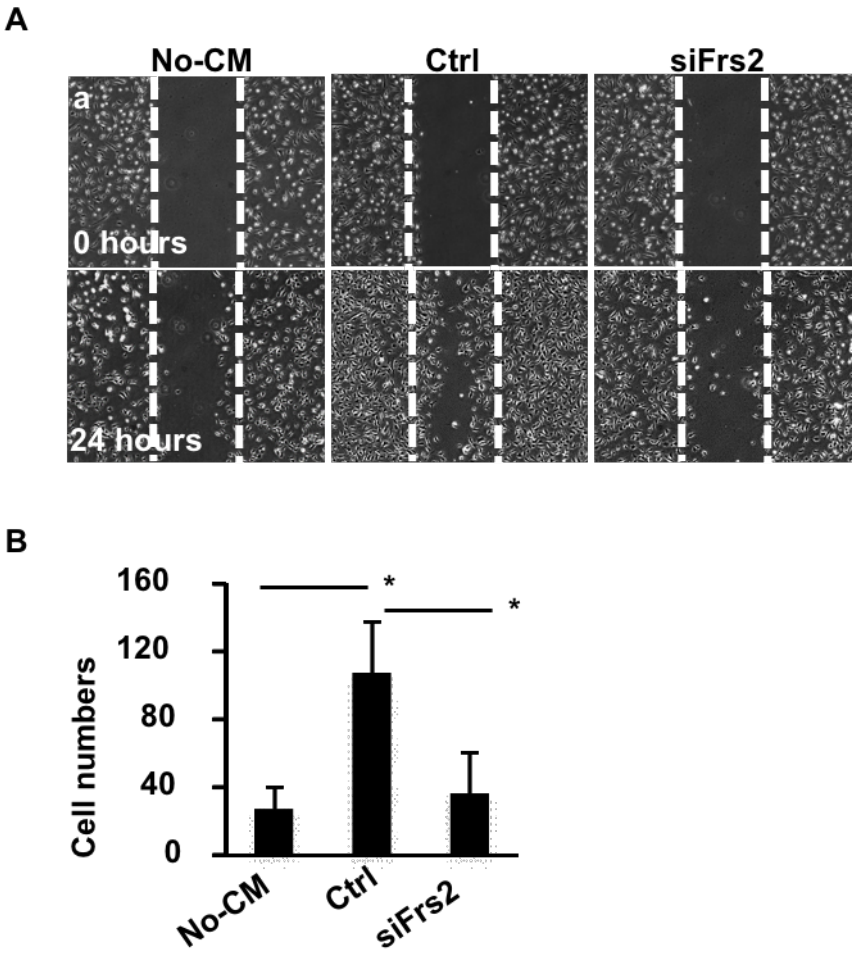


**Fig. 2.5. Frs2α depleted PC3 conditioned medium reduces HUVEC migration HUVEC.**

Confluent HUVEC cultures were injured by linear scrape with a pipette tip followed by addition of medium containing indicated PC3 cell conditioned medium for 24 hours. **A**. Images before and after culture for 24 with the indicated conditioned medium. **B**. Average number of cells that migrated from 3 independent samples. no-CM, negative control without conditioned medium; *, $P<0.05$.

To further study whether Frs2α regulates angiogenesis through a paracrine manner, we used conditioned medium from Frs2α knockdown cells and control PC3 cells to stimulate endothelial cells and evaluated their activities such as migration and tumor formation afterwards. The medium conditioned by Frs2α deletion had reduced ability to promote migration of HUVECs compared to non-conditioned medium and medium from control PC3 cells in the wound healing assay (Fig. 2.5). The result indicate that Frs2α deletion altered the soluble factor composition in the medium secreted by tumor cells. A unique feature of endothelial cells is the ability to form capillary-like structures with a lumen in Matrigel. Therefore, we compared the tube formation ability of endothelial cells treated with conditioned medium from Frs2α depleted and control PC3 cells. The Frs2α deletion PC3 conditioned medium showed less activity for promoting endothelial cell tube formation relative to control medium (Fig. 2.6). Notably, conditioned medium from both PC3 lines did not affect endothelial cell proliferation. Therefore, we concluded that Frs2α deletion in tumor cells impaired endothelial cell function through a paracrine manner.

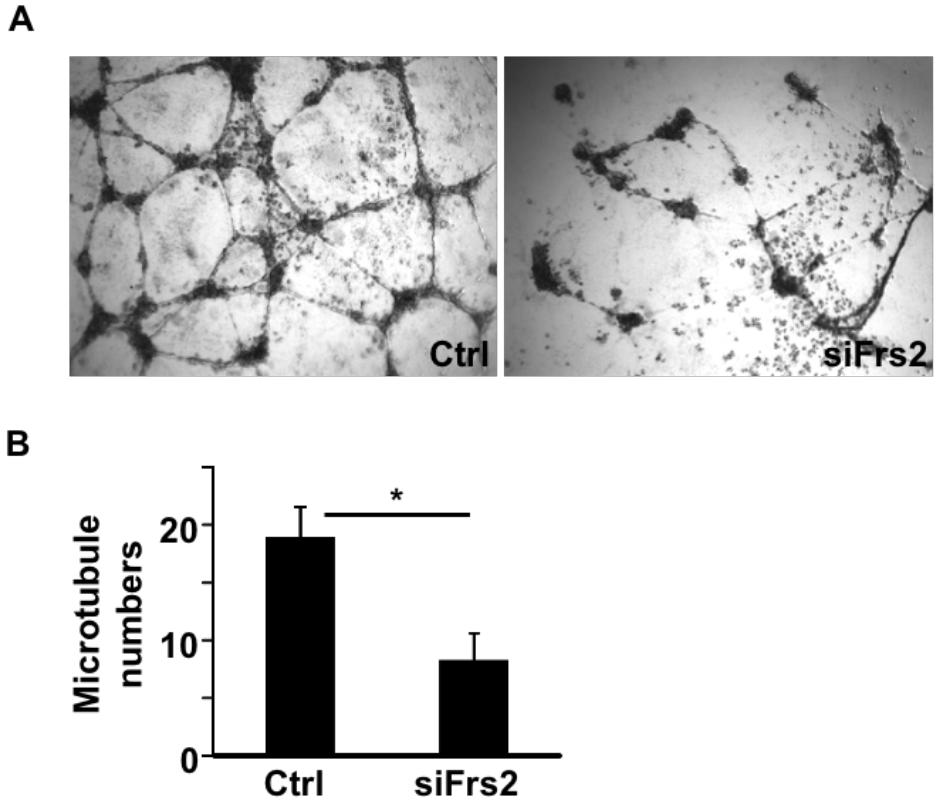


**Fig. 2. 6. Depletion of FRS2α in PC3 cells reduces ability to induce HUVEC tube formation.**

HUVECs were inoculated in Matrigel with 10% conditioned medium from PC3 cells treated with control or FRS2α siRNA. **A.** The indicated images of HUVECs were captured after cells were cultured at 37°C for 8 hours. **B.** The average number of tubes formed from HUVECs were calculated from triplicate samples and presented as mean ± sd. no-CM, negative control without conditioned medium; *, $P<0.05$.

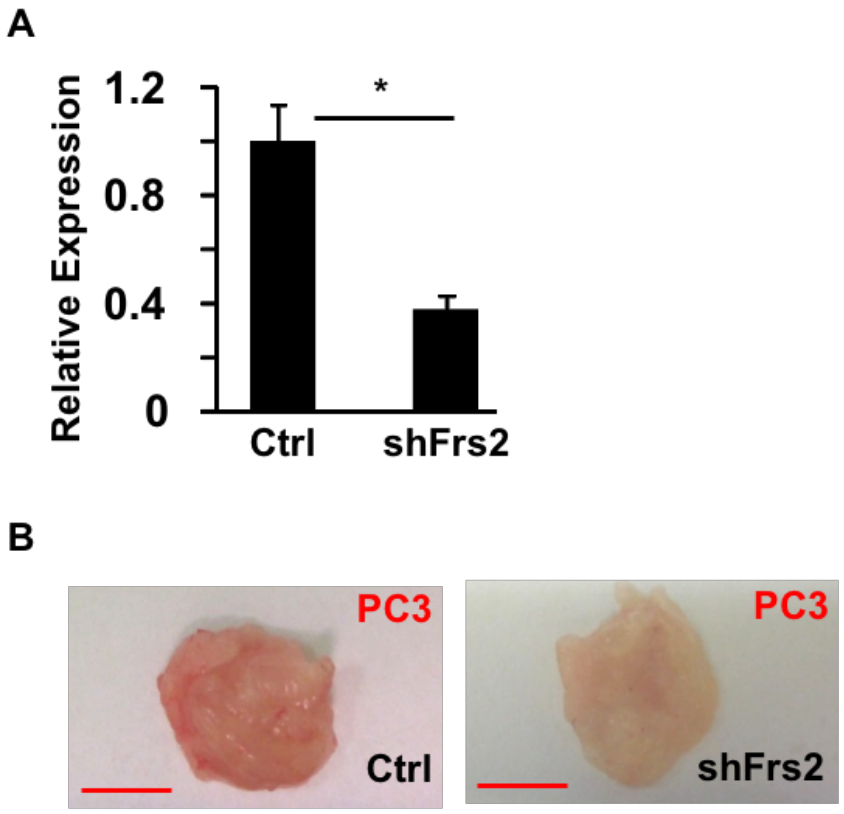


**Fig. 2. 7. Depletion of FRS2α in PC3 cells in Matrigel plugs dampens recruitment of endothelial cells into the plugs in nude mice.**

**A**. Real-time RT-PCR analyses of Frs2α expression in PC3 cells infected with lentivirus carrying Frs2α or control shRNA. **B.** Gross morphology of the Matrigel plugs harvested from nude mice at two weeks after the implantation. shFRS2, FRS2α shRNA; Ctrl, control shRNA; *, P<0.05.

We then determined whether depletion of Frs2α expression in PCa cells also compromised their ability to induce endothelial migration and invasion in vivo. This was accomplished by depletion of Frs2α expression in PC3 cells by stable expression of Frs2α shRNA (Fig. 2.7. A). The Frs2α-depleted PC3 cells were

mixed with Matrigel, and then implanted into the flanks of immune-deficient nude mice. The Matrigel plugs were harvested at day 14 after implantation. The pale tone of Matrigel plugs containing Frs2α-depleted PC3 cells relative to the red color of the plugs containing control PC3 cells indicated a reduced blood vessel density in the Frs2α-depleted group (Fig. 2.7 B).

Immunostaining with $CD31^+$ cells confirmed that the endothelial cell content in the Matrigel plugs was reduced in the Frs2α depleted group (Fig. 2.8). The results further indicate that Frs2α-mediated signals in PCa cells promote attraction of endothelial cells to the tumors formed by PCa cells and angiogenesis of the tumors. Furthermore, quantitative RT-PCR analyses of the RNA extracted from Matrigel plus showed that depletion of Frs2α in PC3 cells reduced human VEGF-A expression (from PC3 cells) and host mouse endothelial cell marker RNAs. This further demonstrated that Frs2α in PCa cells promoted recruitment of host endothelial cells to the tumor (Fig. 2.8 B).

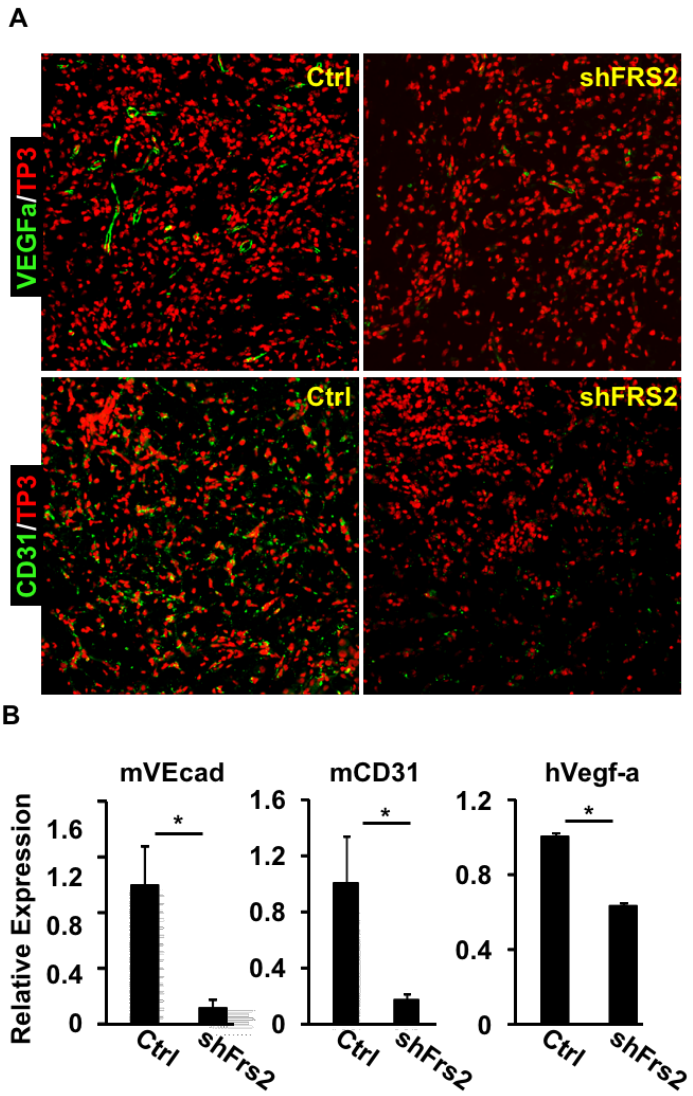


**Fig. 2 .8. Depletion of Frs2α in PC3 cells in Matrigel plugs decreased recruitment of blood vessels and Vegf-a expression.**

**A**. Immunostaining of Matrigel plug sections with anti-CD31 or anti-VEGF-A antibodies. To-Pro3 (TP3) was used for nuclear counter staining. **B**. Real-time RT-PCR analyses of the RNA extracted from the Matrigel plugs containing control (n=6) or Frs2α-depleted (n=6) PC3 cells. mVEcad, mouse VE-cadherin; mCD31, mouse CD31; hVegf-a, human Vegf-a; shFRS2, Frs2α shRNA; Ctrl, control shRNA; *, $P<0.05$.

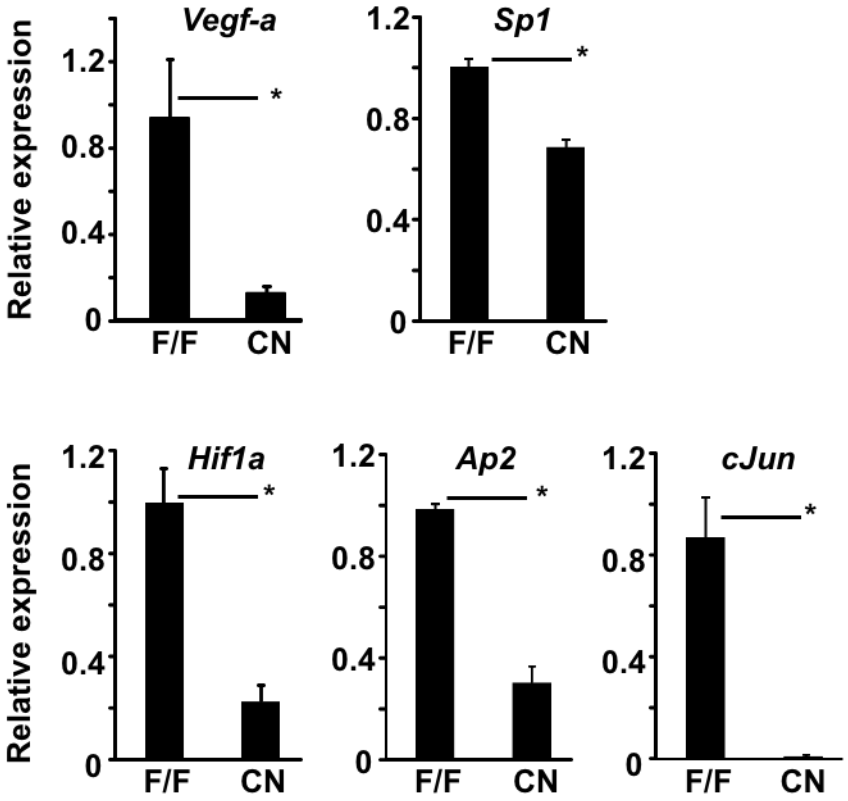


**Fig. 2. 9. Depletion of *Frs2α* reduces expression of *Vegf-a* in mouse TRAMP tumors.**

Real-time RT-PCR analyses of the indicated gene expression in TRAMP tumors with or without tissue-specific ablation of *Frs2α* in the epithelial cells. F/F, $Frs2\alpha^{flox}$; CN, $Frs2\alpha^{CN}$; *, P<0.05.

***Ablation of Frs2α in PCa cells reduced Vegf-A expression via down-regulation of Hif1a and cJun expression.***

Since VEGF-A is a key angiogenic factor, we then asked whether Frs2 deletion affects VEGF-A expression. We employed quantitative RT-PCR analyses to assess Vegf-a expression in TRAMP tumors bearing *Frs2α*$^{Flox}$ or *Frs2α*$^{CN}$ alleles. In comparison with *Frs2α*$^{Flox}$ tumors, the expression of Vegf-a in Frs2αCN tumors was reduced (Fig. 2.9). To investigate the mechanism underlying regulation of Vegf-a by Frs2α-mediated signals, we assessed the expression of potential Vegf-a upstream regulators by quantitative RT-PCR analyses. The expression of Sp1, Hif1α, Ap2, and cJun was reduced in *Frs2α*$^{CN}$ tumors at the mRNA level. Furthermore, immunostaining showed that expression of HIF1α and cJUN was downregulated at the protein level in *Frs2α*$^{CN}$ prostates and PCa (Fig. 2.10 B). There were no changes in SP1 and AP2 expression in the *Frs2α*$^{CN}$ prostate (data not shown), possibly due to other redundant upstream regulators. Western analyses further confirmed that expression of cJUN and HIF1α were reduced at the protein level (Fig. 2.10 A). The results suggest that downregulation of these two upstream regulators contribute to reduced expression of Vegf-a in *Frs2α*$^{CN}$ prostate and prostate tumors.

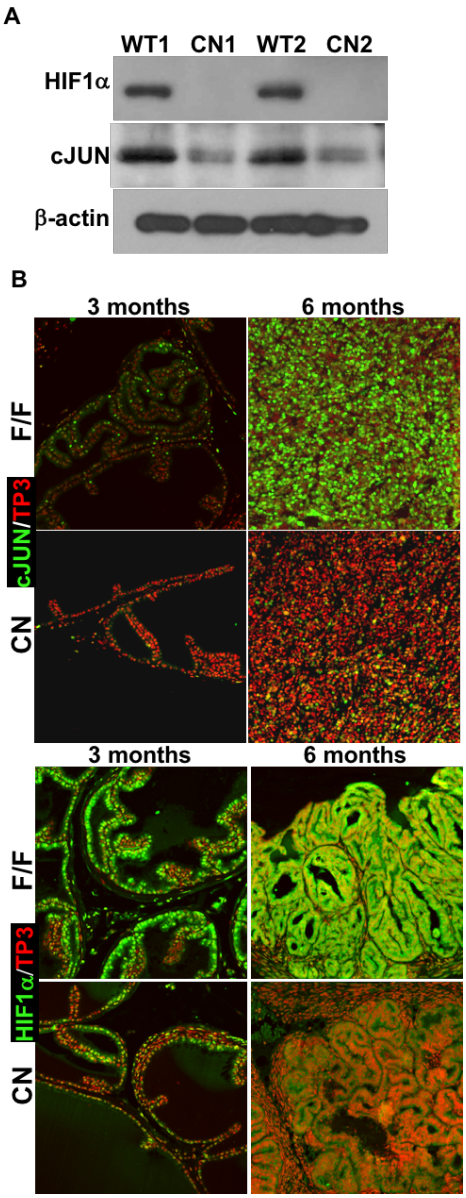


**Fig. 2. 10. Depletion of *FRS2α* reduces expression of *Vegf-a* in mouse TRAMP tumors.**

**A.** Western blot of cJUN and HIF1α expression in the TRAMP tumors.
**B.** Immunostaining analyses of cJUN and HIF1α expression in the TRAMP tumors. F/F, $Frs2\alpha^{flox}$; CN, $Frs2\alpha^{CN}$.

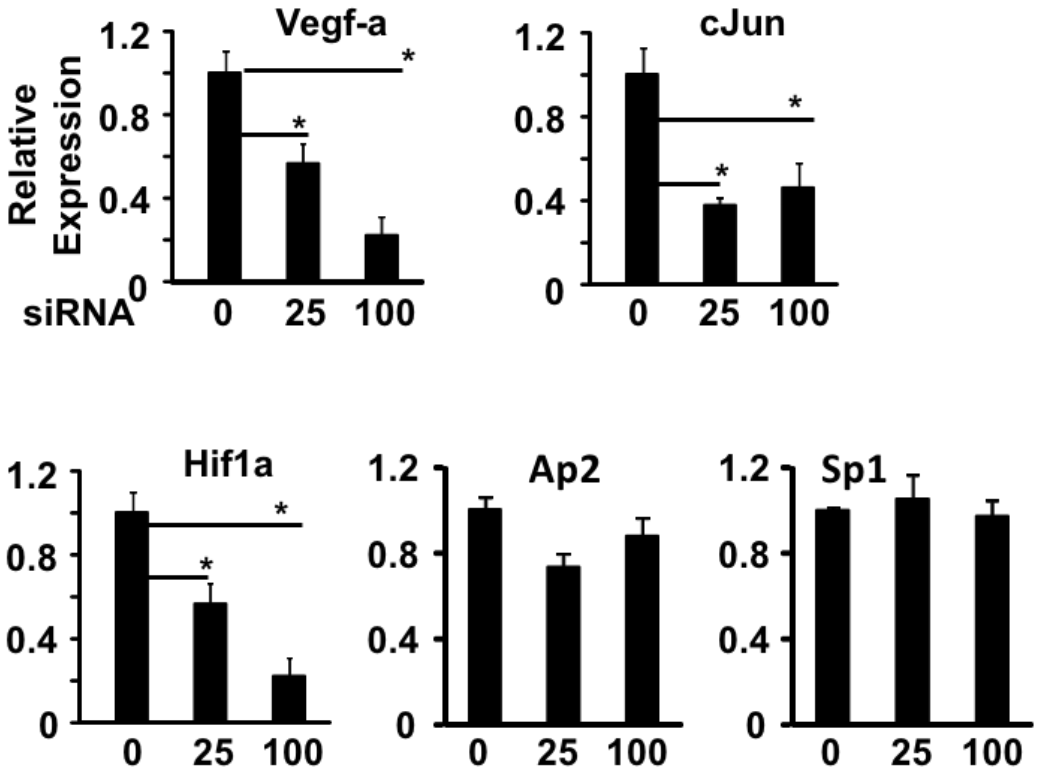


**Fig. 2. 11. Depletion of Frs2α in PCa cells reduces expression of Vegf-a and transcriptional factors that bind to Vegf-a promoter.**

Real-time RT-PCR analyses of PC3 cells at 72 hours after treatment with the indicated siRNA at a final concentration of 25 or 100 nM. mRNA expression of Vegf-a, cJun and Hif1a significantly went down in cells treated with Frs2α siRNA relative to control groups. *, $P<0.05$.

We also noted that depletion of Frs2α also compromised Vegf-a, cJun, and Hif1a expression in human PC3 cells although the expression of Sp1 and Ap2 was not affected (Fig. 2.11). We then focused our efforts to determine whether cJUN and HIF1α were required for Vegf-a expression in human PCa cells. A luciferase reporter construct driven by the Vegf-a promoter was used to determine whether depletion of the two transcription factors compromised expression of the reporter. Consistently, the results showed that depletion of cJUN and HIF1α, but not SP1 or AP2, in PC3 cells reduced expression of the luciferase reporter, suggesting that SP1 and AP2 were dispensable for Vegf-a expression in PC3 cells (Fig. 2.12 A). To further determine whether cJUN, HIF1α, SP1, and AP2 mediated Frs2α signals were required to support Vegf-a expression in PC3 cells, expression of these transcription factors was depleted with siRNA. Western blot analyses showed that expression of VEGF-A was reduced in the cells treated with cJun and Hif1a siRNA (Fig. 2.12B).

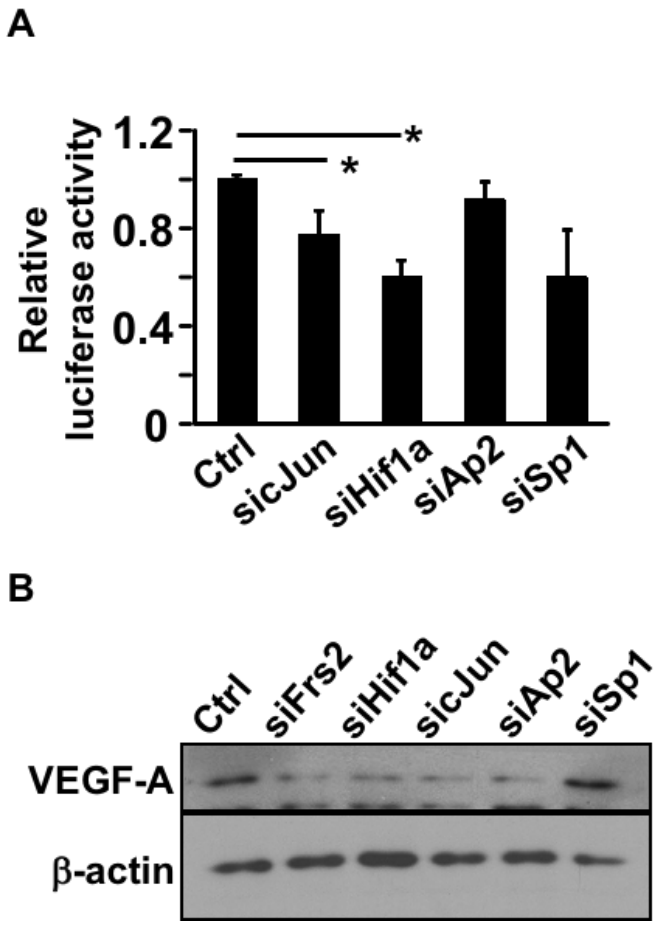


**Fig. 2. 12. Depletion of Frs2α and cJun and Hif1a reduces Vegf-a promoter activity.**

**A**. Luciferase reporter analyses of Vegf-a reporter activities in PC3 cells with or without depletion of indicated genes. Hif1a and cJun knockdown significantly suppressed Vegf-a luciferase activity. **B**. Western blot analyses of VEGF-A expression in PC3 cells after reduction in expression of the indicated genes. *P<0.05.

Consistently, overexpression of either HIF1α or cJUN in Frs2α-depleted PC3 cells partially restored their activity in promoting HUVEC migration (Fig. 2.13 A), although these transcription factors also increased baseline HUVEC migration in control cells. Furthermore, ChIP assays revealed that cJUN binding to the Vegf-a promoter region in pull-down assays was reduced in PC3 cells depleted of Frs2α (Fig. 2.13 B. panels a&b). Since HIF1α is unstable under normoxic conditions and thus it is difficult to do ChIP assays using cultured cells, so similar ChIP experiments for HIF1α were carried out with *Frs2α*$^{CN}$ and control PCa tissues (Fig. 2.13 B. panels c&d). The Vegf-a promoter sequence pulled down by HIF1α was reduced in *Frs2α*$^{CN}$ tumors compared to control tumors. The data demonstrate that HIF1α and cJUN are involved in upregulation of VEGF-A expression by Frs2α-mediated signals in PCa cells.

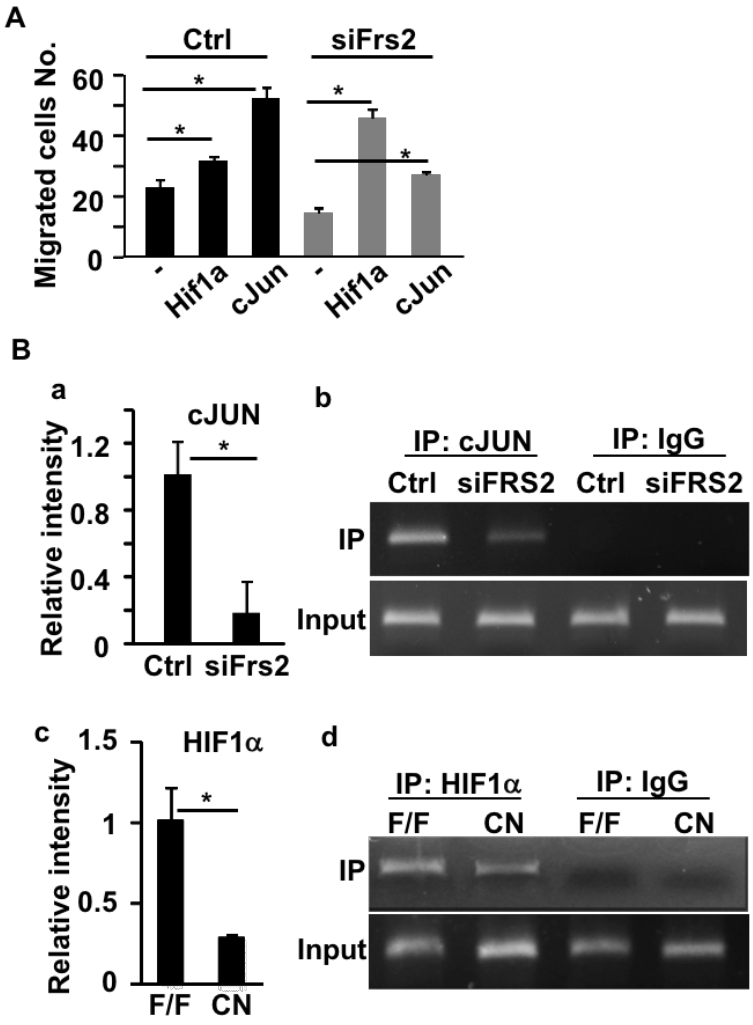


**Fig. 2. 13. Overexpression of Hif1a or c-Jun rescued the migration defect of HUVECs with Frs2α depletion.**

**A.** Transwell cell culture analyses of HUVECs treated with conditioned medium of PC3 cells overexpressing cJUN or HIF1α. **B**. ChIP assays of Vegf-a promoter with anti-cJUN or anti-HIF1α antibodies. Panels a and c are the relative binding of cJUN or HIF1α to the Vegf-A promoter. Data are mean ± sd derived from 3 replicate samples. Panels b and d are images of agarose gel electrophoresis showing a single band of the PCR products. Ctrl, control siRNA; IP, immunoprecipitation; F/F, *Frs2α*$^{f/f}$; CN, *Frs2α*$^{f/f}$; *, P<0.05.

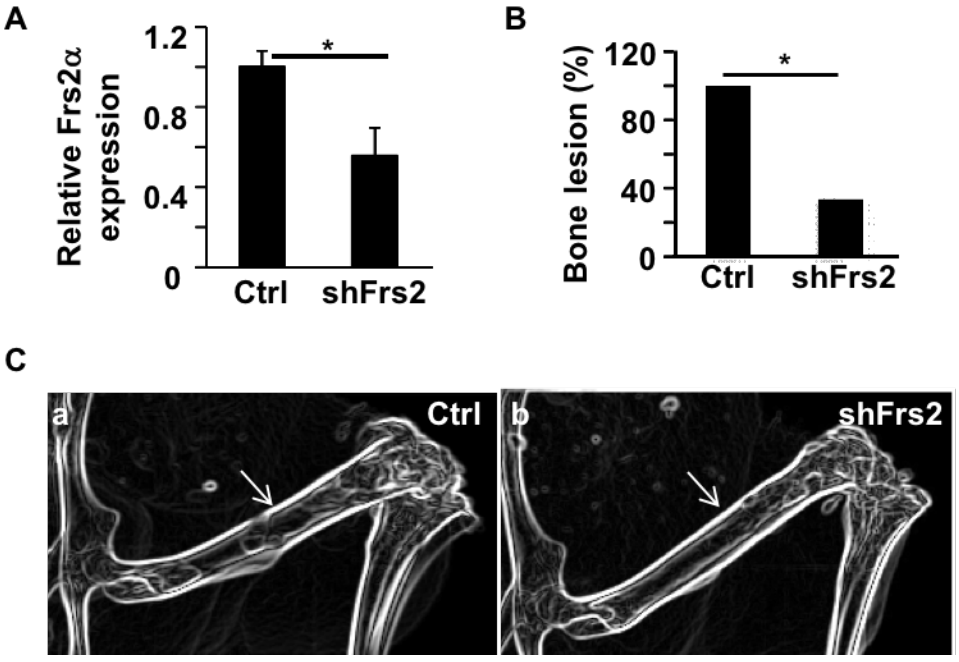


**Fig. 2. 14. Depletion of FRS2α impairs the tumorigenicity of MDA PCa 118b cells.**

**A.** Real-time RT-PCR analyses of MDA PCa 118b cells infected with shFRS2 (n=6) control (n=6) adenoviruses. **B&C**. X-ray analyses of mouse femurs 7 weeks after injection of 1.5 X $10^6$ of the indicated cells. Investigators were blinded when assessing the bone lesions and blood vessels. The tumor incidence rates were calculated and expressed as mean ± sd (B). Representative images are shown in (C). Ctrl, control virus infected PC3 cells; shFrs2, shFrs2 virus infected PC3 cells; *, $P<0.05$.

We then assessed the role of Frs2α in human PCa in bones, the most common site of lethal PCa metastasis. The expression of Frs2α was depleted in tumor cells isolated from MDA PCa 118b tumors, a preclinical human PCa xenograft model, by infection with adenovirus carrying shFrs2α (Fig. 2.14 A). The cells were then implanted to the femurs of SCID mice for assessing their capacity for growth in bone. Frs2α-depleted cells exhibited a lower tumor forming capacity in the mouse femurs than did control cells (Fig. 2.14 B). This suggests that Frs2α deficiency reduces growth of the tumor cells in bone.

Moreover, the density of CD31+ endothelial cells was reduced in the Frs2α-depleted tumors (Fig. 2.15), indicating that the angiogenesis in the tumor was compromised by depletion of Frs2α.

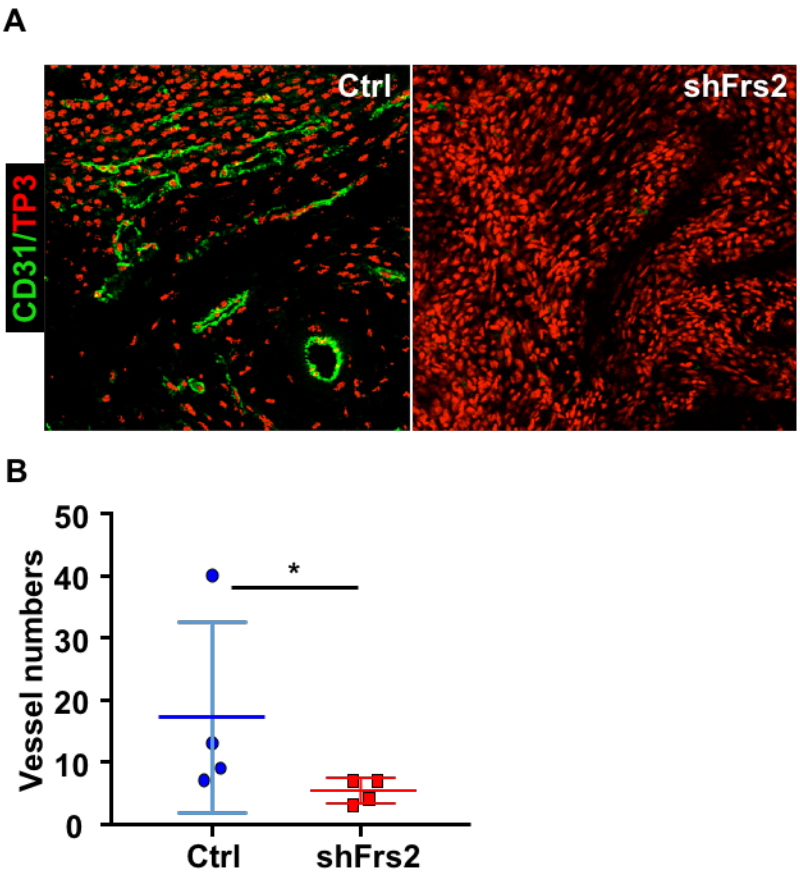


**Fig. 2. 15. Depletion of FRS2α compromises angiogenesis of MDA PCa 118b cell-derived tumors.**

**A.** Immunostaining of tumor sections with anti-CD31 antibodies. **B.** Average percent of CD31 stained areas in randomly viewed areas. Investigators were blinded when assessing the bone lesions and blood vessels. The tumor incidence rates were calculated and expressed as mean ± sd. Ctrl, control virus infected PC3 cells; shFrs2 virus infected PC3 cells *, $P<0.05$.

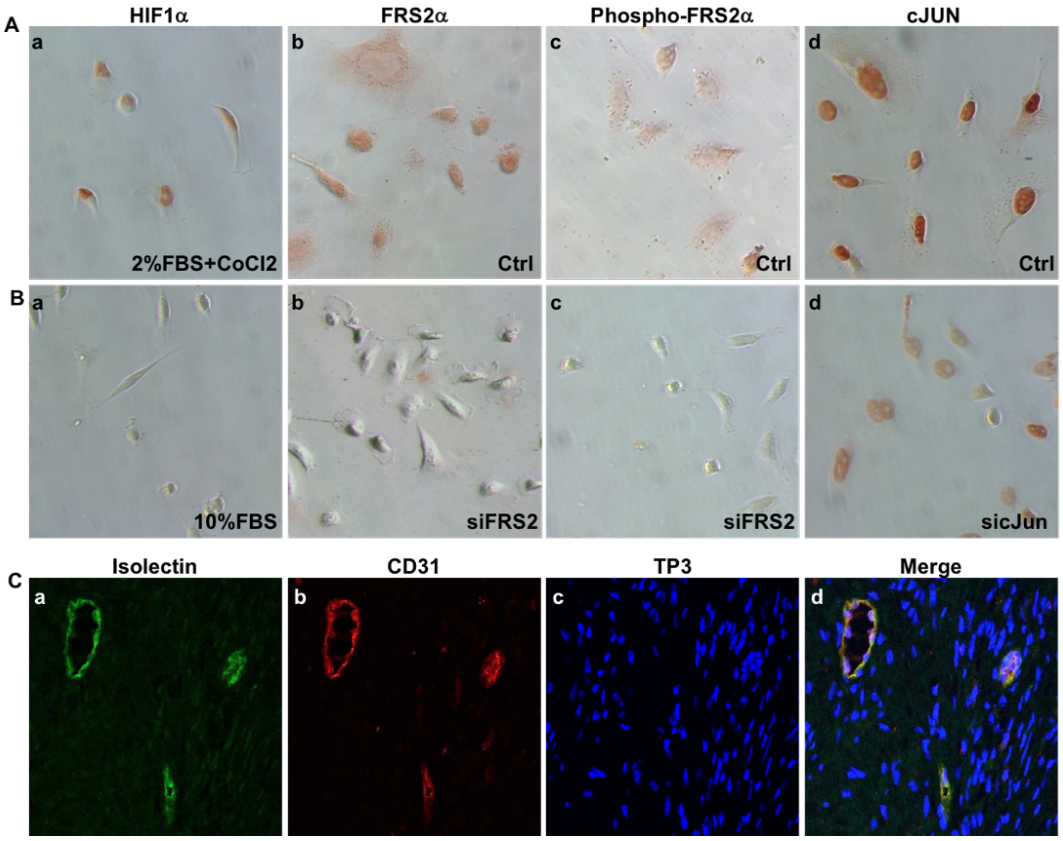


**Fig. 2. 16. Validation of antibodies used for immunostaining.**

**A&B.** Immunostaining of HIF1α, FRS2α, phosphorylated FRS2α, and cJun. Expression of **HIF1α** in PC3 cells was induced by treating the cells with 150 μM $CoCl_2$ in DEMEM containing 2% serum for 24 hours. Untreated cells were used as a negative control for anti-HIF1α antibody. For staining anti-FRS2α, anti-phosphorylated FRS2α, and anti-cJUN, the siRNA depleted cells were used as negative controls. **C**. A human PCa tissue section was co-stained with anti-CD31 antibody and isolectin. The images were captured with a confocal microscope. The data showed that both anti-CD31 and isolectin stained the same areas of the section, indicating that anti-CD31 antibody specifically recognized endothelial cells in the tissue. To-Pro3 (TP3) was used for nuclear counterstaining. Ctrl, control.

### *Overexpression of Frs2α in human PCa is associated with tumor angiogenesis and poor prognosis of PCa patients*

FGFR1 is overexpressed in about 40% of human PCa and forced expression of ectopic FGFR1 in mouse prostate epithelial cells increases tumor angiogenesis. FGF9 promotes VEGF-A expression in LNCaP cells. However, whether aberrant FGF signaling and its key mediator for downstream signaling FRS2α is associated with and contributes to overall tumor angiogenesis in human PCa has not been established. We assessed the clinical relevance of FRS2α expression and its correlation with microvessel density in human PCa by immunohistochemistry with anti-FRS2α and immunostaining with anti-CD31 antibodies. The validation of antibodies was done by using FRS2α, Hif1a and C-JUN small interference RNA (Fig. 2.16). Both analyses were carried out on the same slides from the MGH human prostate tissue microarrays (TMA) that comprised 225 PCa and 27 benign prostate samples (Fig. 2.17). The samples were annotated with detailed patient follow up information, including PSA recurrence, Gleason Scores, pathological stages, patients' age, and survival time. Although only a small group of cases had very strong staining (scores 7–9), the majority of the PCa samples had a score between 4–6. This was higher

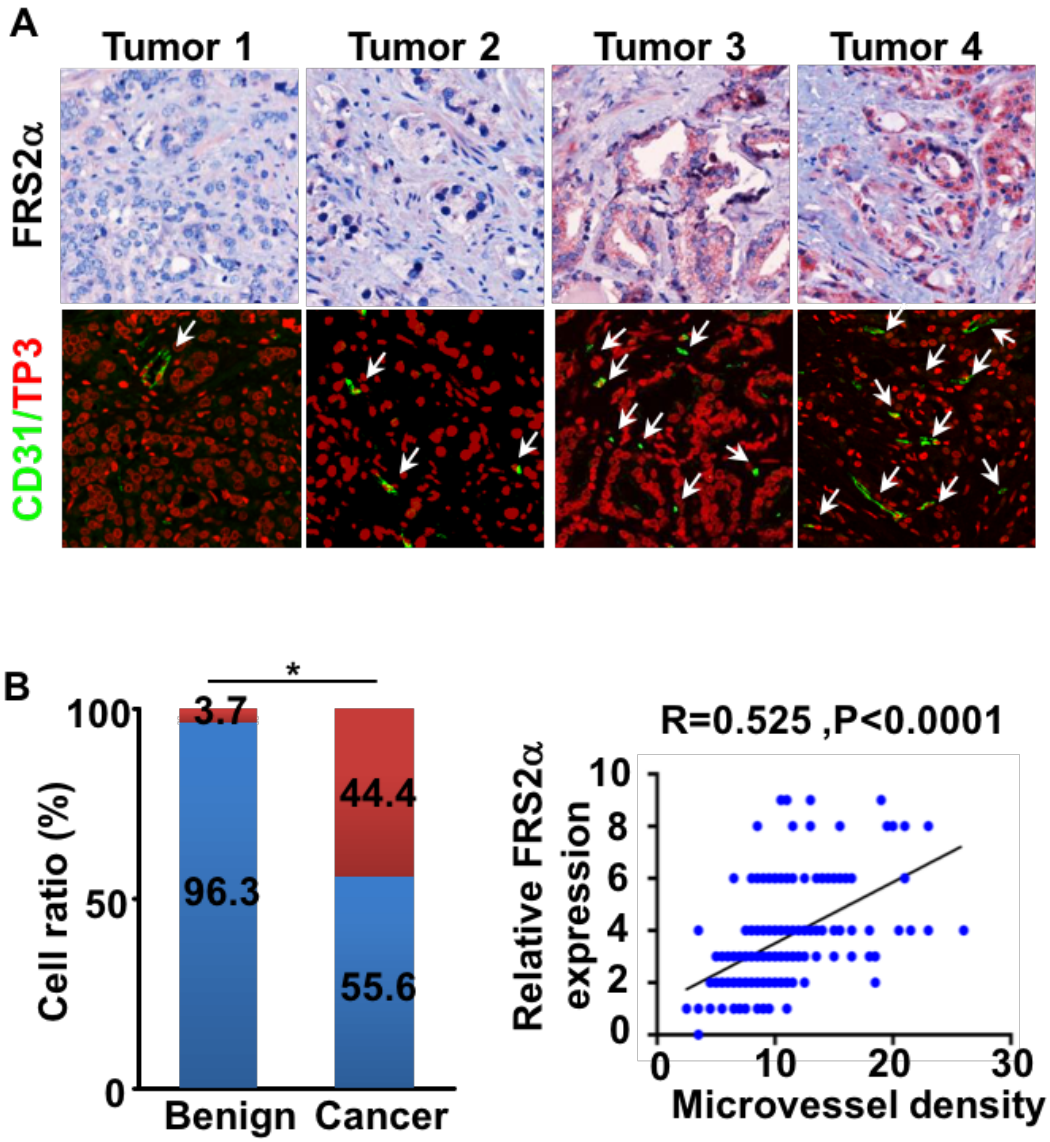


**Fig. 2. 17. Expression and activation of Frs2α in human PCa**

**A.** Representative images of immunochemical staining of FRS2α and CD31 counterstained with nuclear To-Pro3 (TP3) in the MGH PCa TMA. **B.** Statistical comparison of differences in expression of FRS2α in human PCa and benign prostate (left) and Pearson correlation between FRS2α expression and microvessel density determined by CD31 staining (right). Red bar, FRS2α expression score>3; blue bar, FRS2α expression score≤3.

than the expression score in the adjacent non-cancerous tissues (Fig. 2.17 B). In addition, elevated expression of FRS2α was found in PCa with high Gleason scores and in patients with high serum PSA (Fig. 2.18). To determine whether FRS2α expression correlated with the prognosis of PCa patients, the association of FRS2α expression and PCa metastasis, PSA recurrence time, and overall survival time of the 225 patients was analyzed (Fig. 2.17). The data showed that the PSA recurrence-free survival and overall survival time of PCa patients was shorter in the groups exhibiting high FRS2α expression (score >3), compared to the group with low FRS2α expression (score≤3). Furthermore, metastases appeared faster in PCa exhibiting high FRS2α than those with low FRS2α expression. In addition, expression levels of FRS2α positively correlated with microvessel density as determined by CD31 staining (Pearson correlation: $R=0.55$, $P<0.01$).

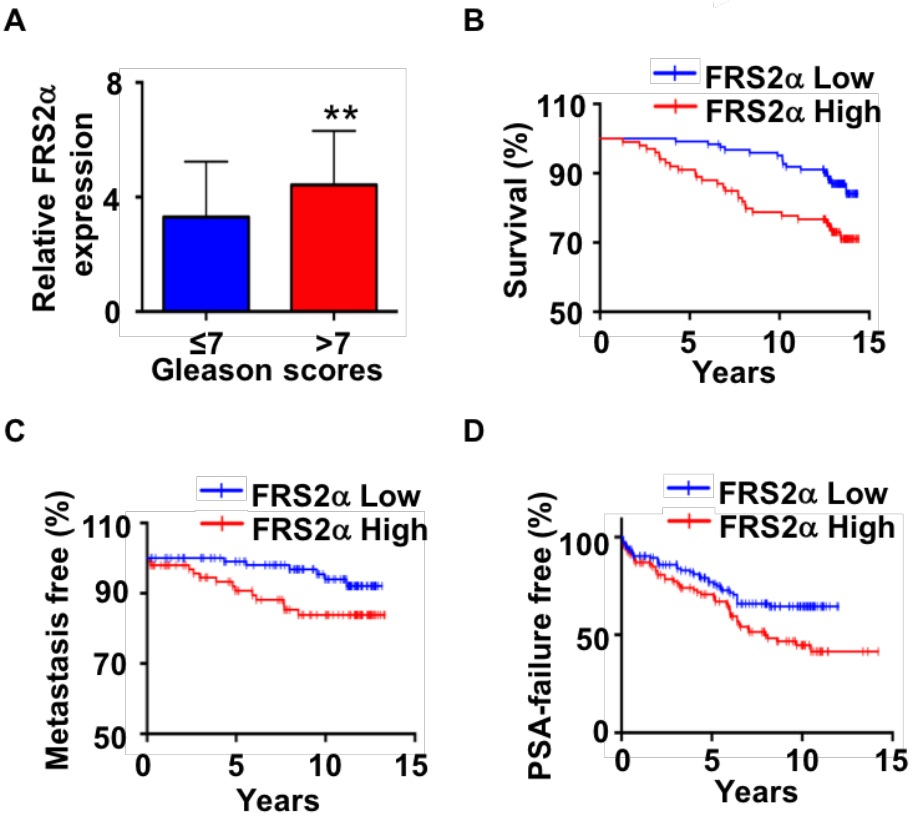


**Fig. 2. 18. High FRS2α expression was observed in patients with high Gleason score and poor prognosis.**

**A.** Statistical analyses of the association of FRS2α expression with Gleason scores. **B.** FRS2α expression predicts overall survival time of the patients. **C.** FRS2α predicts metastasis free survival time of PCa patients. **D.** FRS2α predicts PSA-free survival time.

To further implicate the activity of FRS2α in angiogenesis in human PCa tissues, levels of activity of FRS2α were assessed by immunochemical staining of activated FRS2α (phosphorylated) in a separate PCa TMA. Expression of HIF1α, cJUN, and CD31 were also assessed in the same array. This array included 99 primary PCa and 81 adjacent non- cancerous prostate tissue samples with the pathological features characterized by the vendor (Fig. 2.19). The results showed that phosphorylation of FRS2α was higher in PCa than in benign tissues (2.23±1.78 vs 1.68±1.32, $P<0.02$) and that the expression of cJUN was higher in tumors with Gleason Score ≥7 than in those with Gleason Score ≤7. In addition, the phosphorylation level of FRS2α positively correlated with expression of cJUN ($r=0.358$, $p<0.001$), but not with HIF1α ($r=0.142$, $P=0.164$), and CD31 ($r=0.009$, $P=0.312$).

A

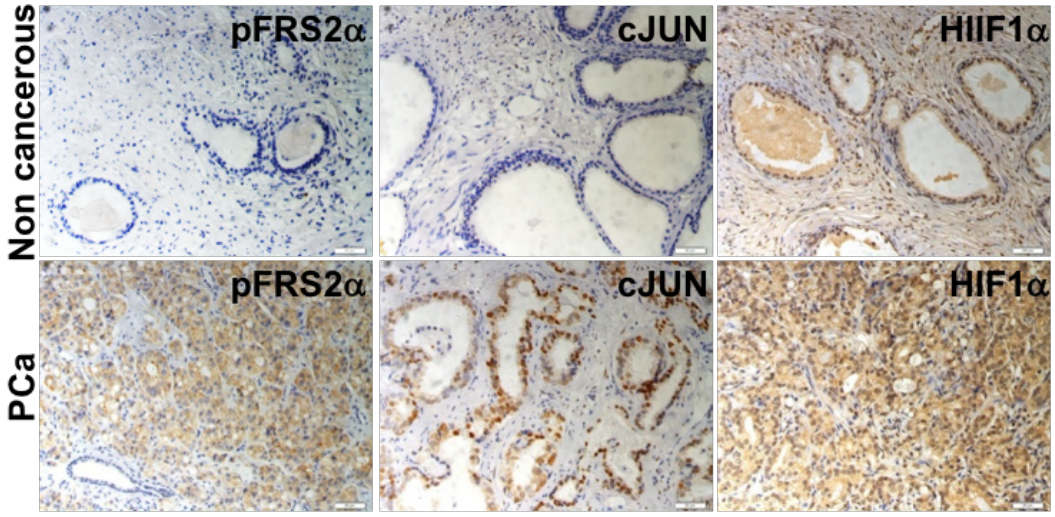


B

| | Taylor dataset | | | | | |
|---|---|---|---|---|---|---|
| | CD31 | | cJUN | | HIF1α | |
| FRS2α | R | P | R | P | R | P |
| | 0.551 | 0.000 | 0.473 | 0.000 | 0.675 | 0.000 |

**Fig. 2. 19. Frs2 is positively associated with CD31, c-JUN and Hif1a in PCa.**

**A.** Representative images of FRS2α phosphorylation and expression of the indicated molecules in PCa TMA (from Shanghai Outdo Biotech Co, LTD). **B.** Statistical analyses of the association between Frs2α and CD31, cJun, or Hif1a expression at the mRNA level in the Taylor dataset. R, Pearson correlation coefficient; P, p value; *, P<0.05

We then further evaluated the correlation coefficients between Frs2α expression and cJun, Hif1α, and CD31 at the mRNA level in the Taylor dataset GSE10645 25. The results showed a positive correlation between FRS2α expression and cJun ($r= 0.473$, $P<0.001$), Hif1a ($r=0.675$, $P<0.001$), and CD31 ($r=0.358$, $P<0.001$) mRNA levels in the PCa tissues that comprise both epithelial and stromal cells. Since microvessel density correlates with poor PCa progression, the data further demonstrated that overexpressed FRS2α in the tumor promotes angiogenesis in PCa and suggest that FRS2α affects the clinical course of human PCa, since microvessel density correlates with poor PCa progression. Together, the data also suggests that the level of FRS2α expression in PCa tissues can serve as a biomarker for predicting outcomes of PCa patients.

## Discussion

In this report, we demonstrated that overactivation of FRS2α-mediated angiogenic signaling was associated with tumor angiogenesis and poor clinical features in human PCa. This included high blood vessel density, high Gleason Score, and high serum PSA. Furthermore, high FRS2α expression correlated with poor outcomes of PCa patients. These included high metastatic rates, shortened time to tumor recurrence and shorter survival times. We also showed that Frs2α underlies the previously established ability of FGF to elicit angiogenic signals. Ablation of *Frs2α i*n prostate epithelial cells reduced VEGF-A expression through downregulating cJUN and HIF1α expression. This was

accompanied by inhibition of tumor angiogenesis and tumor growth in mouse PCa models. Depleting Frs2α expression in human PCa cells also compromised the capability of the cells to recruit endothelial cells both in vivo and in vitro. Our results suggest that overactivation of the Frs2α-mediated angiogenic pathway can be used as a biomarker for PCa diagnosis and prognosis. They also suggest that suppressing Frs2α-mediated angiogenic signaling may be promising for development into a strategy for PCa treatment.

Fgfr1 is overexpressed in about 40% of human PCa and amplification of Frs2α and activation of the FGFR/FRS2α signaling pathway have been shown to be associated with liposarcoma (18,32). It has been reported that although no significant differences in Frs2α and Frs2β expression in small samples of human PCa, double depletion of Frs2α and Frs2β in human PCa cells reduces cell proliferation, migration, and invasion, as well as increase susceptibility to cytotoxic irradiation (33). In this report, we showed data derived from three sample pools that expression and activation of FRS2α were increased in human PCa at the protein level with the MGH PCa TMA, at the activation level with the commercial available PCa TMA, or at the mRNA level based on online datasets. The consistent conclusion derived from both TMA and the online dataset indicates that neither ethnic factors nor detailed screening methods affect the finding that levels of FRS2α are correlated with tumor angiogenesis in human PCa.

The levels of phosphorylation of FRS2α in PCa were higher than adjacent non-cancerous, although the statistical data showed that the difference was moderate. We often found that the FRS2α phosphorylation levels in para-cancer tissues varied significantly. Some areas had a relatively high phosphorylated FRS2α although others had low to undetectable phosphorylated FRS2α. It is possible that the phosphorylation of FRS2α in para-cancer tissues may be affected by PCa in adjacent. In resting adult mouse prostates, expression of FRS2α in luminal epithelial cells is below the detection limit of immunostaining (34). Therefore, it is necessary to assess phosphorylated FRS2α in normal prostate tissues in order to determine whether phosphorylated FRS2α can be used as a biomarker for PCa diagnosis and prognosis. Nevertheless, the data here demonstrated that overactivation of FRS2α-mediated angiogenic signaling is associated with the malignance of prostate lesions and poor prognosis for patients bearing PCa.

Furthermore, the results were consistent with the report that Fgfr1 is overexpressed in PCa and that overexpression of FGF9 increases VEGF-A expression in LNCaP cells and predicts bone metastasis and poor prognosis of PCa (35,36). It has been shown that overexpression of FGFR1 in mouse prostate epithelial cells is oncogenic and that the ectopic FGFR1 signaling promotes tumor angiogenesis (37). In addition, expression of constitutively active mutant of FGFR1 also increases *Vegf1* expression and angiogenesis in hepatocellular carcinoma (38). However, whether FRS2α is required to mediate

the angiogenic signals elicited by FGFR1 has not been reported. Our results not only confirm the tumor angiogenic roles of ectopic FGF signaling, but also unravel its underlying mechanism. This shines new light on the potential for development of new PCa treatments based on disrupting the FRS2α-mediated tumor angiogenic signaling axis.

Depleting FRS2α in PCa cells reduced recruitment of endothelial cells to tumors via secreted factors. This suggests that FRS2α-mediated signals in tumor cells are involved in communication of tumor cells with host cells in the tissue microenvironment. The results are consistent with our recent report that human PCa cells induce host bone cells to overexpress FGF2 and FGFR1, suggesting that the FGF axis mediates a synergistic interaction between PCa cells and bone cells in the tumor metastasis microenvironment to support PCa growth in bone metastasis (39). Since PCa cells overexpress FGFR1 that is activated by FGF2, the host cell expressed FGF2 in turn activates PCa FGFR1 and thus, will also enhances the angiogenic activity of PCa cells mediated by the FRS2α pathway. We further demonstrated here that depletion of FRS2α in MDA PCa 118b cells reduced tumorigenesis in the bone as well as reduced blood vessel density in the prostate tumors hosted by bone (Fig. 2.15). The results further indicated the importance of FRS2α-mediated signals in the crosstalk between PCa and host cells in the bone microenvironment.

The Vegf-a promoter region contains multiple consensus binding sites, which

include SP1/SP3, AP1, AP2, Egr1, STAT3, and HIF1α (40,41). Although SP1 and AP2 can serve as downstream signaling molecules in the FGF pathway, overexpression of both AP2 and SP1 failed to restore the expression of VEGF-A in FRS2α-depleted PCa cells. This suggests that these two transcription factors are not sufficient to mediate angiogenic signals of the FRS2α pathway. Moreover, ablation of *Frs2α* did not affect expression of the two transcription factors. The results suggest that other upstream regulators may also control VEGF-A expression via these transcription factors. Future efforts are needed to characterize the upstream regulators for SP1 and AP2 for VEGF-A expression.

In summary, we report here that FRS2α-mediated signals contribute to PCa angiogenesis and depletion of FRS2α expression suppressed PCa tumor angiogenesis and tumor growth. Since FRS2α is a major mediator of the FGFR1 signaling complex at the intracellular membrane boundary, it likely accounts for the effects of overactive tumor FGFR1 on tumor angiogenesis. Furthermore, overactivation of the FRS2α signaling pathway was associated with blood vessel density and pathological features of human PCa. The results suggest that suppressing the FRS2α-mediated pathway is of therapeutic value for PCa therapies and that the overactivated FRS2α signaling pathway is a potential biomarker for PCa diagnosis.

# CHAPTER III

# ABERRANT FIBROBLAST GROWTH FACTOR (FGF) SIGNALING REPROGRAMS PCA CELL METABOLISM THROUGH STABILIZING LACTATE DEHYDROGENASE A AND REPRESSING THE EXPRESSION OF LACTATE DEHYDROGENASE B

## Introduction

Metabolic reprograming from the oxidative phosphorylation to the aerobic glycolysis is a common event in cancer progression, which provides building blocks to meet the rapid growth of cancer cells. Aerobic glycolysis results in glucose consumption and Lactate accumulation in the tumor microenvironment, which suppress the infiltration of lymphocytes to the tumor and compromises the effects of anti-tumor immunotherapies. In line with these, the glycolytic phenotype is also associated with prostate cancer (PCa) progression and aggressiveness (21,42-47). The molecular mechanism by which cancer cells reprogram their metabolism is not clear. Understanding how tumor cells reprogram their metabolism from oxidative phosphorylation to aerobic glycolysis will provide a novel venue to inhibit aerobic glycolysis selectively in tumor cells.

The prostate consists of epithelial and stromal compartments that are separated by basement membranes. Cells in the two compartments maintain active two-way communication through paracrine mechanisms, including the fibroblast growth factor (FGF) signaling in which FGF and FGF receptors (FGFR) are partitioned

between the two compartments (48). These precisely balanced two-way communications are critical for preserving the tissue homeostasis and function of the prostate. The FGF family consists of 18 receptor-binding polypeptides that exert their regulatory signals by activating the FGFR tyrosine kinases encoded by four highly homologous genes (49-53). Both FGF and FGFR are expressed in a spatiotemporal- and cell type-specific pattern, important for controlling embryonic development, and maintaining tissue homeostasis and function.

Extensive evidence shows that abnormal expression of FGF or FGFR isoforms and activation of the FGF/FGFR signaling axis are associated with PCa development and progression (53-59). Amplification of the Fgfr1 gene is frequently found in human PCa (60). The acquisition of ectopic expression of FGFR1 in tumor epithelial cells stands out as the most remarkable change among FGFR isotypes (61-64). Forced expression of FGFR1, FGF2, FGF8, FGF9 and FGF10 induces prostate lesions in mouse models (36,58,61,64-69). On the other hand, ablation of *Fgfr1* or *Frs2*$\alpha$ significantly reduces PCa development and progression induced by T antigens (57,70). However, the mechanism by which aberrant FGF signals contribute to PCa progression is still not fully understood. FGF signaling promotes aerobic glycolysis by increasing expression of HK2 and tyrosine phosphorylation of multiple enzymes in the aerobic glycolysis (9). However, whether aberrant FGF signaling contributes to PCa progression by promoting aerobic glycolysis remains to be determined.

The last step of glycolysis is the reduction of pyruvate to lactate. It is a reversible

conversion catalyzed by lactate dehydrogenase (LDH). It is a tetrameric enzyme composed of two types of subunits, designated as LDHA or LDHB. The combination of these two subunits yields 5 isozymes, which catalyzes the conversion of pyruvate to lactate. LDH1, which is composed of 4 LDHB subunits favors the conversion from lactate to pyruvate and allows oxidation along the pathway of the tricarboxylic acid cycle, whereas LDH5, which is composed of 4 LDHA subunits favors the conversion from pyruvate to lactate and allows the glycolytic pathway to be completed at lactate (71). Emerging evidence shows that LDHA is required for survival and proliferation of cancer cells. Although still debatable, current data seem to indicate the association of reduced levels of LDHB with an increased malignancy of PCa and other cancers (43,72-83). Targeting lactate metabolism has been proposed for cancer therapeutics (84,85). LDHA in cancer is mainly tyrosine phosphorylated and increased activity of LDHA was believed to associate with its phosphorylation (83).

It has been reported that FGFR1 phosphorylates LDHA at multiple tyrosine residues, which enhances the formation of tetramers and binding of NADH and therefore, the enzymatic activity of LDHA (86). In this report, we demonstrate that FGFR1 signaling promoted aerobic glycolysis via stabilizing LDHA and downregulating LDHB expression via inducing Ldhb promoter hypermethylation. Ablation of LDHA compromised, whereas ablation of LDHB enhanced, the tumorigenicity of DU145 cells. Furthermore, high levels of phosphorylated LDHA and low levels of LDHB in human PCa tissues was associated with short time to

biochemical recurrence and decreased patient survival time. Together, it suggests that aberrantly expressed FGFR1 tyrosine kinase in PCa induces metabolic changes via altering the ratio of LDHA and LDHB, which promotes PCa growth and progression. Furthermore, high levels of phosphorylated LDHA and high expression of LDHB are the potential biomarkers for PCa diagnosis and prognosis.

## Materials and Methods:

### *Animals*

Mice were housed under the Program of Animal Resources of the Institute of Biosciences and Technology in accordance with the principles and procedure of the Guide for the Care and Use of Laboratory Animals. All experimental procedures were approved by the Institutional Animal Care and Use Committee. Mice carrying loxP-flanked *Frs2$\alpha$, Fgfr1,* and *Fgfr2* alleles were bred and genotyped as described (56,87-89). For xenograft studies, wild type, LDHA or LDHB knockout DU145 cells ($2X10^6$) were mixed with Matrigel (BD) at a 1:1 ratio before subcutaneously injection into flanks of nude mice (6 weeks old). The tumor volume was measured with a caliper and calculated as following: volume= (length) X $(width)^2$ X 0.52. The xenografts and other tissues were harvested after the animals were euthanized by $CO_2$ asphyxiation. The tumors were weighed and photographed before being subjected to molecular and cellular analyses.

### *Histology*

Prostate and xenografts were fixed with 4% paraformaldehyde-PBS solution for 2 hours at 4 °C . The tissues were serially dehydrated, embedded in paraffin, and sectioned at 5 μm thickness as described (14). For general histology, slides were re-hydrated and stained with hematoxylin and eosin (H&E). For immunostaining, the antigens were retrieved by boiling in citrate buffer (10 mM, pH 8.0) for 20 minutes. The rabbit anti-pLDHA (1:200) and anti-LDHA (1:200) were purchased from Cell Signaling Technology (Beverly, MA). Mouse anti-LDHB (1:200), rabbit anti-CD31 (1:200), rat anti-F4/80 (1:200) and rabbit anti-Ki67 (1:200) were purchased from Abcam (Cambridge, MA). Fluorometric TUNEL assay kit was purchased from Promega (Fitchburg, WI). The ExtraAvidin Peroxidase System (Sigma) and fluorescence-conjugated secondary antibodies (Invitrogen) were used to visualize specifically bound antibodies. For the immunofluorescence staining, the nuclei were counter stained with To-Pro 3 before being observed under a confocal microscope (Zeiss LSM 510).

For expression of LDHA, LDHB, and Fgfr1, as well as phosphorylated LDHA in human PCa, the Massachusetts General Hospital (MGH) PCa TMA was used. It includes 240 consecutive patients with PCa who underwent radical prostatectomy at the MGH from September 1993 to March 1995 (90). Two experienced pathologists independently scored the results without being given

any information on the samples. Only epithelial staining was counted. The scores were compared, and discrepant scores were subjected to re-examining by both individuals to achieve a consensus score. Immunostaining of PCa and stromal cells was evaluated separately. The percentage of positive cells was calculated and categorized as follows: 0, 0 %; 1, 1–10 %; 2, 11–50 %; 3, 50 - 75%; and 4, 75-100%. The staining intensity was visually scored and defined as 0, negative; 1, weak; 2, moderate; and 3, strong. Final immunoreactivity scores (IRS) were calculated for each case by multiplying the percentage and the intensity score.

***Western blotting***

DU145 cells, MEFs, and xenografts were homogenized in RIPA buffer (50 mM Tris-HCl buffer pH 7.4, 1% NP40, 150 mM NaCl, 0.25% Na-deoxycholate, 1 mM EGTA, 1 mM PMSF), and the extracted proteins were harvested by centrifugation. Samples containing 30 μg proteins were separated by SDS-PAGE and electroblotted onto PVDF membranes for Western analyses with the indicated antibodies. The anti-phosphorylated ERK1/2 (1:1000), anti-phosphorylated AKT (1:1000), anti-ERK1/2 (1:1000), anti-AKT (1:1000), anti-phosphorylated Frs2αα (1:000), and anti-HA (1:1000) antibodies were purchased from Santa Cruz Biotechnology (Santa Cruz, CA). Anti-phosphorylated LDHA (1:1000), anti-LDHB (1:1000), anti-LDHA (1:1000) antibodies, and The Glycolysis Antibody Sampler Kit containing anti-HK1, PFKP,

PFKP2, PFKP3, Aldolase, PGAM, PKM1/2, and pyruvate dehydrogenase antibodies were purchased from Cell Signaling Technology (Danvers, MA). The anti-phosphotyrosine 4G10 (1:1000), anti-TET1, (1:1000); and anti-Flag (1:1000) antibodies were from Millipore Sigma (Danvers, MA). After being washed with TBST buffer to remove nonspecific antibodies, the membranes were then incubated with the horseradish peroxidase conjugated rabbit antibody (1:10000) at room temperature for 1 hour. The specifically bound antibodies were visualized by using the ECL-Plus chemoluminescent reagents. The films were scanned with a densitometer for quantitation.

***RNA expression***

Total RNA was isolated from cells and tissues using the Ribopure RNA isolation reagent (Ambion, TX). Reverse transcription was carried out with SuperScript III (Life Technologies, Grand Island, NY) and random primers according to manufacturer's protocols. Real-time PCR analyses were carried out using the Fast SYBR Green Master Mix (Life Technologies) as instructed by the manufacturer. Relative abundances of mRNA were calculated using the comparative threshold (CT) cycle method and were normalized to β-actin as the internal control. The mean±sd among at least three individual experiments are shown. The primer sequences are listed in Table 2.

**Table 2. Primers of metabolism related genes**

| Gene Name | | Sequence (from 5'-3') |
|---|---|---|
| human-Ldha | forward | ACATCCTGGGCTATTGGACT |
| | reverse | TTCTTCAAACGGGCCTCTTC |
| human-Ldhb | forward | GTGAATGTGGCAGGTGTTTC |
| | reverse | ACCATTGTTGACACGGGATG |
| Gene Name | | Sequence (from 5'-3') |
| human-Gapdh | forward | GAAGGTCGGAGTCAACGGATT |
| | reverse | TGACGGTGCCATGGAATTTG |
| mouse-Tet1 | forward | GAGCCTGTTCCTCGATGTGG |
| | reverse | CAAACCCACCTGAGGCTGTT |
| mouse-Tet2 | forward | AACCTGGCTACTGTCATTGCTCCA |
| | reverse | ATGTTCTGCTGGTCTCTGTGGGAA |
| mouse-Tet3 | forward | TCCGGATTGAGAAGGTCATC |
| | reverse | CCAGGCCAGGATCAAGATAA |
| mouse-Ldha | forward | CTGAGAGCATAATGAAGAACC |
| | reverse | CACAACATCCGAGATTCCA |
| mouse-Ldhb | forward | ATTCACCCCGTGTCTACCAT |
| | reverse | TCTGATTGATGACGCTGGTC |
| mouse-Fgfr1 | forward | AGCATCAACCACACCTACCAGCT |
| | reverse | ATCCGCAGCCTCACATTCAG |
| mouse-Fgfr2 | forward | GGAGCCTTATTATGGAAAGTGTGG |
| | reverse | GGGAAGCCGTGATCTCCTTCTCT |
| mouse-Frs2 | forward | GAGCTGGAAGTCCCTAGGACACCT |
| | reverse | GCTCTCAGCATTAGAAACCCTTGC |
| mouse-β-actin | forward | GCACCAAGGTGTGATGGTG |
| | reverse | GGATGCCACAGGATTCCATA |

***Gene ablation***

The lentivirus based CRISPR-Cas9 system was used to ablate Ldha, Ldhb, and Fgfr1 alleles in DU145 cells. The sequences of the sgRNAs are: Ldha: AAGCTGGTCATTATCACGGC; Ldhb: GGACTGTACTTGACGATCTG; and Fgfr1: AACTTGTTCCGATGGTTATC. Two days after infection of the lentivirus, the cells with were selected by growing in the medium containing 2 μg/ml puromycin.

***Mutagenesis of LDHA***

We used a QuikChange Lightning Multi Site-Directed Mutagenesis Kit, purchased from Agilent Technologies (Santa Clara, California), to create LDHA mutant plasmids. Primer sequences that were used to generate mutants are as follows (from 5' to 3'): Y10F, CTAAAGGATCAGCTGATTTTT AATCTTCTAAAGGAAGAA; Y83F, GATTGTCTCTGGCAAAGACTTTAATGTAACTGCAAACTCC; Y172F, GATTGTCTCTGGCAAAGACTTT AATGTAACTGCAAACTCC, Y239F, CAGGTGGTTGAGAGTGCT TTTGAGGTGATCAAACTCAAA.

***NMR analyses***

The cells ($2 \times 10^7$) were suspended in 450 μl methanol /chloroform (2:1) and lysed by ultrasound. The lysates were mixed with 450 μl chloroform/$H_2O$ (1:1).

The supernatants were collected and lyophilized. The cell extracts were then resuspended in 500 µl $D_2O$ containing 0.25 mM sodium trimethylsily 1 propionate-d4. After centrifugation, the supernatant was transferred to 5-mm NMR tubes. All NMR spectra were recorded at 25°C on a Bruker AVANCE III 600 MHz NMR spectrometer equipped with a triple resonance probe and a z-axis pulsed field gradient. $^1$H NMR spectra were acquired using a one-dimensional NOESY pulse sequence with water suppression during the relaxation delay of 4 s and a mixing time of 150 ms. 128 free induction decays were collected into 32 K data points with a spectral width of 12,000 Hz, an acquisition time of 2.66 s. FID was zero-filled to 64 K prior to Fourier transformation.

***MeDIP***

Genomic DNA of WT and fgfr1/fgfr2/frs2 triple knockout mouse embryonic fibroblasts ($MEF^{\Delta F}$) were isolated with the Qiagen Kit and ultrasound sheared into smaller fragments (200-600 bp). The sheared gDNA was denatured by incubation in 1M NaOH/25mM EDTA at 95°C for 12 minutes. The denatured DNA was incubated with anti-5mc antibodies and then mixed with pre-equilibrated protein G dynabeads. The immunocomplexes were mixed with 250 µl proteinase K buffer and 2 µl 20 mg/ml proteinase K (Roche 03115852001), shaken vigorously at 50 °C for 3 hours. The bound 5-mc containing DNA was then purified with phenol:chloroform:isoamyl alcohol (25:24:1) (Sigma) and

chloroform:isoamyl alcohol (24:1) (Sigma). The purified DNA was used for making the sequencing library with the NEB (E6240S) library prep kit, and sequence by the Agrilife Genomics and Bioinformatics Service, Texas A&M University.

***Sodium bisulfite DNA sequencing***

Genomic DNA was isolated using the Qiangen Genomic DNA Kit, followed by bisulfite conversion using the EpiJET Bisulfite Conversion Kit (Thermo Scientific). Bisulfite specific primers for the PCR amplification were 5'-GAGGGTTGTAAATATTAGTAAGTGATTA-3' (sense) and 5'-ACCAAATTAACCTTAAACTCAAAAAC-3' (antisense). The PCR products contained 6 CpG sites and were expected to be 136bp. The amplicons were then cloned into pDrive Cloning Vectors (Qiangen). Plasmid DNA extracted from each clone was then sequenced. The methylation of each CpG site was determined by comparison with the sequence of the LDHB promoter counterparts.

***Protein stability assay***

Stable transfectants of MEFs expressing HA-tagged LDHA were treated with cycloheximide for the indicated times. The abundance of LDHA was examined by Western blot. The relative level of endogenous or HA-tagged LDHA was quantitated with the Image J.

***Lentivirus plasmids transfection***

$8x10^5$ 293T cells on 6cm dish were planted one day before transfection with 3ml medium for each dish. Two tubes were prepared for each group. The composition of transfection reagents is as follows. Tube 1 contained 200ul DMEM serum free medium 20ul Fugene6 and tube 2 contained 200ul DMEM serum free medium with 5ug shRNA plasmids, 5ug Pspax2, and 2.5ug PMD2G. Tube 1 and tube 2 were mixed together and vortexed at room temperature for 25mins prior to being added to the surface of 293T cells.

***Statistical analysis***

Statistical analysis was performed using the two tailed t test, with significance set to $P<0.05$. Error bars indicate standard deviation.

## Results

***Ablation of the FGF signaling axis reduced glycolysis and increased oxygen consumption in mouse embryonic fibroblasts (MEF).*** FGFR1 has been report to promote LDHA activity by tyrosine phosphorylating LDHA (86). To investigate the role of FGF signaling in cell metabolism, we generated MEFs that are devoid of *Fgfr1*, *Fgfr2*, and *Frs2*$\alpha$ by infecting MEFs bearing floxed *Fgfr1*, *Fgfr2*, and *Frs2*$\alpha$ alleles with adenovirus carrying the Cre-GFP coding sequence. The cells did not respond to FGF2 with respect to activating

downstream signaling molecules and were designated as $MEF^{\Delta F}$ (Fig. 3.1). Western blot analyses revealed that, compared with parental MEF, the expression of LDHA protein was reduced and the expression of LDHB was increased at the protein levels in $MEF^{\Delta F}$ cells.

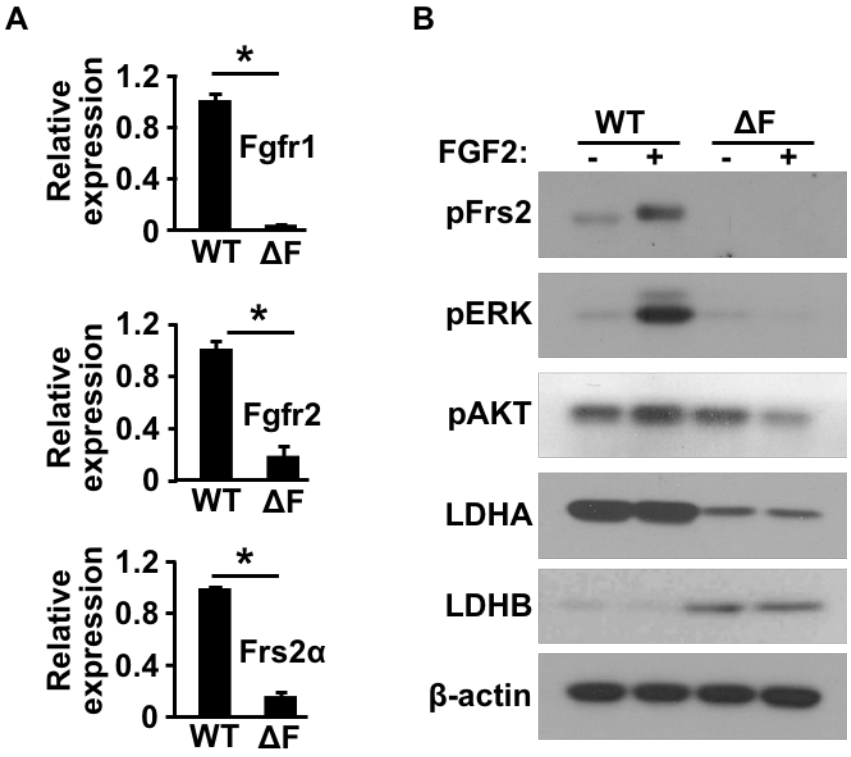


**Fig. 3. 1. FGF signaling deletion decreased LDHA but increased LDHB expression.**

**A.** Real-time RT-PCR analyses showing *Fgfr1, Fgfr2* and *Frs2*$\alpha$ knockout efficiency. **B.** Western blot showing ablation of FGF signaling reduced LDHA expression and increased LDHB expression. WT, wildtype; Ctrl, control; ΔF, $MEF^{\Delta F}$; *, P<0.05.

However, real-time RT-PCR revealed that the expression of *ldha* was not changed whereas the expression of *ldhb* was increased at the mRNA level (Fig. 3.2 A). The results suggest that FGF signaling promotes LDHA expression at the protein level and LDHB at the mRNA level. LDHA displays a higher affinity for pyruvate than LDHB, therefore, LDHA primarily drives the production of lactate and NAD+ whereas LDHB favors the production of pyruvate and NADH (71). To determine whether abrogation of the FGF signaling axis in MEF changed cell metabolism, we compared the lactate production and oxygen consumption in MEF and $MEF^{\Delta F}$ (Fig. 3.2 B). The results demonstrated that abrogation of FGF signaling in MEF reduced lactate production and increased the oxygen consumption rate (OCR).

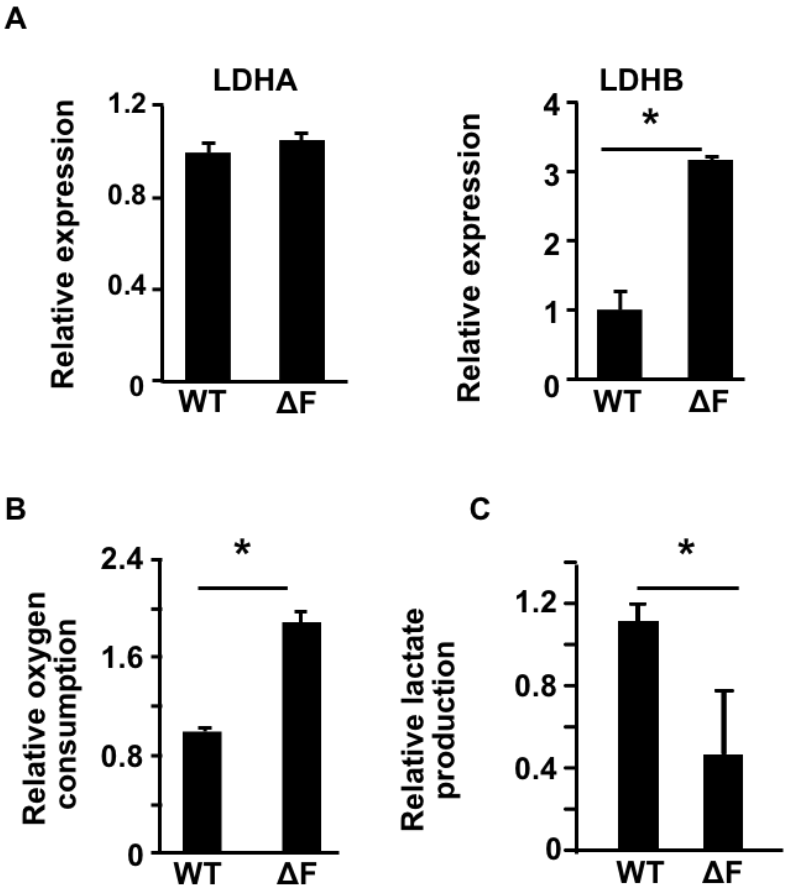


**Fig. 3. 2. Ablation of FGF signaling increased oxygen consumption of MEFs.**

**A.** Real-time RT-PCR showing ablation of FGF signaling increased LDHB mRNA expression but did not change LDHA transcripts. **B.** Ablation of FGF signaling decreased the oxygen consumption rate of control and knockout MEFs. **C.** FGF deletion increased the lactate production of MEFs. WT, wildtype; Ctrl, control; ΔF, $MEF^{\Delta F}$; *, $P<0.05$.

In addition, NMR analysis also revealed that the concentration of isoleucine, valine, and acetate was reduced and the concentration of glutamate, glutamine, succinate, and glutathione was increased in $MEF^{\Delta F}$ (Fig. 3.3). Notably, isoleucine and valine were decreased in $MEF^{\Delta F}$, suggesting that the synthesis of branched chain amino acids (BCAAs) was disrupted in MEFs that lost FGF signaling (Fig. 3.3). The dysregulation of BCAAs synthesis in MEFs lacking FGF signaling is in line with evidence that BCAAs promotes glucose uptake (91). The results further demonstrate changes in cell energy metabolism from aerobic glycolysis to oxidative phosphorylation in $MEF^{\Delta F}$. Thus, it suggests that the cell energy metabolism in MEFs is regulated by FGF signaling. FGF signaling might regulate BCAAs through unique mechanism. More studies are needed to address how FGF regulates the BCAA pathway.

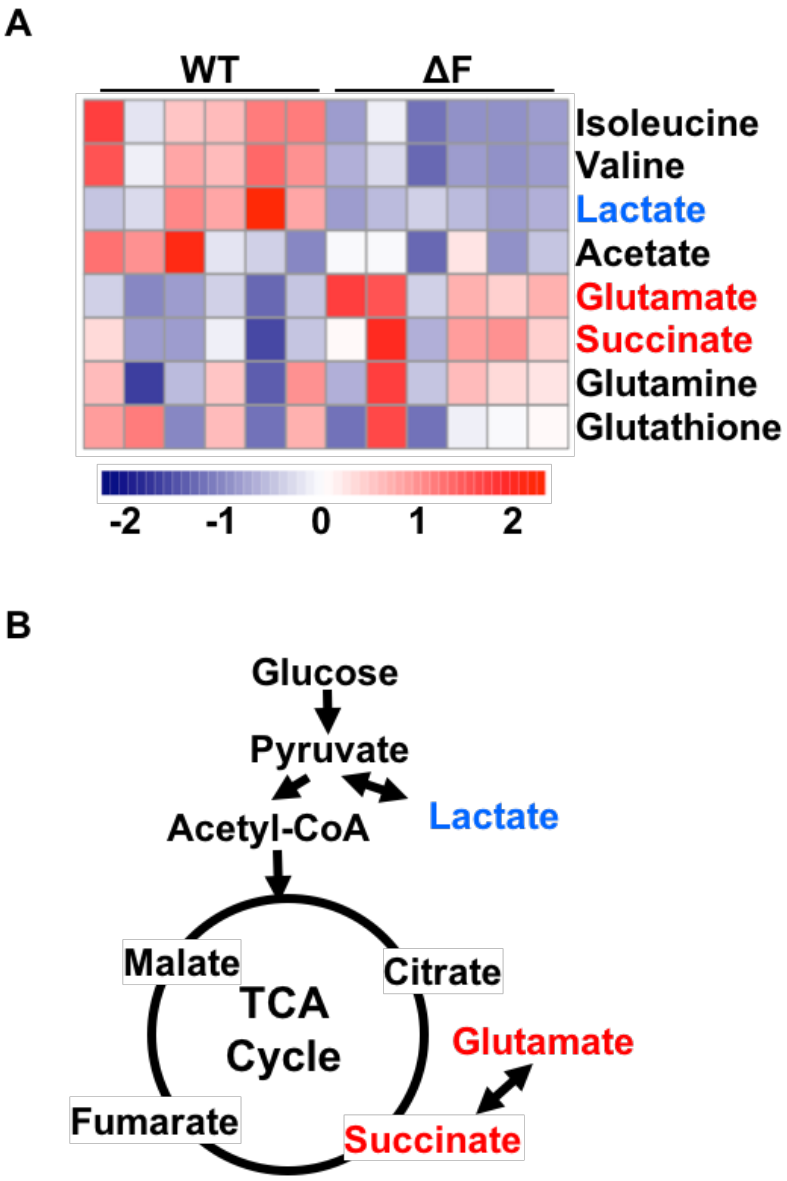


**Fig. 3. 3. Ablation of FGF signaling decreased aerobic glycolysis.**

NMR analysis demonstrated metabolite changes in $MEF^{\Delta F}$ cells. Relative glucose uptake and lactate production of MEFs with or without ablation of the FGF signaling axis. WT, wildtype; Ctrl, control; ΔF, $MEF^{\Delta F}$; *, $P<0.05$.

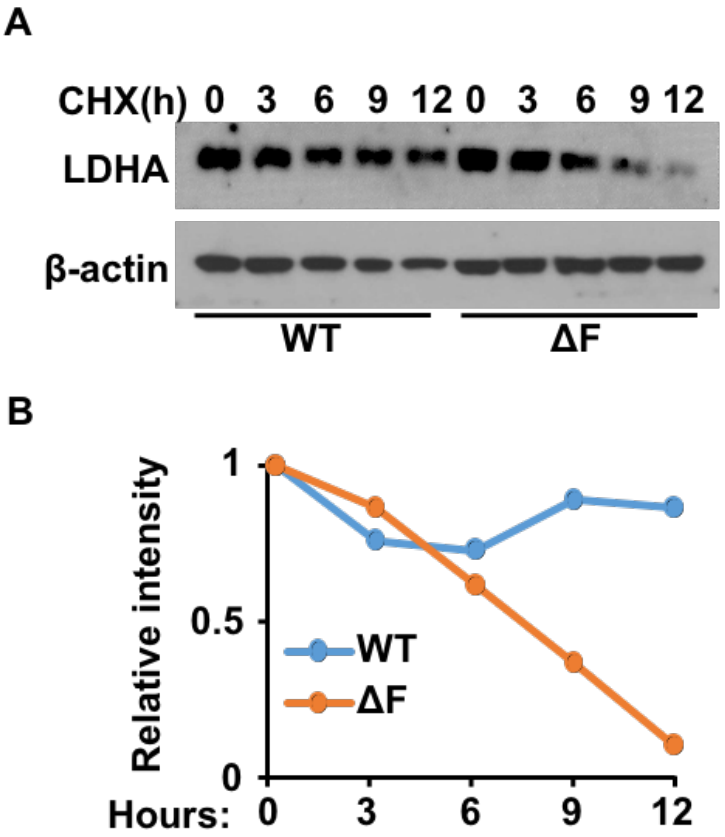


**Fig. 3. 4. Knockout of FGF signaling enhanced degradation of LDHA.**

**A.** MEFs and MEF$^{\Delta F}$ were treated with cycloheximide for 0, 3, 6, 9, 12 h. Endogenous LDHA protein levels were determined by Western blot. **B.** Intensity of LDHA relative to β-actin were determined using Image J.

***FGFR1 enhanced the stability of LDHA by tyrosine phosphorylation.***

To determine the role of FGFR1 in regulating LDHA at the protein level, the MEF and MEF$^{\Delta F}$ cells were treated with cycloheximide to block the protein synthesis. Western blot revealed that the abundance of LDHA protein in MEF$^{\Delta F}$ declined faster compared with that in parental MEFs (Fig. 3.4). The results indicate that the halflife of LDHA is shorter in MEF$^{\Delta F}$ than in parental MEFs, suggesting that the stability of LDHA was promoted by FGFR1. In line with a previous report (86), Western blot with the anti-phosphotyrosine antibody 4G10 demonstrated LDHA was tyrosine phosphorylated (Fig. 3.5). LDHA has four tyrosine phosphorylation sites (86). To identify which tyrosine phosphorylation sites were involved in regulating LDHA stability, site-direct mutagenesis was employed to generate LDHA mutants that had each individual mutation or double mutation, or quadruple mutations as indicated in Fig. 3.5 A. The results showed that only the 4F mutant was not phosphorylated by FGFR1 kinase. Other mutations only partially reduced the phosphorylation, confirming the previous report that all four tyrosine residues were phosphorylated by FGFR1 kinase. Interestingly, the stability of the four individual tyrosine phosphorylation sites did not affect the stability of LDHA. The two 2F mutants had a shorter half-life compared with the wildtype. However, the 4F mutant showed a statistically significant reduction in stability (Fig. 3.6). The results indicate that phosphorylation of the four tyrosine residues promotes the stability of LDHA.

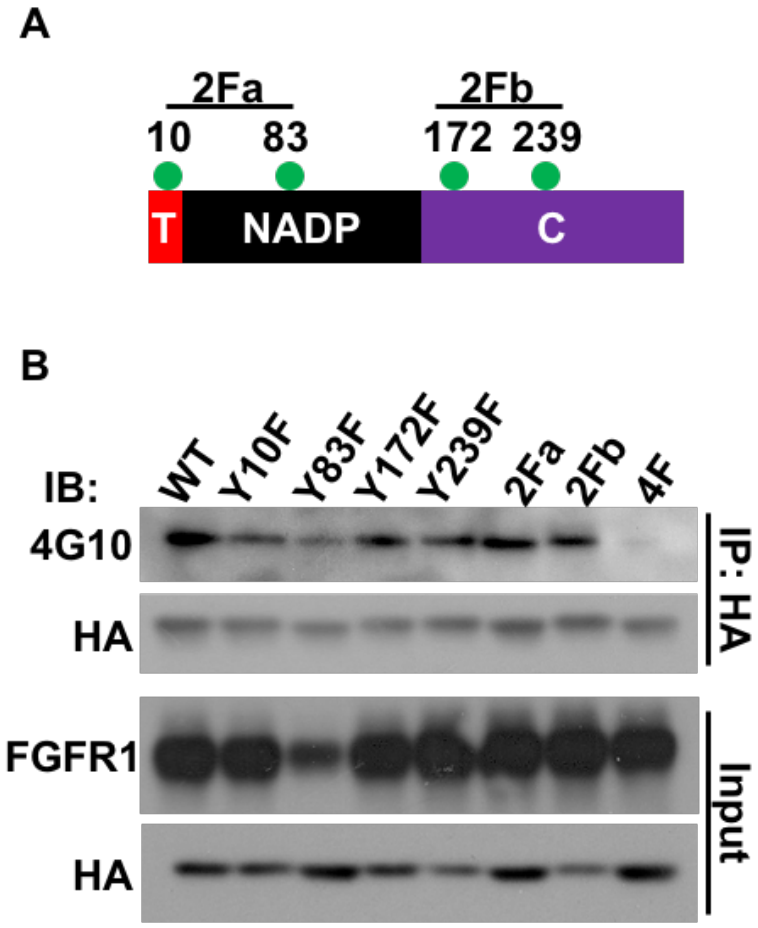


**Fig. 3. 5. Tyrosine phosphorylation suppressed degradation of LDHA.**

**A.** The structure domains and phosphorylation of LDHA. Green dots indicate the tyrosine phosphorylation sites. **B.** HA tagged wildtype or mutant LDHA were expressed in 239T cells with FGFR1.4F, all four tyrosines were changed to phenylalanine. IP, immunoprecipitation; IB, immunoblot; T, region for tetramer formation; NADP, NAD(P) biding domain; C, C-terminal domain; 4G10, anti-phosphotyrosine antibody 4G10.

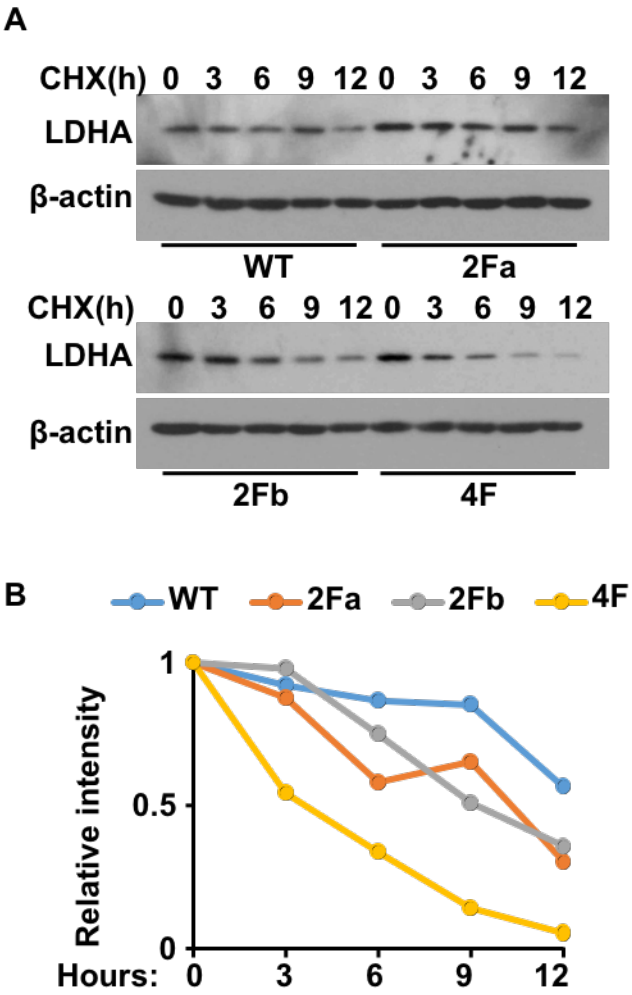


**Fig. 3. 6. Tyrosine phosphorylation stabilizes LDHA protein.**

**A.** MEFs stably expressing wildtype or mutant LDHA were treated with CHX for 0, 3, 6, 9, 12h. The levels of LDHA were determined with Western blot. **B.** The relative intensity of LDHA against β-actin was plotted. 2Fa, Y10F/Y83F mutation; 2Fb, Y172/Y239 mutation; 4F, Y10F/Y83F/Y172/Y239 mutation. IP, immunoprecipitation; IB, immunoblot.

***FRS2α interacts with LDHA independent of LDHB.***

Since FGFR1 phosphorylates LDHA through direct interaction with it (86), we hypothesize that FRS2α, an adaptor protein of FGF receptors, can also interact with LDHA. Therefore, we generated plasmids that express FRS2α or LDHA. Wildtype 293T cells and 293T cells lacking LDHB were co-transfected with FRS2α and LDHA simultaneously. We used anti-LDHA antibodies to pull down the LDHA protein complex, which was followed by immunoblotting of anti-FRS2α antibodies. The data showed a strong interaction between FRS2α and LDHA, and LDHB deletion did not affect the binding between LDHA and Frs2α (Fig. 3.7). These data suggest that FRS2α directly interacts with LDHA, and that it might serve as a mediator for FGFR regulated LDHA phosphorylation. Further study is required to determine if FRS2α is needed for the interaction between FGFR1 and LDHA.

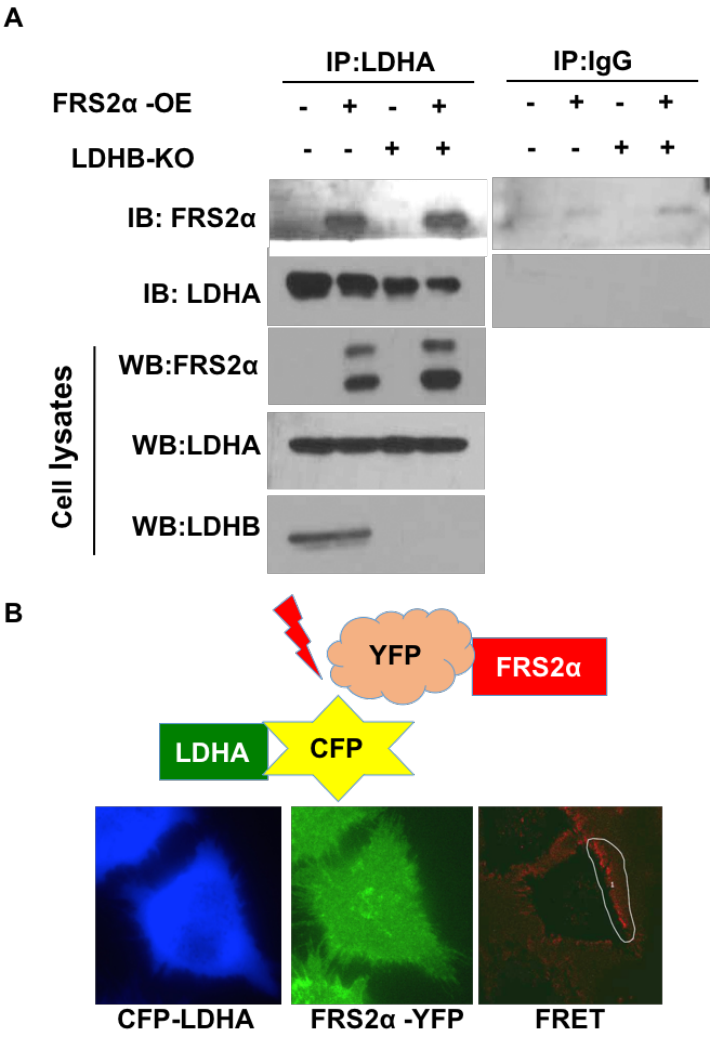


**Fig. 3. 7. FRS2 interacts with LDHA independent of LDHB.**

**A.** Co-immunoprecipitation of LDHA and FRS2α. Anti-IgG and anti-FRS2α antibodies were used to pull down IgG and FRS2α binding proteins. Immunoblotting of LDHA, FRS2α and LDHB was done to detect the expression of indicated proteins in complexes. **B.** FRET experiment to examine the interaction between LDHA-CFP and YFP-FRS2α. Signals of three different channels-donor, acceptor and FRET were recorded using confocal microscopy. IP, immunoprecipitation; WB, western blot; IB, immunoblot; OE, overexpression; KO, knockout; FRET, fluorescence resonant energy transfer.

In addition to the co-IP experiments, we also did the fluorescence resonant energy transfer (FRET) assay to examine the crosstalk between FRS2α and LDHA. The assay is based on the rationale that if the donor (CFP) and acceptor (YFP) are close enough (<6nM), energy transfer between two light-sensitive molecules will occur, thus generating FRET signals. To perform the assay, we added CFP to the C-terminus or N-terminus of LDHA and tagged YFP to the C-terminus l or N-terminus of FRS2α. We then monitored the interaction of the proteins by transfecting them individually or separately into DU145 cells prior to examining cells under confocal microscopy. FRET signals were observed when LDHA with C-terminus tagged CFP and FRS2α with N-terminus tagged YFP were cotransfected, suggesting that there was a crosstalk between the LDHA C-terminus and the FRS2α N-terminus (Fig. 3.7). The FRET assay was able to analyze the interaction of two proteins in live cells and allows for the detailed information regarding the orientation of the interactions. All together, these data suggest that FRS2α binds with LDHA independent of LDHB.

### *FGFR1 interacts with LDHB independent of LDHA.*

FGFR1 interacts with and phosphorylates LDHA, and LDHA forms tetramers with LDHA or LDHB isoforms. Therefore, we examined whether FGFR1 also interacts with LDHB even in the absence of LDHA. Since LDHA forms complexes with LDHA, it is unclear if FGFR1 directly binds with LDHA or needs LDHB in the complex for the interactions. We transfected 293T cells with plasmids expressing FGFR1 and LDHB. By co-immunoprecipitation, FGFR1 interacted with LDHB even in LDHA knockout 293T cells (Fig. 3.8). Surprisingly, the interaction did not result in the phosphorylation of LDHB (data not shown), suggesting that LDHB might not be required for the interaction between FGFR1 and LDHA. Further studies are needed to address this phenomenon.

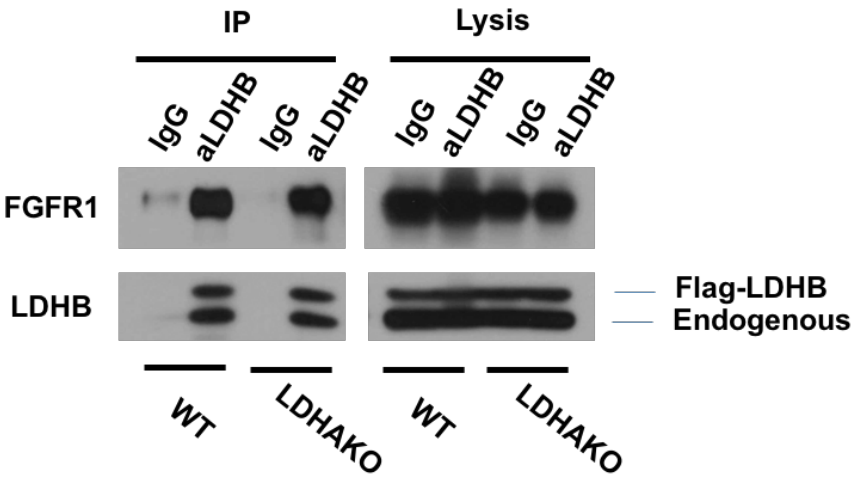


**Fig. 3. 8. FGFR1 binds to LDHB in the absence of LDHA.**

Cells were co-transfected with FGFR1 and LDHB expressing plasmids prior to the co-IP assay. Anti-IgG and LDHB antibodies were used to pull down control IgG and LDHB protein complexes, which was followed by immunoblotting of FGFR1 and LDHB. aLDHB, anti-LDHB antibodies; IP, immunoprecipitation; Endogenous, Endogenous LDHB; LDHAKO, LDHA knockout.

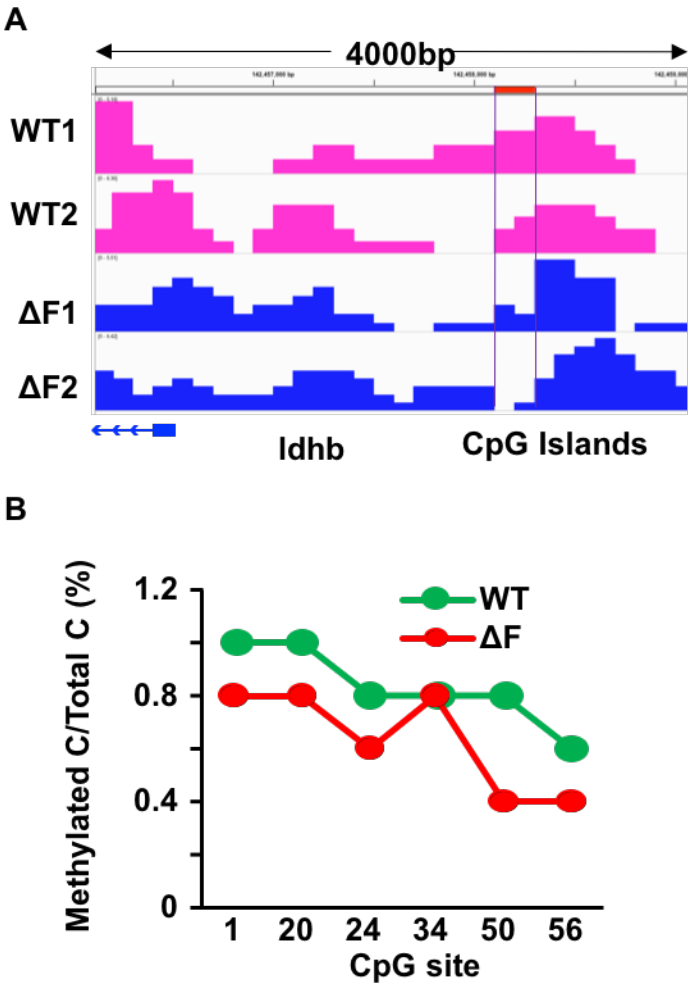


**Fig. 3. 9. Ablation of FGF signaling reduced the DNA methylation of LDHB promoter.**

**A.** Methylated DNA was immunoprecipitated with the anti-methylated DNA antibody and subjected to high throughput sequencing. The level of methylated CpG island in the LDHB promoter region was shown. **B.** Bisulfite DNA sequencing of the Ldhb promoter area showing reduced DNA methylation in $MEF^{\Delta F}$. WT, wildtype; ΔF, $MEF^{\Delta F}$.

***FGFR1 suppressed LDHB transcription by promoting DNA methylation on the LDHB promoter.***

It has been reported that the promoter of LDHB is heavily methylated in PCa, which inhibits the transcription of LDHB (80). To determine whether FGFR1 suppressed LDHB expression via promoter methylation, we employed methylated DNA immunoprecipitation (MeDIP) to pull down methylated DNA for high-throughput sequencing (Fig. 3.9). The results showed that the CpG islands in the Ldhb promoter were less methylated in $MEF^{\Delta R1}$ cells than in parental MEFs. Further bisulfite sequencing of the Ldhb promoter area confirmed that the DNA demethylation is reduced in $MEF^{\Delta F}$ cells (Fig. 3.9). Since DNA demethylation is catalyzed by the three TET enzymes, TET1-3, we then compared the expression of TET1-3 in $MEF^{\Delta F}$ and parental MEFs with real-time RT-PCR. The results revealed the expression of Tet1 at the mRNA level was significantly increased in $MEF^{\Delta F}$ (Fig. 3.10 A). Western blot further confirmed elevated TET1 expression in $MEF^{\Delta F}$ (Fig. 3.10 C), suggesting that FGF signaling suppressed expression of Tet1. Consistent with these findings, *Ldhb* expression was higher in MEF bearing $Tet1^{null}$ alleles than in parental MEFs (Fig. 3.10 B), further indicated that the expression of LDHB was reduced by DNA methylation.

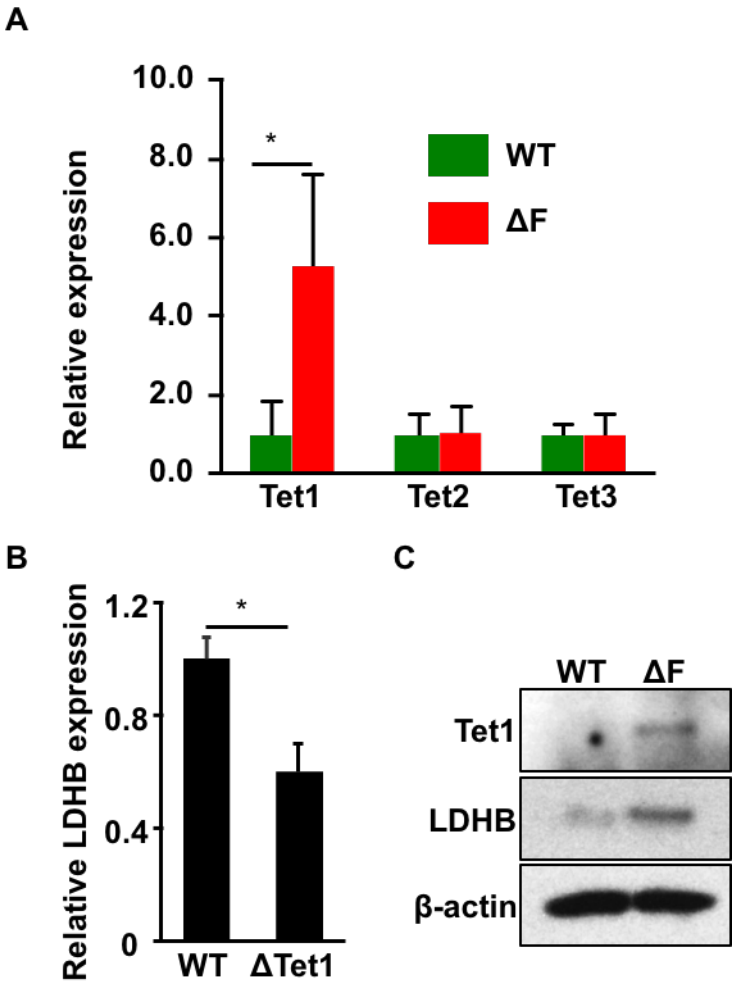


**Fig. 3. 10. Ablation of FGF signaling upregulated Tet1 expression.**

**A.** Real-time RT-PCR showing increased Tet1 in MEF$^{\Delta F}$ cells at the mRNA level. **B.** Real-time RT-PCR analyses showing reduced *ldhb* expression in MEF carrying Tet1 null mutation (ΔTet1). **C.** Western blot analyses showing that Tet1 expression was increased in MEF$^{\Delta F}$ relative to wildtype MEFs. WT, wildtype; ΔF, MEF$^{\Delta F}$; *, P<0.05.

***Ablation of the FGF signaling axis reprograms cell metabolism in human PCa cells.***

The acquisition of ectopic FGFR1 expression and cell metabolic reprogramming are associated with PCa progression. However, whether the acquisition of FGFR1 expression contributes to metabolic changes in PCa cells is not clear. To investigate whether aberrant FGF signaling contributed to PCa metabolic reprogramming, the CRISPR/Cas9 gene editing method was used to ablate the *Fgfr1* alleles in DU145 cells that highly expressed FGFR1. The expression profile of LDHA isozymes was then determined by Western blotting (Fig. 3.11). It was obvious that ablation of Fgfr1 reduced expression of LDHA and increased expression of LDHB in DU145 cells at the protein level. Consistent with the report that FGFR1 tyrosine kinase phosphorylates LDHA, Western blot analyses also revealed that the phosphorylation of LDHA at Y10 residue was reduced in DU145$^{\Delta R1}$ cells. In line with the data in MEF cells, the expression of Ldha mRNA was not affected and the expression of ldhb mRNA was increased in DU145$^{\Delta R1}$ cells (Fig. 3.11 B). This further suggests that the reduction of LDHA was due to regulation at either the translational or posttranslational modification level and the reduction in LDHB was a result of changes in transcription.

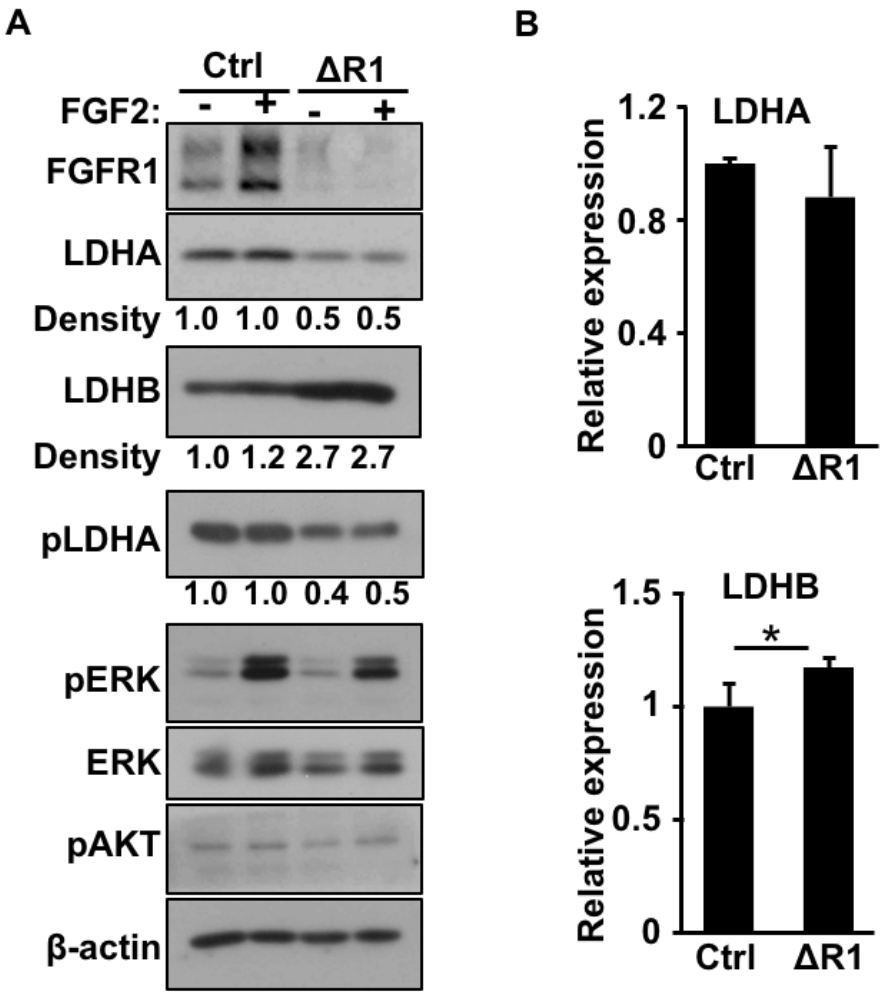


**Fig. 3. 11. Ablation of FGF signaling reduced LDHA and increases LDHB expression in DU145 cells.**

**A.** Western blot showing ablation of Fgfr1 reduced LDHA expression and increases LDHB expression. **B.** Ablation of Fgfr1 increased mRNA expression of LDHB but did not affect LDHA transcription. Ctrl, control; ΔR1, DU145$^{\Delta R1}$; pLDHA, phosphorylated LDHA; pERK, phosphorylated ERK1/2; pAKT, phosphorylated AKT; β-actin was used as loading control. Intensity of indicated proteins relative to β-actin was analyzed using Image J. *, P<0.05

In accord with a FGFR-driven metabolic switch, ablation of Fgfr1 reduced the glucose uptake and lactate production, as well as increased $O_2$ consumption (Fig. 3.12). The results suggest that ablation of Fgfr1 in PCa cells reprograms the cell metabolism from glycolysis to oxidative phosphorylation.

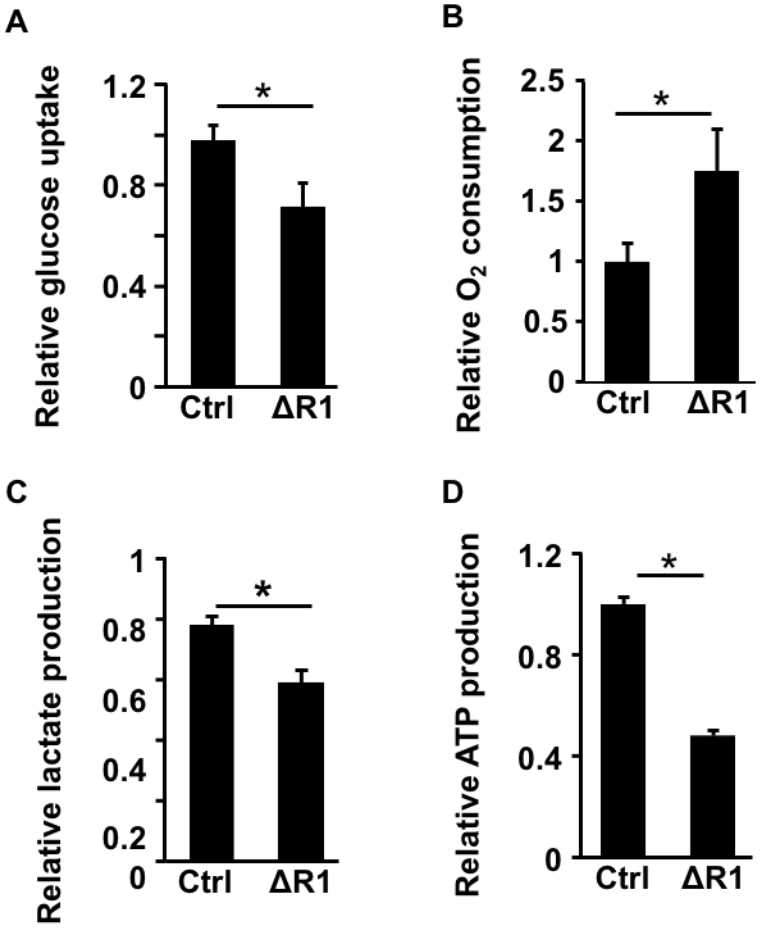


**Fig. 3. 12. Ablation of FGF signaling suppresses aerobic glycolysis and promotes oxidative phosphorylation in DU145 cells.**

**A.** Glucose uptake; **B.** oxygen consumption; **C.** lactate production; **D.** ATP production of control and FGFR1 knockout DU145 cells. Ctrl, control; ΔR1, $DU145^{\Delta R1}$; *, $P<0.05$.

**FGFR1 knockout TRAMP tumors displayed decreased expression of pLDHA and increased expression of LDHB.**

Tissue of origin along with genetic changes that drive the tumor progression both determine tumor metabolic dependencies. Therefore, it is crucial to investigate metabolism regulation in live animals where tumors originally arise. Previous studies have shown that *Fgfr1* null mice were generated through crossing of *Fgfr1*$^{flox/flox}$, *ARR2PBi-Cre* and TRAMP mice (92). To understand whether FGFR1 also regulates pLDHA and LDHB in vivo, we then examined pLDHA levels and LDHB expression in resulted *Fgfr1* knockout and control prostate tumors by immunostaining and real-time PCR analyses. The IHC results showed that pLDHA levels were significantly downregulated, while LDHB was upregulated in tumors with *Fgfr1* deletion (Fig. 3.13). Real-time analyses performed with RNA extracted from control and *Fgfr1* knockout tumors revealed that the transcription of LDHB was enhanced, as shown by the increased expression of LDHB mRNA. These data, in line with the findings done *in vitro*, strongly suggest that FGFR1 positively regulated pLDHA but negatively controlled LDHB in both *in vitro* and *in vivo*.

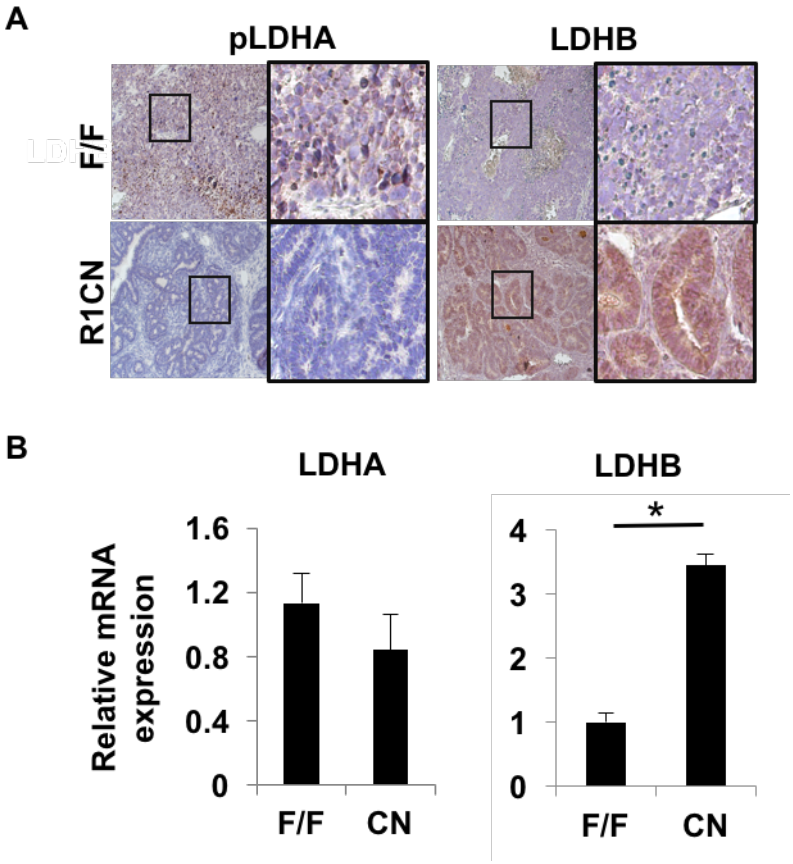


**Fig. 3. 13. FGFR1 deletion reduced pLDHA but increased LDHB expression in TRAMP tumors.**

**A.** Immunostaining of pLDHA and LDHB in *Fgfr1* knockout and control TRAMP tumors using anti-pLDHA and LDHB antibodies. Representative pictures showed that pLDHA was significantly decreased and LDHB was upregulated in poorly differentiated prostate tumors. **B.** mRNA expression of LDHA and LDHB in *Fgfr1* knockout and control prostate tumors. WT, wildtype; R1CN, *Fgfr1*$^{cn}$, *, P<0.05.

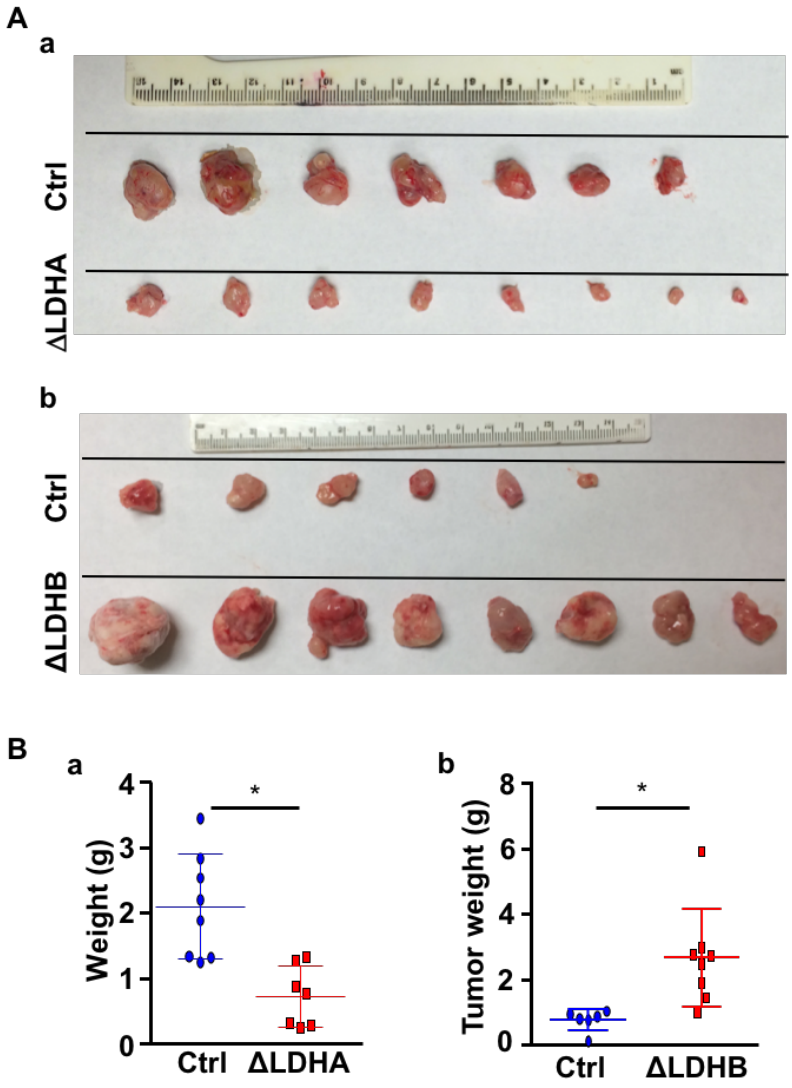


**Fig. 3. 14. Ablation of LDHA reduced and ablation of LDHB enhanced the tumorigenicity of DU145 cells.**

**A.** Xenografts derived from control DU145, DU145$\Delta^{Ldha}$ (**a**) or DU145$\Delta^{Ldhb}$ (**b**). DU145 cells (1 X $10^6$) were mixed with Matrigel and grafted into the hind flanks of nude mice. Note that the tumors of ΔLDHA and ΔLDHB groups were harvested at different days since the ΔLDHB group reached the limit of tumor burdens earlier than the ΔLDHB group. **B.** The average xenograft weight of DU145$^{\Delta Ldha}$ **(a)**, DU145$^{\Delta Ldhb}$ **(b)**, and control tumors. ΔLDHA, DU145$^{\Delta Ldha}$; ΔLDHB, DU145$^{\Delta Ldhb}$; Ctrl, parental DU145 cells as a control.

***Ablation of LDHA reduced, and ablation of LDHB enhanced tumorigenesis of DU145 cells.***

To investigate the function of LDH isoforms on the tumorigenic activity of PCa cells, we employed CRISPR/Cas9 to delete Ldha or Ldhb alleles in DU145 cells, designated as $DU145^{\Delta Ldha}$ and $DU145^{\Delta ldhb}$, respectively. When grafted subcutaneously in nude mice, $DU145^{\Delta Ldha}$ cells only generated small tumors compared with parental DU145 cells (Fig. 3.14). In contrast, the grafts derived from $DU145^{\Delta ldhb}$ cells were larger than parental DU145 cells (Fig. 3.14). Western analysis of the xenografts revealed that ablation of Ldha increased PGAM expression, ablation of Ldhb increased HK1, PFK3 and Aldolase, indicating that depletion of LDHA compromised and depletion of LDHB increased the expression of glycolytic enzymes in prostate cancer cells (Fig. 3.15)

Interestingly, both LDHA and LDHB deletion stimulated the compensatory upregulation of glycolytic related proteins but resulted in opposite effects on tumor growth, suggesting that there might be unidentified proteins that mediate the LDH-regulated tumor growth

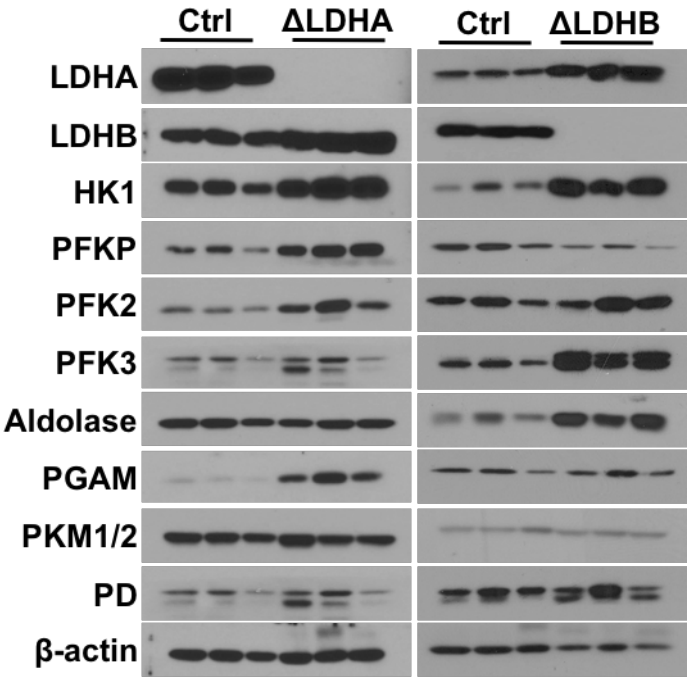


**Fig. 3. 15. Knockout of LDHA or LDHB leads to the reprogramming of the glycolysis pathways.**

Western blot analyses of expression of enzymes related to the aerobic glycolysis. Cell lysates were extracted from control, LDHA or LDHB knockout grafted DU145 tumors. Knockout of LDHA and LDHB stimulated the upregulation of aerobic glycolysis related pathways but had different effects on tumor growth. ΔLDHA, $DU145^{\Delta Ldha}$; ΔLDHB, $DU145^{\Delta Ldhb}$; Ctrl, parental DU145 cells as a control; HK1, hexokinase 1; PD, pyruvate dehydrogenase.

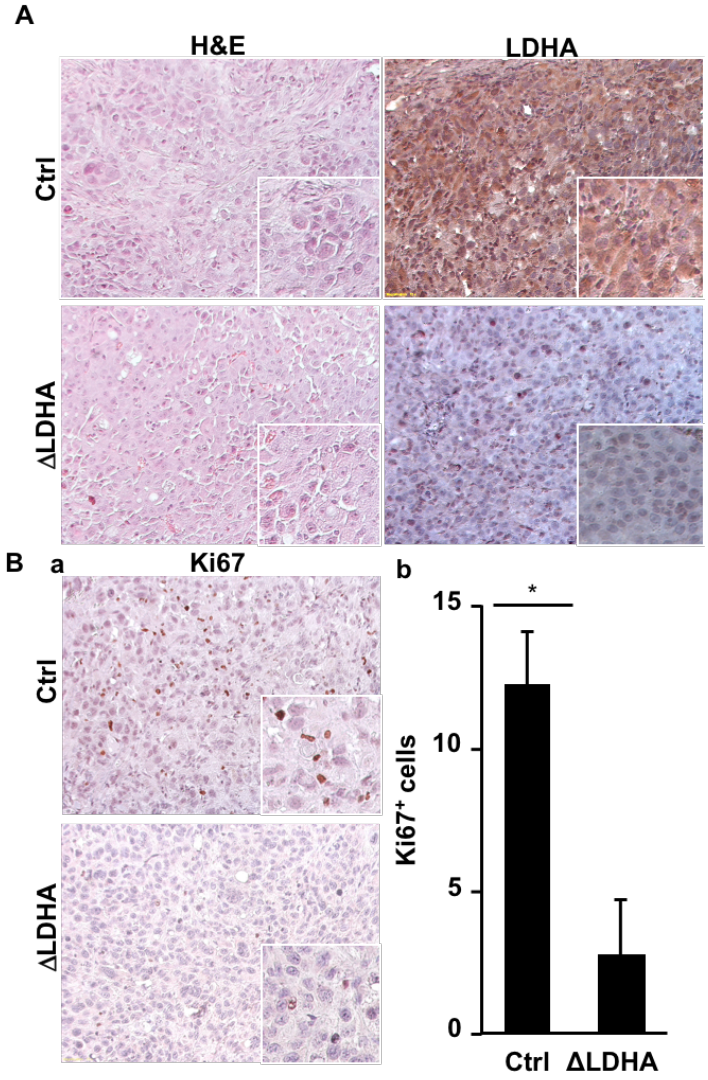


**Fig. 3. 16. Ablation of Ldha reduced cell proliferation in PCa xenografts.**

**A.** Tissue sections of xenografts derived from DU145$^{\Delta Ldha}$ or control DU145 cells. H&E stained, or immunohistochemical staining with anti-LDHA or Ki67 as indicated. **B.** IHC staining for Ki67 (panel a) and averages of Ki67 cells per viewing area were calculated from 20 (6 pairs of tumors) viewing areas and presented as mean ± sd (b).

Although there were no significant differences in histology between the parental DU145, DU145$^{\Delta Ldha}$, and DU145$^{\Delta ldhb}$ xenografts, DU145$^{\Delta Ldha}$ had less and DU145$^{\Delta ldhb}$ had more Ki67$^{+}$ cells, indicating that ablation of Ldha reduced and ablation of Ldhb increased proliferating cells in the xenografts (Fig. 3.16&3.17).

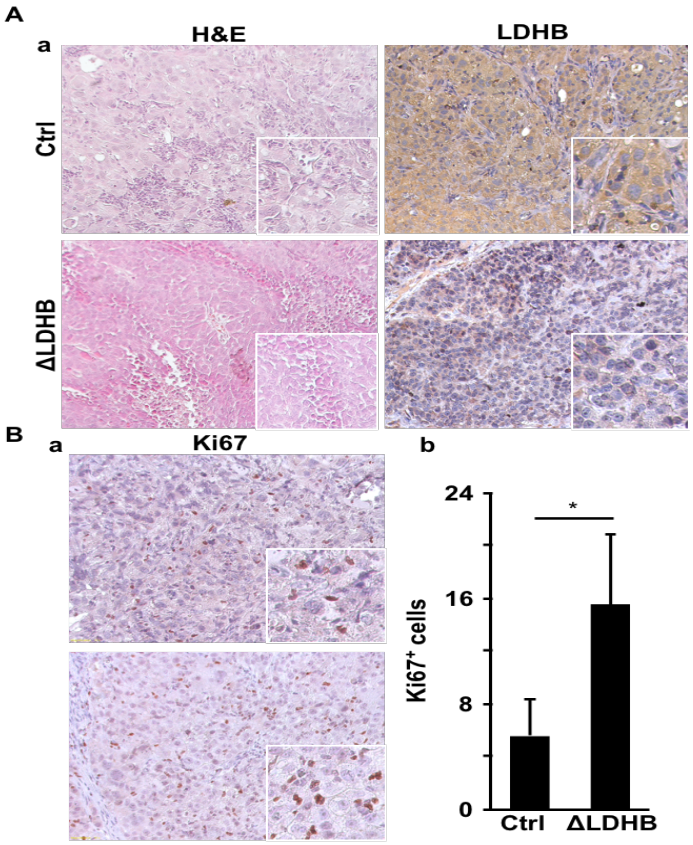


**Fig. 3. 17. Ablation of Ldhb promoted cell proliferation in PCa xenografts.**

**A.** Tissue sections of xenografts derived from DU145$^{\Delta Ldhb}$or control DU145 cells. H&E stained, or immunohistochemical staining with anti-LDHB or Ki67 as indicated. **B.** IHC for Ki67 (panel a) and averages of Ki67 cells per viewing area were calculated from 20 (6 pairs of tumors) viewing areas. *, P<0.05.

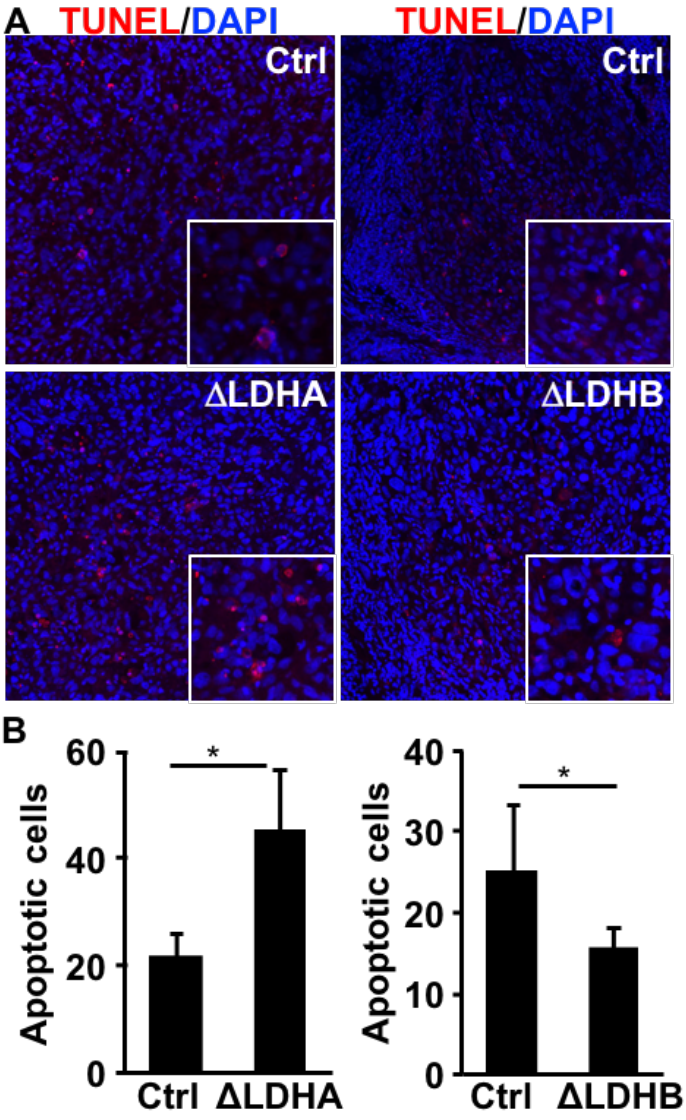


**Fig. 3. 18. Differential impacts of LDHA and LDHB on cell survival in PCa xenografts.**

**A.** Tissue sections of xenografts derived from DU145$^{\Delta Ldha}$, DU145$^{\Delta ldhb}$, and DU145 cells were immunostained with TUNEL. **B.** Averages of positively stained cells per viewing area were calculated from 25 (6 pairs of tumors) viewing areas; *, P<0.05.

Furthermore, there were more apoptotic cells in xenografts derived from DU145$^{\Delta Ldha}$ cells than those derived from parental DU145 cells, whereas the opposite phenomenon was observed in DU145$^{\Delta ldhb}$ xenografts (Fig. 3.18). Lactic acid produced by tumor cells has a critical impact on the tumor microenvironment primarily through triggering angiogenesis and polarizing tumor associated macrophages (93). To investigate the impact of LDHA or LDHB knockout on the tumor microenvironment, we examined the micro vessel density by staining with anti-CD31 antibodies. The results showed that angiogenesis was inhibited in LDHA knockout tumors but stimulated in LDHB knockout tumors compared with control tumors (Fig. 3.19). These data suggest that angiogenesis is accompanied with altered metabolism, which is consistent with the pro-angiogenic role of FRS2 in prostate tumor angiogenesis.

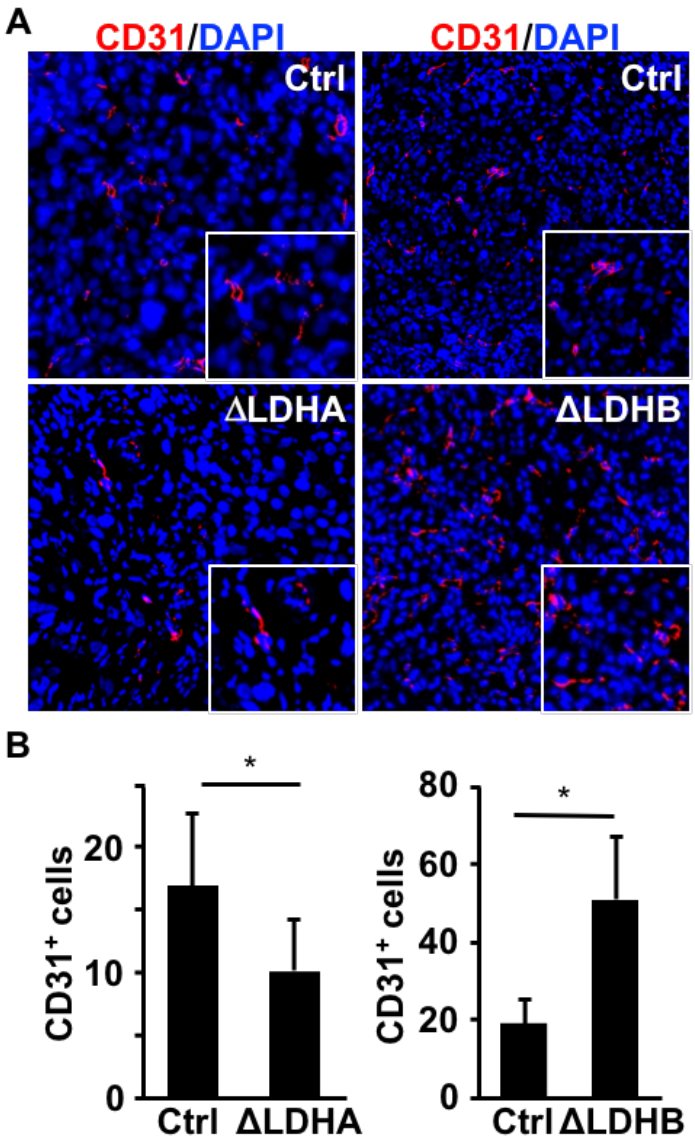


**Fig. 3. 19. Differential impacts of LDHA and LDHB on angiogenesis in PCa xenografts.**

Tissue sections of xenografts derived from DU145$^{\Delta Ldha}$, DU145$^{\Delta ldhb}$, and DU145 cells were immunostained with anti-CD31 antibodies **A.** Representative images of CD31 positive cells in indicated tumors**. B.** Averages of positively stained cells per viewing area were calculated from 25 (6 pairs of tumors) viewing areas. *, P<0.05.

Since inflammation is also associated with malignancy of prostate cancers, we measured macrophages by staining with the F4/80 antibody in xenografts derived from DU145$^{\Delta Ldha}$, DU145$^{\Delta ldhb}$, and parental DU145 cells. The results showed that there were fewer F4/80$^{+}$ cells in xenografts derived from DU145$^{\Delta Ldha}$ than those derived from parental DU145 cells. In contrast, there were, more F4/80$^{+}$ cells in xenografts derived from DU145$^{\Delta Ldhb}$ than those derived from parental DU145 cells (Fig. 3.20). The results demonstrate that ablation of LDHA compromised, whereas ablation of LDHB stimulated, macrophage infiltration. Together, the results indicated that ablation of Ldha compromised, whereas ablation of Ldhb promoted, the tumorigenic activity of DU145 cells. These data once again supported the notion that LDHA and LDHB play different role in tumor initiation and progression.

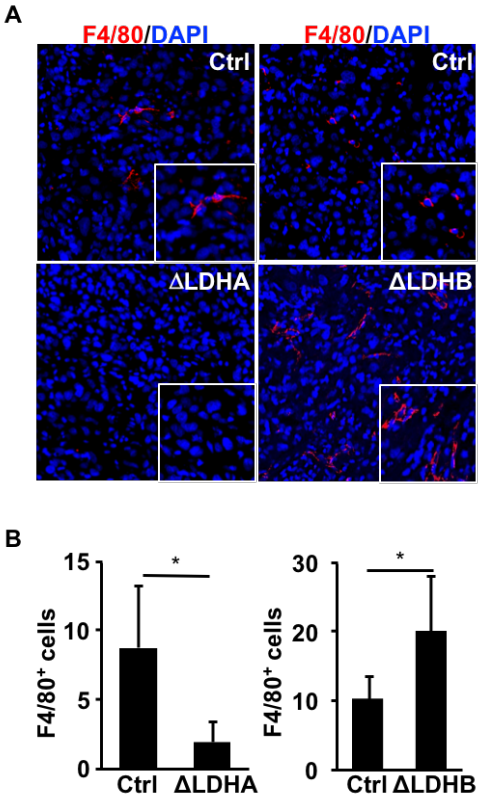


**Fig. 3. 20. Differential impacts of LDHA and LDHB on macrophage infiltration in PCa xenografts.**

Tissue sections of xenografts derived from DU145$^{\Delta Ldha}$, DU145$^{\Delta ldhb}$, and DU145 cells were immunostained with anti-F4/80 antibodies **A.** Representative images of F4/80 positive cells in indicated tumors**. B.** Averages of positively stained cells per viewing area were calculated from 25 (6 pairs of tumors) viewing areas. *, P<0.05.

**LDHA knockout increased the sensitivity of prostate cancer cells to chemotherapeutic drugs.**

One way to develop therapies is to target pathways that are unique to cancer cells. A body of evidence shows that cancer cells with increased mitochondrial activities become more sensitive to drugs that target DNA replication. Mitomycin C (MMC) is one of the drugs that have been applied to prostate cancer patients due to its ability to inhibit DNA replication. Since our data showed that FGFR1 and LDHA deletion increased prostate cancer cell oxygen consumption (Fig. 3.12), which is associated with increased mitochondrial activity, we tested whether FGFR1 ablation alters the chemosensitivity of prostate cancer cells. We treated control and FGFR1 knockout DU145 cells with MMC for 6 hours before subjecting these cells to the apoptosis assay for flow cytometry. FGFR1 ablation increased the number of early apoptotic cells (annexin $V^+$ Sytox $blue^+$) relative to control groups, suggesting that FGFR1 knockout increased the chemosensitivity of prostate cancer cells (Fig 3.21 A).

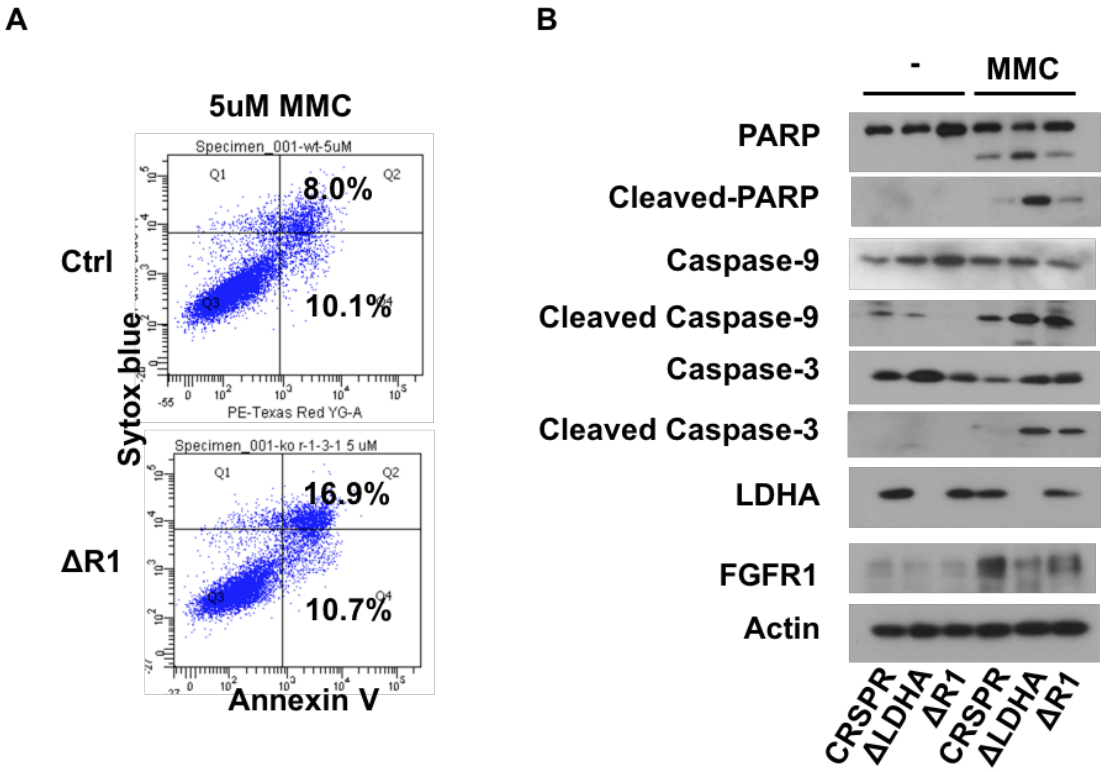


**Fig. 3. 21. FGFR1 and LDHA deletion increased the chemosensitivity of prostate cancer cells.**

**A.** Control and FGFR1 knockout cells were treated with 5uM MMC for 4 hours followed by staining with Annexin V and Sytox blue. The percentages of early apoptotic cells (Sytox blue$^{+}$ and Annexin V$^{+}$) and late apoptotic cells (Sytox blue$^{-}$and Annexin V$^{+}$) are indicated in the contour plots. **B.** Control, FGFR1 or LDHA knockout cells were treated with DMSO or 5uM MMC for 12 hours followed by Western blot analyses. CRISPR**,** control; ΔR1, FGFR1 knockout; ΔLDHA, LDHA knockout.

A series of caspase processing events is one of the common mechanisms through which cells undergo apoptosis. Thus, we further examined the caspase-9/caspase-3 axis by Western blotting and the data showed that cleaved-PARP, cleaved-caspase 9, and cleaved-caspase-3 were significantly upregulated in cells that lack FGFR1 or LDHA compared with controls (Fig. 3.21 B). The data indicated a striking similarity between the mechanisms that FGFR1 and LDHA deletion increased sensitivity of prostate cancer cells to chemotherapeutic drugs.

Although more studies are necessary before these findings are applied to preclinical models, the paradigm we tested in these assays revealed the possibility to target both the pathways that are aberrantly activated due to genetic changes such as FGFR1 amplification and pathways that enable the tumor phenotypes such as aerobic glycolysis. These two types of pathways represent the genetic changes and driver mutations that initiate the outgrowth of tumors, and metabolic changes that adapt transformed cells to the tumor environment.

***LDHB ablation promotes the survival of prostate cancer cells under hypoxic conditions.***

It has been documented that LDHA knockdown inhibits anchorage-independent growth of Rat1a fibroblasts but does not affect their growth when they are adherent to plastic dishes (94). The anaerobic environment of colonies formed on soft agar might provide cancer cells with the idea conditions to rely on the

LDHA dependent glycolysis metabolic pathways. Similarly, LDHB knockout did not change the cell growth in regular culture conditions. However, we observed that the growth of LDHB deleted DU145 cells was significantly impaired when subjected to hypoxia conditions, with most of the knockout cell died off around day 10 (Figure 3.22). These results indicated that hypoxia, which mimics the environment of tumors, imposed growth constraints on DU145 cells and only those cells that lack LDHB survived under the condition.

Since LDHB deletion triggered tumor growth through preventing cell death, we then examined the PTEN pathway, which is a major regulator of apoptosis and a tumor suppressor. Interestingly, LDHB knockout significantly inhibited PTEN levels in DU145 cells regardless of oxygen. The downregulation of PTEN was independent of its transcription since RT-PCR analyses showed that PTEN mRNA levels were not affected by LDHB deletion. However, mRNA expression of IL-6 was decreased in LDHB knockout tumor cells, which is consistent with the rationale that targeting both IL-6 and PTEN deletion may inhibit prostate cancer proliferation, migration and metastasis (95). LDHB deletion also reduced the mRNA expression of BCL-2, a survival marker. All together, these data suggest that LDHB is required for tumor cells to survive under hypoxic conditions.

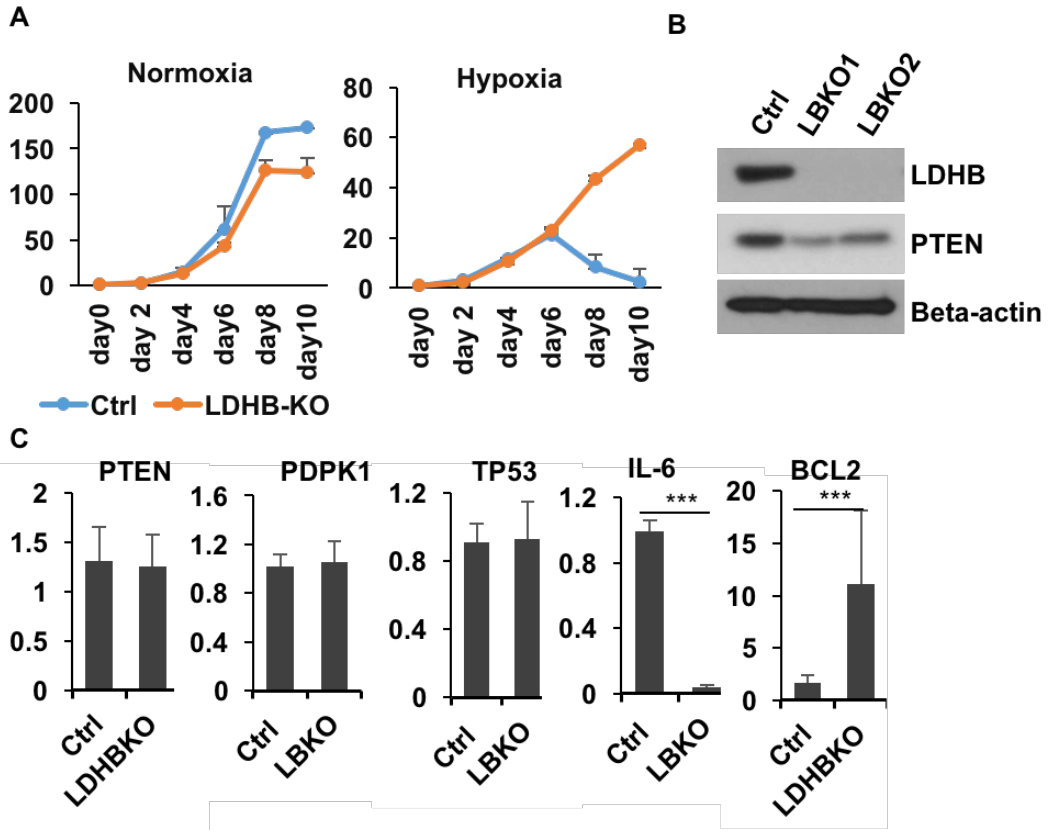


**Fig 3. 22. LDHB knockout inhibited tumor cell growth under hypoxia.**

**A.** Control and knockout DU145 cells were cultured for up to 10 days under normoxia (left panel) or hypoxia (right panel) conditions. **B.** Western blot analyses of control and LDHB knockout DU145 cells. Two LDHB knockout clones (LBKO1 and LBKO2) were used for the analyses. **C.** mRNA expression of PTEN, PDPK1, TP53, IL-6, and BCL2 was analyzed in control and LDHB deleted DU145 cells. Ctrl, control; LBKO, LDHB knockout; *** P<0.01.

***Hyperphosphorylation of LDHA and reduced LDHB expression in human PCa.***

In order to determine the expression pattern of LDHA and LDHB in human PCa,we performed immunohistochemistry on a panel of prostate cancer samples. Immunohistochemical staining showed that the expression of LDHA appeared to be higher in PCa than in adjacent prostate tissues (Fig. 3.23). Human LDHA can be phosphorylated by the FGFR1 kinase at multiple tyrosine residues (86). The level of Y10 phosphorylated LDHA (pLDHA) was increased in PCa compared with the adjacent non-cancerous tissues, whereas the expression of LDHB was reduced in PCa (Fig. 3.23). These results are in line with the evidence we acquired using DU145 and MEF cells, further demonstrating the different biological function of LDHA versus LDHB.

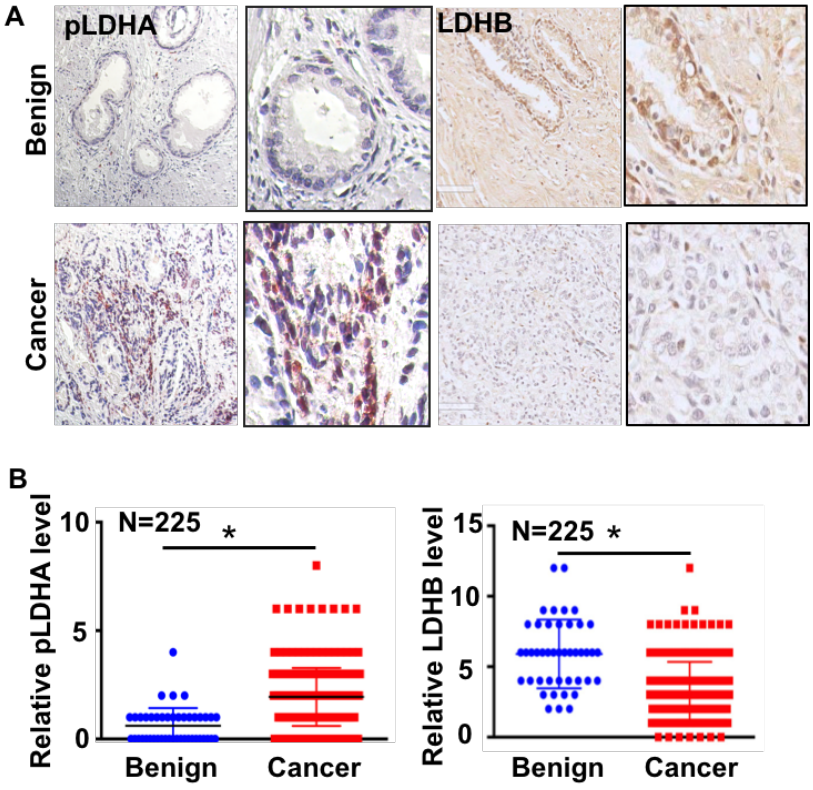


**Fig. 3. 23. High pLDHA and low LDH expression in PCa patients.**

**A**. Representative images of immunochemical staining of pLDHA and LDHB in the MGH PCa TMA. **B**. Statistical analyses of expressions of LDHA and LDHB in PCa and benign prostate. *, P<0.05; N=225.

To assess the clinical relevance of LDH expression profiles in PCa, the levels of pLDHA and expression of LDHB were determined by immunostaining in a human prostate tissue microarray (TMA) that comprised of 225 PCa and 27 benign prostate samples (90). The samples were annotated with detailed patient information and 15-year follow-up of the patients, which includes PSA recurrence, Gleason scores, pathological stages, patients' age, and survival time. In general, the clinical outcomes of the patients with high pLDHA were worse than those with low pLDHA; those with low LDHB expression were worse than those with high LDHB expressions (Fig. 3.24). Furthermore, the group with high pLDHA and low expression of LDHB clearly had shorter biochemical recurrence free time than the group with low pLDHA or high expression of LDHB. The results suggest that the levels of pLDHA and LDHB have the potential to serve as biomarkers for PCa prognosis.

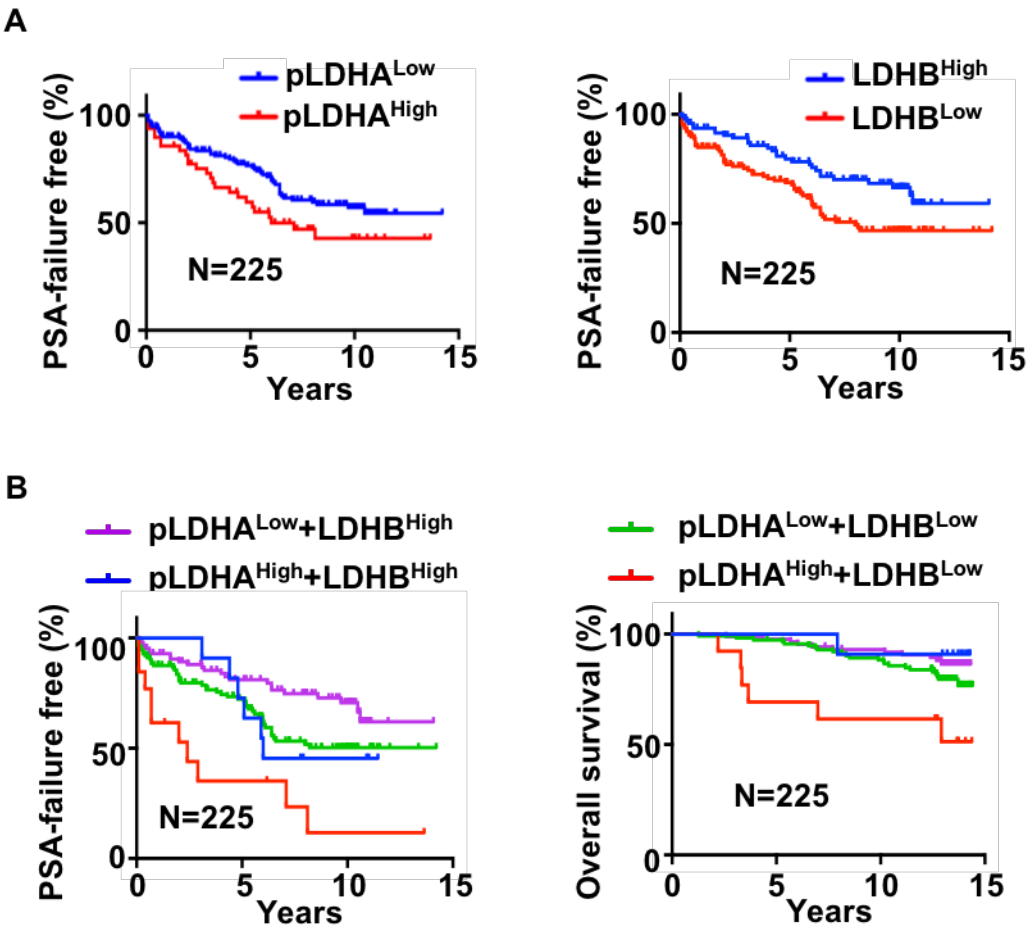


**Fig. 3.24. pLDHA$^{High}$/LDHB$^{Low}$ predicts poor prognosis of PCa patients**

**A.** Statistical analyses of PSA failure free survival time in patients with low (IRS<3) versus high (IRS≥3) phosphorylation of LDHA and in patients with low (IRS<3) versus high LDHB (IRS≥3) expression. **B**. PSA failure-free and overall survival time of patients with pLDHA$^{Low}$/LDHB$^{High}$, pLDHA$^{Low}$/LDHB$^{low}$, pLDHA$^{High}$/LDHB$^{Low}$ and pLDHA$^{High}$/LDHB$^{High}$.

Fgfr1 is overexpressed in about 40% of human PCa (58,62). To determine whether the expression level of Fgfr1 correlates with the abundance of pLDHA, *in situ* hybridization was used to assess the mRNA levels of Fgfr1 in the same set of TMAs. The results showed that Fgfr1 was overexpressed in the epithelial compartment of 73% of this set of PCa samples. Furthermore, expression levels of Fgfr1 were positively associated with the level of pLDHA (Fig. 3.25). In addition, although statistical analysis also revealed that expression of Fgfr1 was negatively associated with the expression of LDHB in the same TMA set (data not shown). Together, the data imply that aberrantly expressed Fgfr1 in PCa deregulates the expression of LDH isozymes and shifts metabolism to favor glycolysis in these cells. Our study also linked the dysregulation of FGFR1 to expression of glycolysis related proteins.

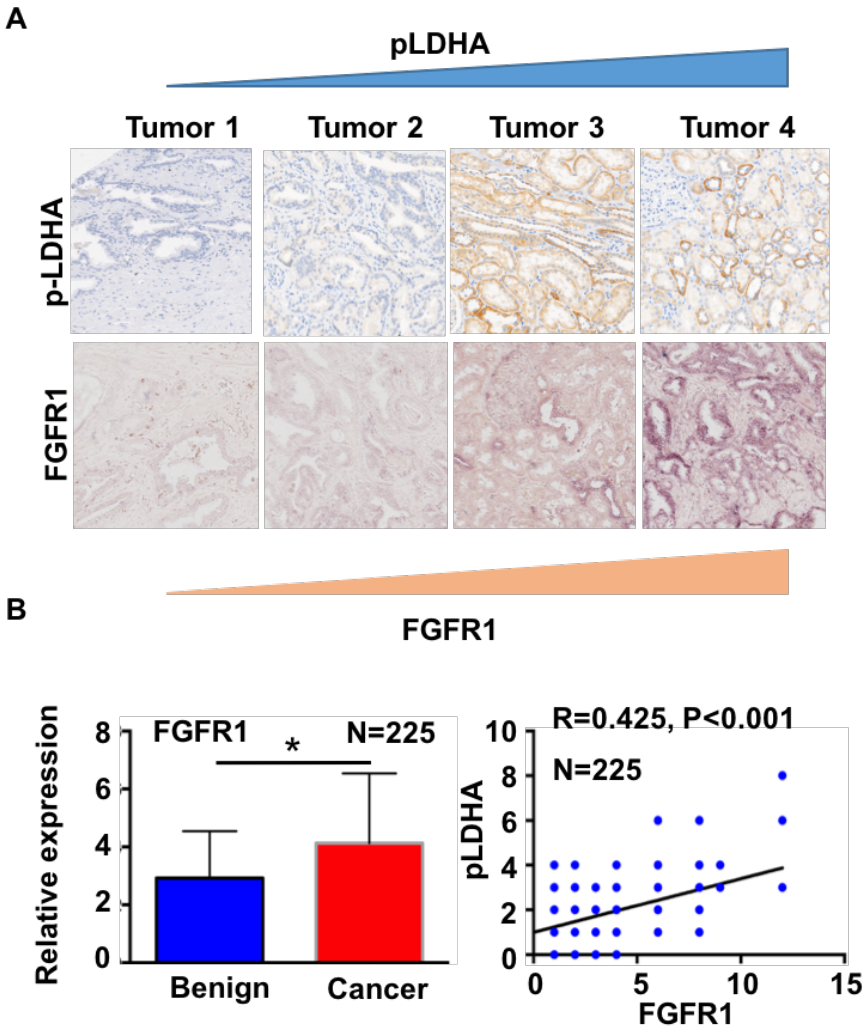


**Fig. 3.25. FGFR1 is positively correlated with LDHA in PCa patients.**

**A.** Representative pictures of pLDHA immunostaining and FGFR1 in situ staining in same selective tumors. **B.** Statistical analyses of FGFR1 in benign and cancer tissues and Pearson correlation of Fgfr1 and pLDHA in the PCa tissue microarray. R=0.425, P<0.01, N=225; *, P<0.05.

## Discussion

Extensive evidence shows that aberrant activation of FGF/FGFR signaling is a contributing factor for PCa development and progression (53-59). The acquisition of ectopic expression of FGFR1 in tumor epithelial cells stands out as the most remarkable change among FGFR isotypes (60-64). FGF-mediated glycolysis plays a pivotal role in developmental (9,96) and FGFR1 has been shown directly phosphorylates LDHA at multiple tyrosine residues and the phosphorylation enhances the LDHA enzymatic activity (86). However, whether aberrant FGFR1 signaling in PCa cells reprograms cellular energy metabolism remains unknown. In this report, we showed that FGFR1 signaling promoted aerobic glycolysis via upregulating LDHA at the protein level and downregulating LDHB at the transcription level. Ablation of LDHA compromised whereas ablation of LDHB enhanced the tumorigenicity of DU145 PCa cells. Furthermore, high levels of phosphorylated LDHA and low levels of LDHB in human PCa tissues was associated with short biochemical recurrence and patient survival time. The results suggest that aberrant FGFR1 signaling contributes to PCa progression via reprograming cell energy metabolism and that high levels of phosphorylated LDHA and high expression of LDHB are potential biomarkers for PCa diagnosis and prognosis.

LDHA has four tyrosine phosphorylation sites. Among them, phosphorylation at tyrosine 10 enhances the formation of tetramers and increases enzymatic activity, and phosphorylation at tyrosine 83 enhances the

binding of substrate NADH (86). In addition, high expression of FGFR1 is associated with high levels of phosphorylated LDHA (97). However, tyrosine residue 10 is not a conserved residue, but only exists in human LDHA, suggesting that FGFR1 activates LDHA not only via Y10 phosphorylation. Here, we showed that phosphorylation of the four LDHA tyrosine residues by FGFR1 extended the half-life of LDHA. Ablation of the FGF signaling axis significantly reduced the half-life of LDHA; substitutions of the four LDHA tyrosine residues with phenylalanine also reduced the half-life of LDHA (Fig. 3.6). Together with the literature, it is suggested that tyrosine phosphorylation of LDHA not only increases the enzymatic activity, but also enhances the stability of LDHA. Western blot analyses did not demonstrate ubiquitination of LDHA with or without coexpression of FGFR1 kinase (data not shown). Therefore, future efforts are needed to determine how tyrosine phosphorylation affects the half-life of LDHA.

It has been reported that the expression of LDHB is silenced by promoter hypermethylation in human PCa (81). Here we further demonstrate that ablation of Fgfr1 reduced methylation of the CpG island in the LDHB promoter, either with high-throughput MeDIP or bisulfide DNA sequencing of the LDHB promoter (Fig. 3.9). Interestingly, ablation of FGF signaling in MEF increased expression of Tet1, which catalyzed the conversion of methylated guanidine to hydroxyl-methylated guanidine, the first step of DNA demethylation. Moreover, ablation of

Tet1 increased LDHB expression. Thus, this demonstrated that FGF signaling suppressed LDHB expression by promoting Tet1 expression.

Targeting lactate metabolism has been tested for cancer treatment in clinical trials (84). Our data here reveal that LDHA and LDHB have opposite effects on PCa growth. Therefore, it is essential to develop new strategies to specifically inhibit LDHA without compromising LDHB activity. FGFR1 selectively phosphorylates LDHA on multiple tyrosine residues, which stabilizes LDHA, and concurrently blocked the expression of LDHB. Therefore, inhibition of FGFR1 is of clinical significance for PCa treatment.

Acquisition of ectopic FGFR1 is a hallmark change in PCa progression and high Fgfr1 expression is associated with poor prognosis of PCa. Although it has been shown that ectopic FGFR1 promotes cell proliferation, survival, and migration, how aberrant FGFR1 signaling contributes to PCa progression is still not fully understood. Here we showed that FGFR1 reprogramed cell metabolism from oxidative phosphorylation to aerobic glycolysis. Emerging evidence shows that the reprogramming to aerobic glycolysis provides building blocks needed for fast proliferation of cancer cells. In addition, accumulation of lactates, the product of aerobic glycolysis in the tumor microenvironment suppresses the infiltration, proliferation, and differentiation of lymphocytes. Therefore, the data here suggest that aberrant FGF signaling also promotes PCa progression by increasing supplies needed for cancer cell growth and by suppressing immunosurveillance.

Overexpression of LDHA and downregulation of LDHB have been separated reported in PCa (98). However, whether the expression pattern of LDH is associated with PCa prognosis remains unclear. In this report, we demonstrated that although either high expression of LDHA or downregulation of LDHB was weakly associated with biochemical recurrence survival time (Fig. 3.24), combined expression profiles of LDHA and LDHB was strongly associated with biochemical recurrence survival and overall survival time of the patient (Fig. 3.24). The results demonstrate the potential of combined expression profiles of LDHA and LDHB as biomarkers for PCa prognosis and warrant future efforts to investigate whether it can be used to guide the selection of more aggressive or conservative treatments for PCa.

In conclusion, herein we demonstrated that FGF signaling promoted aerobic glycolysis and that aberrant FGF signaling in PCa reprogramed cell metabolism; conversely, suppression of FGF signaling reduced aerobic glycolysis and promoted oxidative phosphorylation. Deletion of LDHA suppressed and deletion of LDHB promoted the tumorigenic activity of PCa cells. Furthermore, overexpression of LDHA and downregulation of LDHB correlated with short biochemical recurrence and survival time of PCa patients. Therefore, the results shed new lights on manipulation of aberrant FGF signaling as a strategy for PCa treatment.

# CHAPTER IV

# SUMMARY

Prostate cancer is one of the leading diseases in America. Intensive studies have been done for building an understanding of this disease and hold hopes for developing new therapies against prostate cancer based on the scientific findings deprived from prostate cancer research.

In 1921, Otto Warburg argued that cancer cells, unlike normal cells, tend to use aerobic glycolysis as their energy sources and this phenotype was mainly caused by the defects in the mitochondria of cancer cells. The concepts have been updated since then and scientific research centering on it has also expanded. More evidence suggests that despite the instant energy-ATP, other biological building blocks and reducing equivalents such as NADPH also hold the keys to our understanding towards the rewired metabolic pathways in tumor cells. However, more research has unraveled the complexity of cancer metabolism and new findings have raised new questions and challenges.

Another pioneer of cancer biology-Judah Folkman, in 1972, for the first time, proposed the concept of starving tumor cells to death by inhibiting tumor angiogenesis (99). Rapid expansion and proliferation of tumor cells leads to the depletion of energy and oxygen needed to sustain tumor growth. New blood vessels arise from an existing vasculature and grow towards tumors to supply them with nutrients and oxygen. Angiogenesis is considered a rate limiting process for the outgrowth of tumor cells because tumor cells cannot grow more

than 1mm$^2$ without the support of new blood vessels. With the fast expansion of research on this topic, now it is realized that 1) tumor blood vessel formation is a multi-step process; 2) tumor vasculature is drastically different from normal vessels; 3) there are different hypothesis regarding the origin of newly formed blood vessels within certain tumors.

Our understating of tumor angiogenesis and cancer metabolism have been hindered by the fact that cells behave differently in culture and in the human body. For example, most cell culture media contain a higher concentration of glucose (25mM) than the physiological conditions in vivo (5mM). Even inside the same multicellular organism, different tissue contexts provide unique microenvironments where specific tumors arise. Due to this reason, the interaction of tumor cells and cells that reside in the environment, such as endothelial cells and stromal cells, defines the tumor pathways dependencies. Identifying these dependencies in order to target the vulnerabilities of specific tumors is the most common approach to develop therapies against cancers. To bridge the gap between cell culture and the human body, we used conditional knockout mice model to study how FGF signaling regulates tumor angiogenesis and cancer metabolism, which better represents the disease under physiological conditions. The tissue specific deletion technique also provides the information regarding pathways in specific tissues and overcome the unavailabilities of animal subjects due the lethality of Frs2α whole body knockout. By crossing floxed Frs2α and ARR2Bi-Cre mice, we deleted Frs2α in prostatic tissues which

could not be achieved by total knockout because *Frs2α* null mice are embryonic lethal. Then we crossed the resultant mice with the TRAMP model to acquire prostate tumors with Frs2α deletion in the epithelium. Similarly, we investigated cancer metabolism by using FGFR1 knockout TRAMP tumors. We also i.p. injected DU145 cells with FGFR1, LDHA or LDHB deletion into nude mice, and monitored the tumor growth *in vivo*. The usage of animal models gives us an in-depth understanding of the behaviors of tumors under pathological conditions and it more likely resembles how they behave in patients.

Tumor cells to elicit signals that stimulate the environment to continuously supply them with new nutrients. The onset of angiogenesis could be viewed as the consequence of an interaction between tumor cells and the environment. Under hypoxia, tumor cells gradually shift their metabolism from oxidative phosphorylation to glycolysis without needing oxygen. It is believed that the shift was driven by the genetic changes in cancer cells, but the environmental stresses such as hypoxia and deprivation of other energy sources eventually lead to the complete reprogramming of metabolic pathways, which enables tumor cells to utilize glucose as the major energy source even in the presence of oxygen. Hypoxic conditions also drive another fundamental process during cancer progression-angiogenesis. Hypoxia inducible factor Hif1 promotes the expression of proangiogenic factors such as VEGF-A to induce the proliferation, migration and tube formation of capillaries towards the tumor mass. Therefore, angiogenesis and aerobic glycolysis are interconnected and regulated by a

similar set of genes and possibly the same driver mutations. Epithelial tumors such as prostate cancers were initially separated from blood supply by a basement membrane which becomes broken by lactate that is secreted by tumor cells due to the activation of glycolysis. Lactate, an end product of aerobic glycolysis that had been considered useless, is now believed to play key roles to create an acidic environment to break down the extracellular matrix and the basement membrane, which are barriers that prevent blood vessels reach tumors and prevent tumor cells from invading into the circulatory system.

Our investigation of tumor angiogenesis during the process of prostate cancer progression revealed a new mechanism of how Frs2a mediated FGF signaling promotes angiogenesis. Our data showed that Frs2αa deletion reduced the angiogenesis of prostate cancer, evident by a decreased number of blood vessels in TRAMP tumors that lack frs2 compared with controls. Conditioned medium of Frs2α depleted prostate cancer cells impaired the recruitment of HUVECS by tumor cells. Other functions of endothelial cells, such as migration and tube formation were also undermined due to the deletion of Frs2α in prostate cells. These data demonstrate that aberrant FGF signaling rewires the angiogenic pathways of cancers, and thus impairing the angiogenesis through a paracrine manner.

We further discovered that VEGF-A is a paracrine factor that is suppressed by ablation of Frs2α. The deletion of Frs2α significantly decreased VEGF-A expression in TRAMP tumors and in transplanted matrigel plugs, providing

strong evidence of the crosstalk between FGF and VEGF signaling. Luciferase and Chip assays further demonstrate that Frs2α promotes the binding of the transcriptional factors-Hif1a and c-Jun to the promoter of VEGF-A, and thus controls its expression. Since Hif1a is a transcriptional factor that is induced by the hypoxic conditions of tumor cells, our study demonstrated the possibility of preventing hypoxia-induced tumor angiogenesis through inhibiting Frs2α mediated FGF signaling. The regulation of HIF1a by FGF signaling also reveals that nutrients such as growth factors are interconnected with the pathways of hypoxia.

Since late stage prostate cancers metastasize to bones and are usually lethal, we tested whether Frs2α depletion inhibited the growth of a patient derived bone metastasis prostate cancer – MDA - 118b by using a bone implantation model. Results showed that Frs2α depletion significantly decreased the bone lesions caused by the growth of MDA-118b in mouse femurs. Tumor angiogenesis was also inhibited in tumors that lack Frs2α expression. Our study demonstrates that FGF signaling inhibition could suppress prostate cancer bone metastasis cells by targeting angiogenesis. However, the lack of animal models to mimic the bone metastasis of prostate cancers prevents us from understating the mechanism of the subtype of prostate cancers that usually cause lethality of patients. Starving tumor cells by blood supply deprivation could hold a key to inhibiting metastatic types of prostate cancers.

The development of new therapies relies on identifying pathways that are unique to certain types of tumors. Overactivation of FGFR1 signaling is one of the hallmarks that differentiate prostate cancers from other types of tumors. Since Frs2α is the adaptor protein of FGFR1, the transduction of FGF signaling greatly relies on the availability of Frs2α. In agreement with this notion, we investigated whether Frs2α could be a potential predictive or diagnostic biomarker of prostate cancer by measuring its expression in a cohort of 225 prostate cancer patients and paired normal tissues with detailed follow up information. In the tissue microarrays, we demonstrate that Frs2α, as well as transcriptional factors HIF1a and c-Jun, are associated with increased angiogenesis and poor prostate cancer patient prognosis. High expression levels of Frs2α predict shortened overall survival time, PSA failure free survival and metastasis free survival time.

Tyrosine phosphorylation is one of the most important post-translational modifications of cellular proteins. FGFR, as a tyrosine kinase, phosphorylates a series of downstream proteins such as Frs2α, MAPK and AKT, thus controlling the activation of the signaling cascades. In agreement with the fact that tyrosine phosphorylation is increased during transformation from normal cells to cancers, FGFR1 is believed to be a driver of prostate cancer tumor progression. The amplification of FGFR1 is associated with multiple tumors and chemical induced activation of FGFR1 is sufficient to induce prostate tumors in a mouse model. Our data showed that, in addition to stimulating proliferation promoting pathways such as MAPK, FGFR promoted aerobic glycolysis by stabilizing LDHA by

phosphorylation and suppressing LDHB transcription through promoter methylation.

Mitochondrial function of tumor cells is not intrinsically inactive or inhibited in many tumors. There has been a debate over whether tumors derive ATP exclusively from aerobic glycolysis or oxidative phosphorylation (OXPHOS). Therefore, it is important to investigate the energy source of prostate cancers during proliferation. Our data showed that deletion of FGFRs led to an increase in oxygen consumption, suggesting of a switch from aerobic glycolysis to oxidative phosphorylation upon deletion of FGFR. Notably, ATP production decreased despite the rise of mitochondrial respiration. These data demonstrated that the upregulation of OXPHOS was not sufficient to make up for the loss of energy due to FGFR ablation, indicating that prostate tumor cells derive ATP primarily from aerobic glycolysis.

Our data suggest that FGFR1 is required for the phosphorylation of LDHA, which results in enhanced LDHA stability. Consistent with a previous report, LDHA is phosphorylated at four tyrosine residues: Y10, Y83, Y172 and Y239. Site specific mutations of Y to F at all four sites resulted in dephosphorylation of LDHA, which further inhibited the half-life of LDHA. Our data supported the existing model that FGFR1 phosphorylates LDHA and, for the first time, linked the phosphorylation of LDHA to its protein stability. It provides a new venue to inhibit LDHA activity by simply suppressing its phosphorylation. Degradation of LDHA primarily relies on chaperone-mediated autophagy, which is a lysosome

dependent degradation mechanism (100). Further study needs to be done to determine which pathways cells use to degrade LDHA.

Our data also suggest that FGF signaling regulates expression of LDHB at the transcriptional level, which is different from protein stability regulation of LDHA. The promoter locus of Ldhb that contains multiple CpG sites was hypermethylated in MEFs, However, the ablation of FGF signaling caused demethylation of the Ldhb promoter, which resulted in the upregulation of Ldhb transcripts. These findings are in line with the clinical observations that Ldhb promoter was hypermethylated in multiple cancers and its expression is negatively associated with malignancies.

Lactic acid, produced by tumor cells, has a critical impact on the tumor microenvironment primarily through triggering angiogenesis and polarizing tumor associated macrophages. To investigate the impact of LDHA or LDHB knockout on the tumor microenvironment, we examined the number of blood vessels, stained by the anti CD31 antibody, and the number of F4/80 positive stained macrophage cells in DU145 xenografted tumors. The results showed that LDHA knockout significantly compromised, whereas LDHB knockout stimulated the number of newly formed blood vessels of tumors. Furthermore, LDHA knockout tumors displayed an increased macrophage infiltration, suggesting that LDHA ablation might trigger immune response through recruitment of macrophages. In contrast, LDHB knockout increased the recruitment of macrophage by tumor cells. Altogether, these data suggest that LDHA and LDHB differentially regulate

angiogenesis as well as the immune response mediated by macrophages differentially. These results are in line with the findings that LDHA promotes whereas LDHB suppresses the production of lactate, which is known to influence tumor microenvironment through angiogenesis and inflammation.

We also investigated whether we can exploit the altered glucose metabolism for clinical prediction and diagnostic purposes in PCa. The data showed that p-LDHA is overexpressed but LDHB is downregulated in prostate cancers compared with non-cancerous adjacent tissues. Individually, high pLDHA is associated with short PSA-failure free survival time of patients while low expression of LDHB also predicts shorter PSA-free survival time. Notably, LDHA expression is not a significantly factor in predicting the prognosis of patients which is contrast to p-LDHA, although elevated levels of LDHA protein was observed in prostate cancers. This suggested that the enhanced sensitivity of p-LDHA in predicting prognosis might be due to the fact that it is directly correlated with the tyrosine kinase activity of FGFR1 in prostate cancers. Therefore, the expression profile of LDH1-5 might be of limited use clinically in determining the prognosis of patients. Importantly, the combination of p-LDHA and low LDHB expression better predicts the biochemical recurrence-free and overall survival time of prostate cancer patients. There was a dramatic difference in PSA free and overall survival time between patients that have high p-LDHA and low LDHB and patients that express low p-LDHA and high LDHB, suggesting that p-LDHA and low LDHB can be exploited for predictive and diagnostic benefits.

To summarize, our findings demonstrate the unique roles of FGF signaling during prostate cancer progression. Targeting oncogenic FGF signaling suppressed tumor angiogenesis through inhibiting VEGF-A, blocking the communication of cancer and blood vessels cells. FGF inhibition also suppresses the Warburg effect of cancer cells through downregulating LDHA and upregulating LDHB. Intrinsic factors, such as activation of FGFR1, Frs2α, VEGF-A and LDHA, along with extrinsic factors, such as hypoxia and energy restrictions, define the unique metabolism and pathways of prostate cancers.

Tumors adapt to these factors, which causes the tumor to signal to its environment to reshape the vasculature networks to acquire energy and nutrients to sustain its rapid growth and expansion. Therefore, in addition to identifying pathways that are unique to cancer cells, we need to consider tumors as a well-structured organization. Our studies reveal the complexity of the organization and highlight the broad functions of FGF signaling in various contexts, therefore shedding new lights for the invention of new therapies against prostate cancer.

## REFERENCES


1. Vander Heiden, M. G., Lunt, S. Y., Dayton, T. L., Fiske, B. P., Israelsen, W. J., Mattaini, K. R., Vokes, N. I., Stephanopoulos, G., Cantley, L. C., Metallo, C. M., and Locasale, J. W. (2011) Metabolic pathway alterations that support cell proliferation. *Cold Spring Harb Symp Quant Biol* **76**, 325-334
2. Vander Heiden, M. G., and DeBerardinis, R. J. (2017) Understanding the Intersections between Metabolism and Cancer Biology. *Cell* **168**, 657-669
3. Gatenby, R. A., and Gillies, R. J. (2004) Why do cancers have high aerobic glycolysis? *Nat Rev Cancer* **4**, 891-899
4. Upadhyay, M., Samal, J., Kandpal, M., Singh, O. V., and Vivekanandan, P. (2013) The Warburg effect: insights from the past decade. *Pharmacol Ther* **137**, 318-330
5. Vander Heiden, M. G., Cantley, L. C., and Thompson, C. B. (2009) Understanding the Warburg effect: the metabolic requirements of cell proliferation. *Science* **324**, 1029-1033
6. Bostwick, D. G., and Iczkowski, K. A. (1998) Microvessel density in prostate cancer: prognostic and therapeutic utility. *Semin Urol Oncol* **16**, 118-123
7. Hanahan, D., and Weinberg, R. A. (2011) Hallmarks of cancer: the next generation. *Cell* **144**, 646-674

8. Lin, C., McGough, R., Aswad, B., Block, J. A., and Terek, R. (2004) Hypoxia induces HIF-1alpha and VEGF expression in chondrosarcoma cells and chondrocytes. *Journal of orthopaedic research : official publication of the Orthopaedic Research Society* **22**, 1175-1181

9. Yu, P., Wilhelm, K., Dubrac, A., Tung, J. K., Alves, T. C., Fang, J. S., Xie, Y., Zhu, J., Chen, Z., De Smet, F., Zhang, J., Jin, S. W., Sun, L., Sun, H., Kibbey, R. G., Hirschi, K. K., Hay, N., Carmeliet, P., Chittenden, T. W., Eichmann, A., Potente, M., and Simons, M. (2017) FGF-dependent metabolic control of vascular development. *Nature* **545**, 224-228

10. Helmlinger, G., Yuan, F., Dellian, M., and Jain, R. K. (1997) Interstitial pH and pO2 gradients in solid tumors in vivo: high-resolution measurements reveal a lack of correlation. *Nat Med* **3**, 177-182

11. Jemal, A., Siegel, R., Ward, E., Hao, Y., Xu, J., and Thun, M. J. (2009) Cancer statistics, 2009. *CA Cancer J Clin* **59**, 225-249

12. Wang, Y., Hayward, S., Cao, M., Thayer, K., and Cunha, G. (2001) Cell differentiation lineage in the prostate. *Differentiation* **68**, 270-279

13. Leong, K. G., Wang, B. E., Johnson, L., and Gao, W. Q. (2008) Generation of a prostate from a single adult stem cell. *Nature* **456**, 804-808

14. Xin, L., Lukacs, R. U., Lawson, D. A., Cheng, D., and Witte, O. N. (2007) Self-renewal and multilineage differentiation in vitro from murine prostate stem cells. *Stem Cells* **25**, 2760-2769

15. Peters, K. G., Marie, J., Wilson, E., Ives, H. E., Escobedo, J., Del Rosario, M., Mirda, D., and Williams, L. T. (1992) Point mutation of an FGF receptor abolishes phosphatidylinositol turnover and Ca2+ flux but not mitogenesis. *Nature* **358**, 678-681

16. Mohammadi, M., Dionne, C. A., Li, W., Li, N., Spivak, T., Honegger, A. M., Jaye, M., and Schlessinger, J. (1992) Point mutation in FGF receptor eliminates phosphatidylinositol hydrolysis without affecting mitogenesis. *Nature* **358**, 681-684

17. Seghezzi, G., Patel, S., Ren, C. J., Gualandris, A., Pintucci, G., Robbins, E. S., Shapiro, R. L., Galloway, A. C., Rifkin, D. B., and Mignatti, P. (1998) Fibroblast growth factor-2 (FGF-2) induces vascular endothelial growth factor (VEGF) expression in the endothelial cells of forming capillaries: an autocrine mechanism contributing to angiogenesis. *The Journal of cell biology* **141**, 1659-1673

18. Zhang, K., Chu, K., Wu, X., Gao, H., Wang, J., Yuan, Y. C., Loera, S., Ho, K., Wang, Y., Chow, W., Un, F., Chu, P., and Yen, Y. (2013) Amplification of FRS2 and activation of FGFR/FRS2 signaling pathway in high-grade liposarcoma. *Cancer Res* **73**, 1298-1307

19. Ho, T. H., Liu, X. D., Huang, Y., Warneke, C. L., Johnson, M. M., Hoang, A., Tamboli, P., Wang, F., and Jonasch, E. (2015) The impact of FGFR1 and FRS2alpha expression on sorafenib treatment in metastatic renal cell carcinoma. *BMC Cancer* **15**, 304

20. Luo, L. Y., Kim, E., Cheung, H. W., Weir, B. A., Dunn, G. P., Shen, R. R., and Hahn, W. C. (2015) The Tyrosine Kinase Adaptor Protein FRS2 Is Oncogenic and Amplified in High-Grade Serous Ovarian Cancer. *Mol Cancer Res* **13**, 502-509

21. Pertega-Gomes, N., Felisbino, S., Massie, C. E., Vizcaino, J. R., Coelho, R., Sandi, C., Simoes-Sousa, S., Jurmeister, S., Ramos-Montoya, A., Asim, M., Tran, M., Oliveira, E., Lobo da Cunha, A., Maximo, V., Baltazar, F., Neal, D. E., and Fryer, L. G. (2015) A glycolytic phenotype is associated with prostate cancer progression and aggressiveness: a role for monocarboxylate transporters as metabolic targets for therapy. *J Pathol* **236**, 517-530

22. Ros, S., Santos, C. R., Moco, S., Baenke, F., Kelly, G., Howell, M., Zamboni, N., and Schulze, A. (2012) Functional metabolic screen identifies 6-phosphofructo-2-kinase/fructose-2,6-biphosphatase 4 as an important regulator of prostate cancer cell survival. *Cancer Discov* **2**, 328-343

23. Ganapathy-Kanniappan, S., and Geschwind, J. F. (2013) Tumor glycolysis as a target for cancer therapy: progress and prospects. *Molecular cancer* **12**, 152

24. Fanciulli, M., Bruno, T., Giovannelli, A., Gentile, F. P., Di Padova, M., Rubiu, O., and Floridi, A. (2000) Energy metabolism of human LoVo colon

carcinoma cells: correlation to drug resistance and influence of lonidamine. *Clin Cancer Res* **6**, 1590-1597

25. Hanahan, D., and Folkman, J. (1996) Patterns and emerging mechanisms of the angiogenic switch during tumorigenesis. *Cell* **86**, 353-364

26. Carmeliet, P., and Jain, R. K. (2000) Angiogenesis in cancer and other diseases. *Nature* **407**, 249-257

27. Bouis, D., Kusumanto, Y., Meijer, C., Mulder, N. H., and Hospers, G. A. (2006) A review on pro- and anti-angiogenic factors as targets of clinical intervention. *Pharmacol Res* **53**, 89-103

28. Casanovas, O., Hicklin, D. J., Bergers, G., and Hanahan, D. (2005) Drug resistance by evasion of antiangiogenic targeting of VEGF signaling in late-stage pancreatic islet tumors. *Cancer Cell* **8**, 299-309

29. Nissen, L. J., Cao, R., Hedlund, E. M., Wang, Z., Zhao, X., Wetterskog, D., Funa, K., Brakenhielm, E., and Cao, Y. (2007) Angiogenic factors FGF2 and PDGF-BB synergistically promote murine tumor neovascularization and metastasis. *J Clin Invest* **117**, 2766-2777

30. Borre, M., Offersen, B. V., Nerstrom, B., and Overgaard, J. (1998) Microvessel density predicts survival in prostate cancer patients subjected to watchful waiting. *Br J Cancer* **78**, 940-944

31. Zhang, Y., Zhang, J., Lin, Y., Lan, Y., Lin, C., Xuan, J. W., Shen, M. M., McKeehan, W. L., Greenberg, N. M., and Wang, F. (2008) Role of

epithelial cell fibroblast growth factor receptor substrate 2alpha in prostate development, regeneration and tumorigenesis. *Development* **135**, 775-784

32. Wang, X., Asmann, Y. W., Erickson-Johnson, M. R., Oliveira, J. L., Zhang, H., Moura, R. D., Lazar, A. J., Lev, D., Bill, K., Lloyd, R. V., Yaszemski, M. J., Maran, A., and Oliveira, A. M. (2011) High-resolution genomic mapping reveals consistent amplification of the fibroblast growth factor receptor substrate 2 gene in well-differentiated and dedifferentiated liposarcoma. *Genes, chromosomes & cancer* **50**, 849-858
33. Valencia, T., Joseph, A., Kachroo, N., Darby, S., Meakin, S., and Gnanapragasam, V. J. (2011) Role and expression of FRS2 and FRS3 in prostate cancer. *BMC cancer* **11**, 484
34. Zhang, Y., Zhang, J., Lin, Y., Lan, Y., Lin, C., Xuan, J. W., Shen, M. M., McKeehan, W. L., Greenberg, N. M., and Wang, F. (2008) Role of epithelial cell fibroblast growth factor receptor substrate 2{alpha} in prostate development, regeneration and tumorigenesis. *Development* **135**, 775-784
35. Teishima, J., Yano, S., Shoji, K., Hayashi, T., Goto, K., Kitano, H., Oka, K., Nagamatsu, H., and Matsubara, A. (2014) Accumulation of FGF9 in prostate cancer correlates with epithelial-to-mesenchymal transition and induction of VEGF-A expression. *Anticancer research* **34**, 695-700

36. Li, Z. G., Mathew, P., Yang, J., Starbuck, M. W., Zurita, A. J., Liu, J., Sikes, C., Multani, A. S., Efstathiou, E., Lopez, A., Wang, J., Fanning, T. V., Prieto, V. G., Kundra, V., Vazquez, E. S., Troncoso, P., Raymond, A. K., Logothetis, C. J., Lin, S. H., Maity, S., and Navone, N. M. (2008) Androgen receptor-negative human prostate cancer cells induce osteogenesis in mice through FGF9-mediated mechanisms. *J Clin Invest* **118**, 2697-2710

37. Winter, S. F., Acevedo, V. D., Gangula, R. D., Freeman, K. W., Spencer, D. M., and Greenberg, N. M. (2007) Conditional activation of FGFR1 in the prostate epithelium induces angiogenesis with concomitant differential regulation of Ang-1 and Ang-2. *Oncogene* **26**, 4897-4907

38. Huang, X., Yu, C., Jin, C., Kobayashi, M., Bowles, C. A., Wang, F., and McKeehan, W. L. (2006) Ectopic activity of fibroblast growth factor receptor 1 in hepatocytes accelerates hepatocarcinogenesis by driving proliferation and vascular endothelial growth factor-induced angiogenesis. *Cancer research* **66**, 1481-1490

39. Wan, X., Corn, P. G., Yang, J., Palanisamy, N., Starbuck, M. W., Efstathiou, E., Tapia, E. M., Zurita, A. J., Aparicio, A., Ravoori, M. K., Vazquez, E. S., Robinson, D. R., Wu, Y. M., Cao, X., Iyer, M. K., McKeehan, W., Kundra, V., Wang, F., Troncoso, P., Chinnaiyan, A. M., Logothetis, C. J., and Navone, N. M. (2014) Prostate cancer cell-stromal

cell crosstalk via FGFR1 mediates antitumor activity of dovitinib in bone metastases. *Science translational medicine* **6**, 252ra122

40. Pages, G., and Pouyssegur, J. (2005) Transcriptional regulation of the Vascular Endothelial Growth Factor gene--a concert of activating factors. *Cardiovascular research* **65**, 564-573

41. Tischer, E., Mitchell, R., Hartman, T., Silva, M., Gospodarowicz, D., Fiddes, J. C., and Abraham, J. A. (1991) The human gene for vascular endothelial growth factor. Multiple protein forms are encoded through alternative exon splicing. *The Journal of biological chemistry* **266**, 11947-11954

42. Ciccarese, C., Santoni, M., Massari, F., Modena, A., Piva, F., Conti, A., Mazzucchelli, R., Cheng, L., Lopez-Beltran, A., Scarpelli, M., Tortora, G., and Montironi, R. (2015) Metabolic Alterations in Renal and Prostate Cancer. *Curr Drug Metab*

43. Chen, R., Zhou, X., Yu, Z., Liu, J., and Huang, G. (2015) Low Expression of LDHB Correlates With Unfavorable Survival in Hepatocellular Carcinoma: Strobe-Compliant Article. *Medicine (Baltimore)* **94**, e1583

44. Mraz, J., Vrubel, F., and Hanselova, M. (1979) Carcinoma of the prostate. II. Serum activity of acid phosphatase, prostatic acid phosphatase, LDH and its isoenzymes. *International urology and nephrology* **11**, 301-309

45. Oliver, J. A., el-Hilali, M. M., Belitsky, P., and MacKinnon, K. J. (1970) LDH isoenzymes in benign and malignant prostate tissue. The LDH V-I ratio as an index of malignancy. *Cancer* **25**, 863-866

46. Naruse, K., Yamada, Y., Aoki, S., Taki, T., Nakamura, K., Tobiume, M., Zennami, K., Katsuda, R., Sai, S., Nishio, Y., Inoue, Y., Noguchi, H., and Hondai, N. (2007) Lactate dehydrogenase is a prognostic indicator for prostate cancer patients with bone metastasis. *Hinyokika kiyo. Acta urologica Japonica* **53**, 287-292

47. Keshari, K. R., Sriram, R., Van Criekinge, M., Wilson, D. M., Wang, Z. J., Vigneron, D. B., Peehl, D. M., and Kurhanewicz, J. (2013) Metabolic reprogramming and validation of hyperpolarized 13C lactate as a prostate cancer biomarker using a human prostate tissue slice culture bioreactor. *The Prostate* **73**, 1171-1181

48. Cunha, G. R., Cooke, P. S., and Kurita, T. (2004) Role of stromal-epithelial interactions in hormonal responses. *Arch Histol Cytol* **67**, 417-434

49. Powers, C. J., McLeskey, S. W., and Wellstein, A. (2000) Fibroblast growth factors, their receptors and signaling. *Endocr Relat Cancer* **7**, 165-197.

50. Faham, S., Linhardt, R. J., and Rees, D. C. (1998) Diversity does make a difference: fibroblast growth factor-heparin interactions. *Curr Opin Struct Biol* **8**, 578-586.

51. Kanda, S., Shono, T., Tomasini-Johansson, B., Klint, P., and Saito, Y. (1999) Role of thrombospondin-1-derived peptide, 4N1K, in FGF-2-induced angiogenesis. *Experimental cell research* **252**, 262-272

52. Ornitz, D. M. (2000) FGFs, heparan sulfate and FGFRs: complex interactions essential for development. *Bioessays* **22**, 108-112.

53. McKeehan, W. L., Wang, F., and Luo, Y. (2009) *The fibroblast growth factor (FGF) signaling complex. Handbook of Cell Signaling*, 2dn ed., Academic/Elsevier Press, New York

54. Thomson, A. A. (2001) Role of androgens and fibroblast growth factors in prostatic development. *Reproduction* **121**, 187-195.

55. Gowardhan, B., Douglas, D. A., Mathers, M. E., McKie, A. B., McCracken, S. R., Robson, C. N., and Leung, H. Y. (2005) Evaluation of the fibroblast growth factor system as a potential target for therapy in human prostate cancer. *Br J Cancer* **92**, 320-327

56. Abate-Shen, C., and Shen, M. M. (2007) FGF signaling in prostate tumorigenesis--new insights into epithelial-stromal interactions. *Cancer Cell* **12**, 495-497

57. Chen, Y., Zhang, D., Xin, N., Xiong, Y., Chen, P., Li, B., Tu, X., and Lan, F. (2008) Construction of sperm-specific lactate dehydrogenase DNA vaccine and experimental study of its immunocontraceptive effect on mice. *Science in China. Series C, Life sciences / Chinese Academy of Sciences* **51**, 308-316

58. Acevedo, V. D., Gangula, R. D., Freeman, K. W., Li, R., Zhang, Y., Wang, F., Ayala, G. E., Peterson, L. E., Ittmann, M., and Spencer, D. M. (2007) Inducible FGFR-1 activation leads to irreversible prostate adenocarcinoma and an epithelial-to-mesenchymal transition. *Cancer Cell* **12**, 559-571

59. Wesche, J., Haglund, K., and Haugsten, E. M. (2011) Fibroblast growth factors and their receptors in cancer. *The Biochemical journal* **437**, 199-213

60. Taylor, B. S., Schultz, N., Hieronymus, H., Gopalan, A., Xiao, Y., Carver, B. S., Arora, V. K., Kaushik, P., Cerami, E., Reva, B., Antipin, Y., Mitsiades, N., Landers, T., Dolgalev, I., Major, J. E., Wilson, M., Socci, N. D., Lash, A. E., Heguy, A., Eastham, J. A., Scher, H. I., Reuter, V. E., Scardino, P. T., Sander, C., Sawyers, C. L., and Gerald, W. L. (2010) Integrative genomic profiling of human prostate cancer. *Cancer Cell* **18**, 11-22

61. Giri, D., Ropiquet, F., and Ittmann, M. (1999) Alterations in expression of basic fibroblast growth factor (FGF) 2 and its receptor FGFR-1 in human prostate cancer. *Clin Cancer Res* **5**, 1063-1071.

62. Ozen, M., Giri, D., Ropiquet, F., Mansukhani, A., and Ittmann, M. (2001) Role of fibroblast growth factor receptor signaling in prostate cancer cell survival. *J Natl Cancer Inst* **93**, 1783-1790

63. Devilard, E., Bladou, F., Ramuz, O., Karsenty, G., Dales, J. P., Gravis, G., Nguyen, C., Bertucci, F., Xerri, L., and Birnbaum, D. (2006) FGFR1 and WT1 are markers of human prostate cancer progression. *BMC Cancer* **6**, 272

64. Chen, X., Gu, X., Shan, Y., Tang, W., Yuan, J., Zhong, Z., Wang, Y., Huang, W., Wan, B., and Yu, L. (2009) Identification of a novel human lactate dehydrogenase gene LDHAL6A, which activates transcriptional activities of AP1(PMA). *Molecular biology reports* **36**, 669-676

65. Jin, C., McKeehan, K., Guo, W., Jauma, S., Ittmann, M. M., Foster, B., Greenberg, N. M., McKeehan, W. L., and Wang, F. (2003) Cooperation between ectopic FGFR1 and depression of FGFR2 in induction of prostatic intraepithelial neoplasia in the mouse prostate. *Cancer Res* **63**, 8784-8790

66. Song, Z., Powell, W. C., Kasahara, N., van Bokhoven, A., Miller, G. J., and Roy-Burman, P. (2000) The effect of fibroblast growth factor 8, isoform b, on the biology of prostate carcinoma cells and their interaction with stromal cells. *Cancer Res* **60**, 6730-6736.

67. Memarzadeh, S., Xin, L., Mulholland, D. J., Mansukhani, A., Wu, H., Teitell, M. A., and Witte, O. N. (2007) Enhanced paracrine FGF10 expression promotes formation of multifocal prostate adenocarcinoma and an increase in epithelial androgen receptor. *Cancer Cell* **12**, 572-585

68. Polnaszek, N., Kwabi-Addo, B., Peterson, L. E., Ozen, M., Greenberg, N. M., Ortega, S., Basilico, C., and Ittmann, M. (2003) Fibroblast growth factor 2 promotes tumor progression in an autochthonous mouse model of prostate cancer. *Cancer Res* **63**, 5754-5760

69. Valta, M. P., Tuomela, J., Bjartell, A., Valve, E., Vaananen, H. K., and Harkonen, P. (2008) FGF-8 is involved in bone metastasis of prostate cancer. *Int J Cancer* **123**, 22-31

70. Chang, J. Y., Wang, C., Jin, C., Yang, C., Huang, Y., Liu, J., McKeehan, W. L., D'Souza, R. N., and Wang, F. (2013) Self-renewal and multilineage differentiation of mouse dental epithelial stem cells. *Stem Cell Res* **11**, 990-1002

71. Fritz, P. J. (1965) Rabbit muscle lactate dehydrogenase 5; a regulatory enzyme. *Science* **150**, 364-366

72. Dennison, J. B., Molina, J. R., Mitra, S., Gonzalez-Angulo, A. M., Balko, J. M., Kuba, M. G., Sanders, M. E., Pinto, J. A., Gomez, H. L., Arteaga, C. L., Brown, R. E., and Mills, G. B. (2013) Lactate dehydrogenase B: a metabolic marker of response to neoadjuvant chemotherapy in breast cancer. *Clin Cancer Res* **19**, 3703-3713

73. McCleland, M. L., Adler, A. S., Deming, L., Cosino, E., Lee, L., Blackwood, E. M., Solon, M., Tao, J., Li, L., Shames, D., Jackson, E., Forrest, W. F., and Firestein, R. (2013) Lactate dehydrogenase B is

required for the growth of KRAS-dependent lung adenocarcinomas. *Clin Cancer Res* **19**, 773-784

74. McCleland, M. L., Adler, A. S., Shang, Y., Hunsaker, T., Truong, T., Peterson, D., Torres, E., Li, L., Haley, B., Stephan, J. P., Belvin, M., Hatzivassiliou, G., Blackwood, E. M., Corson, L., Evangelista, M., Zha, J., and Firestein, R. (2012) An integrated genomic screen identifies LDHB as an essential gene for triple-negative breast cancer. *Cancer Res* **72**, 5812-5823

75. Isozaki, Y., Hoshino, I., Nohata, N., Kinoshita, T., Akutsu, Y., Hanari, N., Mori, M., Yoneyama, Y., Akanuma, N., Takeshita, N., Maruyama, T., Seki, N., Nishino, N., Yoshida, M., and Matsubara, H. (2012) Identification of novel molecular targets regulated by tumor suppressive miR-375 induced by histone acetylation in esophageal squamous cell carcinoma. *Int J Oncol* **41**, 985-994

76. Lai, L., Liu, J., Zhai, D., Lin, Q., He, L., Dong, Y., Zhang, J., Lu, B., Chen, Y., Yi, Z., and Liu, M. (2012) Plumbagin inhibits tumour angiogenesis and tumour growth through the Ras signalling pathway following activation of the VEGF receptor-2. *British journal of pharmacology* **165**, 1084-1096

77. Shao, Q., Byrum, S. D., Moreland, L. E., Mackintosh, S. G., Kannan, A., Lin, Z., Morgan, M., Stack, B. C., Jr., Cornelius, L. A., Tackett, A. J., and Gao, L. (2013) A Proteomic Study of Human Merkel Cell Carcinoma. *J Proteomics Bioinform* **6**, 275-282

78. Ciregia, F., Giusti, L., Molinaro, A., Niccolai, F., Agretti, P., Rago, T., Di Coscio, G., Vitti, P., Basolo, F., Iacconi, P., Tonacchera, M., and Lucacchini, A. (2013) Presence in the pre-surgical fine-needle aspiration of potential thyroid biomarkers previously identified in the post-surgical one. *PLoS One* **8**, e72911

79. Huang, Y., Hamana, T., Liu, J., Wang, C., An, L., You, P., Chang, J. Y., Xu, J., Jin, C., Zhang, Z., McKeehan, W. L., and Wang, F. (2015) Type 2 Fibroblast Growth Factor Receptor Signaling Preserves Stemness and Prevents Differentiation of Prostate Stem Cells from the Basal Compartment. *J Biol Chem* **290**, 17753-17761

80. Maekawa, M., Taniguchi, T., Ishikawa, J., Sugimura, H., Sugano, K., and Kanno, T. (2003) Promoter hypermethylation in cancer silences LDHB, eliminating lactate dehydrogenase isoenzymes 1-4. *Clinical chemistry* **49**, 1518-1520

81. Leiblich, A., Cross, S. S., Catto, J. W., Phillips, J. T., Leung, H. Y., Hamdy, F. C., and Rehman, I. (2006) Lactate dehydrogenase-B is silenced by promoter hypermethylation in human prostate cancer. *Oncogene* **25**, 2953-2960

82. Cui, J., Quan, M., Jiang, W., Hu, H., Jiao, F., Li, N., Jin, Z., Wang, L., Wang, Y., and Wang, L. (2015) Suppressed expression of LDHB promotes pancreatic cancer progression via inducing glycolytic phenotype. *Med Oncol* **32**, 143

83. Bae, Y. H., Park, H. J., Kim, S. R., Kim, J. Y., Kang, Y., Kim, J. A., Wee, H. J., Kageyama, R., Jung, J. S., Bae, M. K., and Bae, S. K. (2011) Notch1 mediates visfatin-induced FGF-2 up-regulation and endothelial angiogenesis. *Cardiovascular research* **89**, 436-445

84. Doherty, J. R., and Cleveland, J. L. (2013) Targeting lactate metabolism for cancer therapeutics. *J Clin Invest* **123**, 3685-3692

85. Xie, H., Hanai, J., Ren, J. G., Kats, L., Burgess, K., Bhargava, P., Signoretti, S., Billiard, J., Duffy, K. J., Grant, A., Wang, X., Lorkiewicz, P. K., Schatzman, S., Bousamra, M., 2nd, Lane, A. N., Higashi, R. M., Fan, T. W., Pandolfi, P. P., Sukhatme, V. P., and Seth, P. (2014) Targeting lactate dehydrogenase--a inhibits tumorigenesis and tumor progression in mouse models of lung cancer and impacts tumor-initiating cells. *Cell metabolism* **19**, 795-809

86. Fan, J., Hitosugi, T., Chung, T. W., Xie, J., Ge, Q., Gu, T. L., Polakiewicz, R. D., Chen, G. Z., Boggon, T. J., Lonial, S., Khuri, F. R., Kang, S., and Chen, J. (2011) Tyrosine phosphorylation of lactate dehydrogenase A is important for NADH/NAD(+) redox homeostasis in cancer cells. *Molecular and cellular biology* **31**, 4938-4950

87. Trokovic, R., Trokovic, N., Hernesniemi, S., Pirvola, U., Vogt Weisenhorn, D. M., Rossant, J., McMahon, A. P., Wurst, W., and Partanen, J. (2003) FGFR1 is independently required in both developing mid- and hindbrain

for sustained response to isthmic signals. *The EMBO journal* **22**, 1811-1823

88. Forough, R., Wang, X., Martinez-Lemus, L. A., Thomas, D., Sun, Z., Motamed, K., Parker, J. L., and Meininger, G. A. (2003) Cell-based and direct gene transfer-induced angiogenesis via a secreted chimeric fibroblast growth factor-1 (sp-FGF-1) in the chick chorioallantoic membrane (CAM). *Angiogenesis* **6**, 47-54

89. Kim, B. S., Park, J. Y., Kang, H. J., Kim, H. J., and Lee, J. (2014) Fucoidan/FGF-2 induces angiogenesis through JNK- and p38-mediated activation of AKT/MMP-2 signalling. *Biochem Biophys Res Commun* **450**, 1333-1338

90. Zhong, W. D., Liang, Y. X., Lin, S. X., Li, L., He, H. C., Bi, X. C., Han, Z. D., Dai, Q. S., Ye, Y. K., Chen, Q. B., Wang, Y. S., Zeng, G. H., Zhu, G., Zhang, Z., Chen, Z. N., and Wu, C. L. (2012) Expression of CD147 is associated with prostate cancer progression. *Int J Cancer* **130**, 300-308

91. Nishitani, S., Takehana, K., Fujitani, S., and Sonaka, I. (2005) Branched-chain amino acids improve glucose metabolism in rats with liver cirrhosis. *Am J Physiol Gastrointest Liver Physiol* **288**, G1292-1300

92. Yang, F., Zhang, Y., Ressler, S. J., Ittmann, M. M., Ayala, G. E., Dang, T. D., Wang, F., and Rowley, D. R. (2013) FGFR1 is essential for prostate cancer progression and metastasis. *Cancer Res* **73**, 3716-3724

93. Colegio, O. R., Chu, N. Q., Szabo, A. L., Chu, T., Rhebergen, A. M., Jairam, V., Cyrus, N., Brokowski, C. E., Eisenbarth, S. C., Phillips, G. M., Cline, G. W., Phillips, A. J., and Medzhitov, R. (2014) Functional polarization of tumour-associated macrophages by tumour-derived lactic acid. *Nature* **513**, 559-563

94. Shim, H., Dolde, C., Lewis, B. C., Wu, C. S., Dang, G., Jungmann, R. A., Dalla-Favera, R., and Dang, C. V. (1997) c-Myc transactivation of LDH-A: implications for tumor metabolism and growth. *Proceedings of the National Academy of Sciences of the United States of America* **94**, 6658-6663

95. Pencik, J., Schlederer, M., Gruber, W., Unger, C., Walker, S. M., Chalaris, A., Marie, I. J., Hassler, M. R., Javaheri, T., Aksoy, O., Blayney, J. K., Prutsch, N., Skucha, A., Herac, M., Kramer, O. H., Mazal, P., Grebien, F., Egger, G., Poli, V., Mikulits, W., Eferl, R., Esterbauer, H., Kennedy, R., Fend, F., Scharpf, M., Braun, M., Perner, S., Levy, D. E., Malcolm, T., Turner, S. D., Haitel, A., Susani, M., Moazzami, A., Rose-John, S., Aberger, F., Merkel, O., Moriggl, R., Culig, Z., Dolznig, H., and Kenner, L. (2015) STAT3 regulated ARF expression suppresses prostate cancer metastasis. *Nature communications* **6**, 7736

96. Sugiura, K., Su, Y. Q., Diaz, F. J., Pangas, S. A., Sharma, S., Wigglesworth, K., O'Brien, M. J., Matzuk, M. M., Shimasaki, S., and

Eppig, J. J. (2007) Oocyte-derived BMP15 and FGFs cooperate to promote glycolysis in cumulus cells. *Development* **134**, 2593-2603

97. Jin, L., Chun, J., Pan, C., Alesi, G. N., Li, D., Magliocca, K. R., Kang, Y., Chen, Z. G., Shin, D. M., Khuri, F. R., Fan, J., and Kang, S. (2017) Phosphorylation-mediated activation of LDHA promotes cancer cell invasion and tumour metastasis. *Oncogene*

98. Fantin, V. R., St-Pierre, J., and Leder, P. (2006) Attenuation of LDH-A expression uncovers a link between glycolysis, mitochondrial physiology, and tumor maintenance. *Cancer Cell* **9**, 425-434

99. Folkman, J. (1971) Tumor angiogenesis: therapeutic implications. *N Engl J Med* **285**, 1182-1186

100. Zhao, D., Zou, S. W., Liu, Y., Zhou, X., Mo, Y., Wang, P., Xu, Y. H., Dong, B., Xiong, Y., Lei, Q. Y., and Guan, K. L. (2013) Lysine-5 acetylation negatively regulates lactate dehydrogenase A and is decreased in pancreatic cancer. *Cancer Cell* **23**, 464-476